

When Does Preconditioning Help or Hurt Generalization?

*Shun-ichi Amari[†], Jimmy Ba[‡], Roger Grosse[‡], Xuechen Li[§],
Atsushi Nitanda[¶], Taiji Suzuki[¶], Denny Wu[‡], Ji Xu^{||}

June 6, 2022

Abstract

While second order optimizers such as natural gradient descent (NGD) often speed up optimization, their effect on generalization remains controversial. For instance, it has been pointed out that gradient descent (GD), in contrast to many preconditioned updates, converges to small Euclidean norm solutions in overparameterized models, leading to favorable generalization properties. This work presents a more nuanced view on the comparison of generalization between first- and second-order methods. We provide an exact asymptotic bias-variance decomposition of the generalization error of overparameterized ridgeless regression under a general class of preconditioner \mathbf{P} , and consider the inverse population Fisher information matrix (used in NGD) as a particular example. We determine the optimal \mathbf{P} for both the bias and variance, and find that the relative generalization performance of different optimizers depends on the label noise and the “shape” of the signal (true parameters): when the labels are noisy, the model is misspecified, or the signal is misaligned with the features, NGD can achieve lower risk; conversely, GD generalizes better than NGD under clean labels, a well-specified model, or aligned signal. Based on this analysis, we discuss several approaches to manage the bias-variance tradeoff, and the potential benefit of interpolating between GD and NGD. We then extend our analysis to regression in the reproducing kernel Hilbert space and demonstrate that preconditioned GD can decrease the population risk faster than GD. Lastly, we empirically compare the generalization performance of first- and second-order optimizers in neural network experiments, and observe robust trends matching our theoretical analysis.

1 Introduction

Due to the significant and growing cost of training large-scale machine learning systems (e.g. neural networks [RWC⁺]), there has been much interest in algorithms that speed up optimization. Many such algorithms make use of various types of second-order information, and can be interpreted as minimizing the empirical risk (or the training error) $L(f_{\theta})$ via a preconditioned gradient descent update:

$$\theta_{t+1} = \theta_t - \eta \mathbf{P}(t) \nabla_{\theta_t} L(f_{\theta_t}), \quad t = 0, 1, \dots \quad (1.1)$$

Setting $\mathbf{P} = \mathbf{I}$ recovers ordinary gradient descent (GD). Choices of \mathbf{P} which exploit second-order information include the inverse Fisher information matrix, which gives the natural gradient descent (NGD) [Ama98]; the inverse Hessian, which gives Newton’s method [LBOM12]; and diagonal matrices estimated from past gradients, corresponding to various adaptive gradient methods [DHS11, KB14]. By using second-order information, these preconditioners often alleviate the effect of pathological curvature and speed up optimization.

*Alphabetical ordering. Correspondence to: Denny Wu (dennywu@cs.toronto.edu).

[†]RIKEN Center for Brain Science. amari@brain.riken.jp.

[‡]University of Toronto and Vector Institute for Artificial Intelligence. {jba, rgrosse, dennywu}@cs.toronto.edu.

[§]Google Research, Brain Team. Member of the Google AI Residency Program. lxuechen@cs.toronto.edu.

[¶]University of Tokyo and RIKEN Center for Advanced Intelligence Project. {nitanda, taiji}@mist.i.u-tokyo.ac.jp.

^{||}Columbia University. jixu@cs.columbia.edu.

However, the typical goal of learning is not to fit a finite training set, but to construct predictors that generalize beyond the training data. Although second-order methods can lead to faster optimization, their effect on generalization has been largely under debate. NGD [Ama98], as well as Adagrad [DHS11] and its successors [KB14], was originally justified in online learning, where efficiency in learning directly translates to generalization. Nonetheless, there remains the possibility that, in the finite data setting, these preconditioned updates are more (or less) prone to overfitting than GD. For example, several works reported that in neural network optimization, adaptive or second-order methods generalize worse than GD and its stochastic variants [WRS⁺17, WMW18, KS17], while other empirical studies suggested that second-order methods can achieve comparable, if not better generalization [XRM20, ZWXG18]. We aim to understand when preconditioning using second-order information can help or hurt generalization under fixed training data.

The comparison of the generalization performance of different optimizers relates to the discussion of *implicit regularization* [GLSS18a, ZBH⁺16]. While many explanations have been proposed (see Section 2), the starting point of this work is the well-known observation that GD often implicitly regularizes the Euclidean norm, leading to good generalization. For instance in overparameterized least squares regression [WRS⁺17], GD and many other first-order methods find the minimum ℓ_2 norm solution from zero initialization (without explicit regularization), but preconditioned updates often do not. However, while this minimum norm solution provides reasonable generalization in the overparameterized regime [HMRT19, BLLT19], it is unclear whether preconditioned gradient descent always finds inferior solutions.

Motivated by the observations above, we focus on the analysis of overparameterized least squares regression, a setting that is convenient and also interesting for several reasons: (i) the Hessian and Fisher matrix coincide and are not time varying, (ii) the optimization trajectory and stationary solution admit an analytical form both with and without preconditioning, (iii) due to overparameterization (which is common in modern machine learning models), different \mathbf{P} may give solutions with contrasting generalization properties. Despite its simplicity, linear regression often yields insights and testable predictions for more complex problems such as neural network optimization; indeed we validate the conclusions of our analysis with neural network experiments (although a rigorous connection is not established).

Our results are organized as follows. In Section 3, we compute the stationary ($t \rightarrow \infty$) generalization error of update (1.1) for overparameterized linear regression under a fixed preconditioner. Extending the proportional asymptotic setup in [HMRT19, DW⁺18], we consider a more general random effects model and use random matrix theoretical tools to derive the exact population risk in its bias-variance decomposition. We characterize choices of \mathbf{P} that achieve the optimal bias or variance within a general class of preconditioners. Our analysis focuses on the comparison between GD, in which \mathbf{P} is identity, and NGD, in which \mathbf{P} is the inverse population Fisher information matrix¹. Our characterization reveals that the comparison of generalization performance is affected by the following factors:

1. **Label Noise:** Additive noise in the labels contributes to the variance term in the risk. We show that NGD achieves the optimal variance among a general class of preconditioned updates.
2. **Model Misspecification:** Under misspecification, there does not exist f_θ that achieves perfect generalization. While this influences the bias term in the risk, we argue that the impact is similar to label noise. Thus, NGD is also beneficial when the model is misspecified.
3. **Data-Signal-Alignment:** Alignment describes how the target signal distributes among input features. We show that NGD is advantageous under misalignment — when large variance directions of the features match the small signal directions (learning is “difficult”) — whereas GD achieves lower bias under isotropic signals.

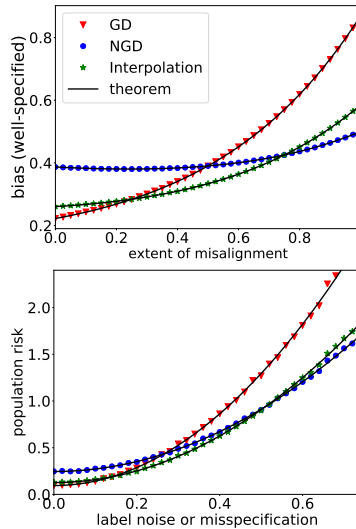


Figure 1: Population risk of the stationary solution of GD, NGD, and interpolation between the two in overparameterized ridgeless regression (detailed setup in Section 3). The relative generalization performance of optimizers depends on label noise, model misspecification and misalignment.

¹From now on we use NGD to denote the preconditioned update with the inverse *population* Fisher, and we write “sample NGD” when \mathbf{P} is the inverse or pseudo-inverse of the sample Fisher (computed on the same training set).

In addition to the decomposition of stationary risk, our findings in Section 4 and 5 can be summarized as:

- In Section 4.1 and 4.2 we discuss how the bias-variance tradeoff can be realized by different choices of preconditioner \mathbf{P} (e.g. interpolating between GD and NGD) or early stopping.
- In Section 4.3 we extend our analysis to regression in reproducing kernel Hilbert spaces (RKHS) and show that under early stopping, a preconditioned update interpolating between GD and NGD achieves minimax optimal convergence rate in much fewer steps, and thus reduces the population risk faster than GD.
- In Section 5 we empirically test how well our predictions from the linear regression setting carry over to neural networks: under a student-teacher setup, we compare the generalization of GD with preconditioned updates and illustrate the influence of all aforementioned factors. The performance of neural networks under a variety of manipulations results in trends that align with our analysis of linear model.

2 Background and Related Works

Natural Gradient Descent. NGD is a second-order optimization method originally proposed in [Ama97]. Consider a data distribution $p(\mathbf{x})$ on the space \mathcal{X} , a function $f_{\boldsymbol{\theta}} : \mathcal{X} \rightarrow \mathcal{Z}$ parameterized by $\boldsymbol{\theta}$, and a loss function $L(\mathbf{X}, f_{\boldsymbol{\theta}}) = \frac{1}{n} \sum_{i=1}^n l(y_i, f_{\boldsymbol{\theta}}(\mathbf{x}_i))$, where $l : \mathcal{Y} \times \mathcal{Z} \rightarrow \mathbb{R}$. Also suppose a probability distribution $p(y|z) = p(y|f_{\boldsymbol{\theta}}(\mathbf{x}))$ is defined on the space of labels as part of the model. Then, the natural gradient is the direction of steepest ascent in the Fisher information norm given by $\tilde{\nabla}_{\boldsymbol{\theta}} L(\mathbf{X}, f_{\boldsymbol{\theta}}) = \mathbf{F}^{-1} \nabla_{\boldsymbol{\theta}} L(\mathbf{X}, f_{\boldsymbol{\theta}})$, where

$$\mathbf{F} = \mathbb{E}[\nabla_{\boldsymbol{\theta}} \log p(\mathbf{x}, y|\boldsymbol{\theta}) \nabla_{\boldsymbol{\theta}} \log p(\mathbf{x}, y|\boldsymbol{\theta})^{\top}] = -\mathbb{E}[\nabla_{\boldsymbol{\theta}}^2 \log p(\mathbf{x}, y|\boldsymbol{\theta})] \quad (2.1)$$

is the *Fisher information matrix*, or simply the (population) Fisher. Note the expectations in (2.1) are under the joint distribution of the model $p(\mathbf{x}, y|\boldsymbol{\theta}) = p(\mathbf{x})p(y|f_{\boldsymbol{\theta}}(\mathbf{x}))$. In the literature, the Fisher is sometimes defined under the empirical data distribution, i.e. based on a finite set of training examples $\{\mathbf{x}_i\}_{i=1}^n$ [APF00]. We instead refer to this quantity as the *sample Fisher*, the properties of which influence optimization and have been studied in various works [KAA18, KAA19, KBH19]. Note that in linear and kernel regression (unregularized) under the squared loss, sample Fisher-based preconditioned updates give the same stationary solution as GD (see [ZMG19] and Section 3), whereas the population Fisher-based update may not.

While the population Fisher is typically difficult to obtain, extra unlabeled data can be used in its estimation, which empirically improves generalization under appropriately chosen damping [PB13]. Moreover, under structural assumptions, estimating the Fisher with parametric approaches can be more sample-efficient [MG15, GM16, Oll15, MCO16], and thus closing the gap between the sample and population Fisher.

When the per-instance loss l is the negative log-probability of an exponential family, the sample Fisher coincides with the *generalized Gauss-Newton matrix* [Mar14]. In least squares regression, which is the focus of this work, the quantity also coincides with the Hessian due to the linear prediction function. Therefore, we take NGD as a representative example of preconditioned update, and we expect our findings to also translate to other second-order methods (not including adaptive gradient methods) applied to regression problems.

Implicit Regularization in Optimization. In overparameterized linear models, GD finds the minimum ℓ_2 norm solution under many loss functions. For the more general mirror descent, the implicit bias is determined by the Bregman divergence of the update [AH18, ALH19, GLSS18b, SPR18]. Under the exponential or logistic loss, recent works demonstrated that GD finds the max-margin direction in various models [JT18, JT19, SHN⁺18, LL19, CB20]. The implicit bias of Adagrad has been analyzed under similar setting [QQ19]. The implicit regularization of the optimizer often relates to the model architecture; examples include matrix factorization [GWB⁺17, SMG13, GBLJ19, ACHL19] and various types of neural network [LMZ17, GLSS18b, WTS⁺19, WGL⁺20]. For neural networks in the kernel regime [JGH18], the implicit bias of GD relates to properties of the limiting neural tangent kernel (NTK) [XLS16, ADH⁺19, BM19]. We also note that the implicit bias of GD is not always explained by the minimum norm property [RC20].

Asymptotics of Interpolating Estimators. In Section 3 we analyze overparameterized estimators that interpolate the training data. Recent works have shown that interpolation may not lead to overfitting [LR18, BRT18, BHM18, BLLT19], and the optimal risk may be achieved under no regularization and extreme

overparameterization [BHMM18, XH19]. The asymptotic risk of overparameterized models has been characterized in various settings, such as linear regression [Kar13, DW+18, HMRT19], random features regression [MM19, dRBK20, GLK+20], max-margin classification [MRSY19, DKT19], and certain neural networks [LLC+18, BES+20]. Our analysis is based on results in random matrix theory developed in [RM11, LP11]. Similar tools can also be used to study the gradient descent dynamics of linear regression [LC18, AKT19].

Analysis of Preconditioned Gradient Descent. While [WRS+17] outlined an example of fixed training set where GD generalizes better than adaptive methods, in the online learning setting, for which optimization speed directly relates to generalization, several works have shown the advantage of preconditioned updates [DHS11, LD19, ZLN+19]. In addition, global convergence and generalization guarantees have been derived for the sample Fisher-based update in overparameterized neural networks [ZMG19, CGH+19], in which case the preconditioned update achieves comparable generalization as GD. Lastly, the generalization of different optimizers often connects to the “sharpness” of the solution [KMN+16, DPBB17], and it has been argued that second-order updates tend to find sharper minima [WMM18].

3 Asymptotic Risk of Ridgeless Interpolants

We consider a student-teacher setup, in which labels are generated by a teacher model (target function) $f^*: \mathbb{R}^d \rightarrow \mathbb{R}$ with additive noise $y_i = f^*(\mathbf{x}_i) + \varepsilon_i$, and we learn a linear student f_θ that minimizes the squared loss: $L(\mathbf{X}, f) = \frac{1}{2n} \sum_{i=1}^n (y_i - \mathbf{x}_i^\top \theta)^2$, where $\mathbf{x}_i = \Sigma_{\mathbf{X}}^{1/2} \mathbf{z}_i$, \mathbf{z}_i is an i.i.d. random vector with zero-mean, unit-variance, and finite 12th moment, and ε is i.i.d. noise independent to \mathbf{z} with mean 0 and variance σ^2 . To compute the population risk $R(f) = \mathbb{E}_{P_{\mathbf{X}}} [(f^*(\mathbf{x}) - f(\mathbf{x}))^2]$, we work under the following assumptions:

- **(A1) Proportional Asymptotics:** $n, d \rightarrow \infty$, $d/n \rightarrow \gamma \in (1, \infty)$.
- **(A2) Converging Eigenvalues:** $c_l \mathbf{I}_d \preceq \Sigma_{\mathbf{X}} \preceq c_u \mathbf{I}_d$ for some $c_l, c_u > 0$ independent of d ; denote $\kappa_{\mathbf{X}} = c_u/c_l \in (0, \infty)$. The spectral measure of $\Sigma_{\mathbf{X}}$ converges weakly to the limiting $F_{\Sigma_{\mathbf{X}}}$.

(A1) entails that the number of features (or trainable parameters) is larger than the number of samples. In this overparameterized setting, the population risk is equivalent to the generalization error, and there exist multiple empirical risk minimizers with potentially different generalization properties.

Denote $\mathbf{X} = [\mathbf{x}_1^\top, \dots, \mathbf{x}_n^\top]^\top \in \mathbb{R}^{n \times d}$ the matrix of training data and $\mathbf{y} \in \mathbb{R}^n$ the corresponding label vector. We optimize the parameters θ via a preconditioned gradient flow with preconditioner $\mathbf{P}(t) \in \mathbb{R}^{d \times d}$,

$$\frac{\partial \theta(t)}{\partial t} = -\mathbf{P}(t) \frac{\partial L(\theta(t))}{\partial \theta(t)} = \frac{1}{n} \mathbf{P}(t) \mathbf{X}^\top (\mathbf{y} - \mathbf{X} \theta(t)), \quad \theta(0) = 0.$$

As previously mentioned, in this linear setup, many common choices of preconditioner do not change through time: under Gaussian likelihood, the sample Fisher (and also Hessian) corresponds to the sample covariance $\mathbf{X}^\top \mathbf{X}/n$ up to variance scaling, whereas the population Fisher corresponds to the population covariance $\mathbf{F} = \Sigma_{\mathbf{X}}$. We thus limit our analysis to fixed preconditioner of the form $\mathbf{P}(t) =: \mathbf{P}$.

Denote parameters at time t under preconditioned gradient update with fixed \mathbf{P} as $\theta_{\mathbf{P}}(t)$. For positive definite \mathbf{P} , the gradient flow trajectory from zero initialization is given as

$$\theta_{\mathbf{P}}(t) = \mathbf{P} \mathbf{X}^\top \left[\mathbf{I}_n - \exp\left(-\frac{t}{n} \mathbf{X} \mathbf{P} \mathbf{X}^\top\right) \right] (\mathbf{X} \mathbf{P} \mathbf{X}^\top)^{-1} \mathbf{y},$$

The stationary solution is obtained by taking the large t limit, which we denote as: $\hat{\theta}_{\mathbf{P}} := \lim_{t \rightarrow \infty} \theta_{\mathbf{P}}(t) = \mathbf{P} \mathbf{X}^\top (\mathbf{X} \mathbf{P} \mathbf{X}^\top)^{-1} \mathbf{y}$. It is straightforward to check that the discrete time gradient descent update (with appropriately chosen step size) and other variants that do not alter the span of the gradient (e.g. stochastic gradient or momentum update) converge to this stationary solution as well.

Remark. For positive definite \mathbf{P} , the estimator $\hat{\theta}_{\mathbf{P}}$ is the minimum $\|\theta\|_{\mathbf{P}^{-1}}$ norm interpolant: $\hat{\theta}_{\mathbf{P}} = \arg \min_{\theta} \|\theta\|_{\mathbf{P}^{-1}}$, s.t. $\mathbf{X} \theta = \mathbf{y}$. For GD this translates to the ℓ_2 norm of the parameters, whereas for NGD ($\mathbf{P} = \mathbf{F}^{-1} = \Sigma_{\mathbf{X}}^{-1}$), the implicit bias is the $\|\theta\|_{\mathbf{F}}$ norm. Since $\mathbb{E}_{P_{\mathbf{X}}} [f(\mathbf{x})^2] = \|\theta\|_{\Sigma_{\mathbf{X}}}^2$, NGD finds an interpolating function with smallest norm under the data distribution (from zero initialization). We empirically observe this divide between small parameter norm and function norm in neural networks as well (see Appendix A).

We highlight the following choices of preconditioners and the corresponding stationary estimator $\hat{\theta}_{\mathbf{P}}$ as $t \rightarrow \infty$.

- **Identity:** $\mathbf{P} = \mathbf{I}_d$ recovers GD that converges to the minimum ℓ_2 norm interpolant (also true for momentum GD and SGD), which we write as $\hat{\theta}_{\mathbf{I}} := \mathbf{X}^\top (\mathbf{X}\mathbf{X}^\top)^{-1} \mathbf{y}$ and refer to as the *GD solution*.
- **Population Fisher:** $\mathbf{P} = \mathbf{F}^{-1} = \Sigma_{\mathbf{X}}^{-1}$, i.e. preconditioning with the inverse *population Fisher*, leads to the estimator $\hat{\theta}_{\mathbf{F}^{-1}}$, which is referred to as the *NGD solution*.
- **Variants of Sample Fisher:** since the sample Fisher is rank-deficient, we may add a damping term to ensure invertibility $\mathbf{P} = (\mathbf{X}^\top \mathbf{X} + \lambda \mathbf{I}_d)^{-1}$ or take the pseudo-inverse $\mathbf{P} = (\mathbf{X}^\top \mathbf{X})^\dagger$. In both cases, the gradient is still spanned by the rows of \mathbf{X} , and thus the preconditioned update also ends up at the unique minimum-norm solution $\hat{\theta}_{\mathbf{I}}$, although the trajectory differs, as shown in Figure 2.

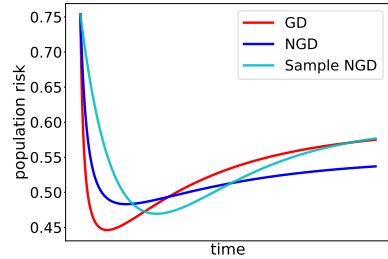


Figure 2: Population risk of preconditioned linear regression vs. time with the following \mathbf{P} : \mathbf{I} (red), $\Sigma_{\mathbf{X}}^{-1}$ (blue) and $(\mathbf{X}^\top \mathbf{X})^\dagger$ (cyan). Time is rescaled differently for each curve (convergence speed is not comparable). Note that GD and sample NGD give the same stationary risk.

Remark. The above choices illustrate the gap between sample-based and population-based preconditioners: while the sample Fisher accelerates optimization [ZMG19, CGH⁺19], the following sections demonstrate generalization properties of the population Fisher that the sample Fisher does not possess.

We compare the population risk of the GD solution $\hat{\theta}_{\mathbf{I}}$ and the NGD solution $\hat{\theta}_{\mathbf{F}^{-1}}$ in its bias-variance decomposition w.r.t. the label noise, and discuss the two components separately:

$$R(\theta) = \underbrace{\mathbb{E}_{P_{\mathbf{X}}}[(f^*(\mathbf{x}) - \mathbf{x}^\top \mathbb{E}_{P_{\epsilon}}[\theta])^2]}_{B(\theta), \text{ bias}} + \underbrace{\text{tr}(\text{Cov}(\theta)\Sigma_{\mathbf{X}})}_{V(\theta), \text{ variance}}.$$

3.1 The Variance Term: NGD is Optimal

We first characterize the variance term which depends on the label noise but not the teacher model f^* . We restrict ourselves to preconditioners satisfying (A2) and the additional assumption²:

- **(A3) Codiagonalizability:** $\Sigma_{\mathbf{X}}$ and \mathbf{P} can be decomposed as $\Sigma_{\mathbf{X}} = \mathbf{U}\mathbf{D}_{\mathbf{X}}\mathbf{U}^\top$, $\mathbf{P} = \mathbf{U}\mathbf{D}_{\mathbf{P}}\mathbf{U}^\top$ for orthogonal matrix \mathbf{U} and diagonal matrices $\mathbf{D}_{\mathbf{X}}$, $\mathbf{D}_{\mathbf{P}}$.

Although (A3) does not cover all possible preconditioners, it still allows us to analyze many common choices of \mathbf{P} , such as the inverse population Fisher, and the pseudo-inverse or ridge-regularized inverse of the sample Fisher³. We compute the asymptotic variance and decide the corresponding optimal preconditioner.

Theorem 1. Given \mathbf{P} satisfying (A3) and $\mathbf{X}\mathbf{P}$ satisfying the same condition as $\Sigma_{\mathbf{X}}$ in (A2),

$$V(\hat{\theta}_{\mathbf{P}}) \rightarrow \sigma^2 \left(\lim_{\lambda \rightarrow 0^+} \frac{m'(-\lambda)}{m^2(-\lambda)} - 1 \right), \quad (3.1)$$

as $n, d \rightarrow \infty$, where $m(z) > 0$ is the Stieltjes transform of the limiting distribution of eigenvalues of $\frac{1}{n} \mathbf{X}\mathbf{P}\mathbf{X}^\top$ (for z beyond its support) defined as the solution to $m^{-1}(z) = -z + \gamma \int \tau(1 + \tau m(z))^{-1} dF_{\mathbf{X}\mathbf{P}}(\tau)$, where $F_{\mathbf{X}\mathbf{P}}$ denotes the limiting spectral measure of $\mathbf{D}_{\mathbf{X}}\mathbf{D}_{\mathbf{P}}$.

Furthermore, $V(\hat{\theta}_{\mathbf{P}}) \geq \sigma^2(\gamma - 1)^{-1}$, and the equality is obtained by $\hat{\theta}_{\mathbf{F}^{-1}}$, i.e. when $\mathbf{P} = \Sigma_{\mathbf{X}}^{-1}$.

Formula (3.1) is a direct extension of [HMRT19, Thorem 4], which can be obtained from [DW⁺18, Thorem 2.1] or the general result of [LP11, Thorem 1.2]. Theorem 1 implies that preconditioning with the inverse population Fisher results in the optimal stationary variance, which is supported by Figure 3(a). In other words, when the labels contain large amount of noise, i.e. the generalization error is dominated by the variance term, we expect NGD to generalize better upon convergence. We emphasize that this advantage is only present when the population Fisher is used, but not the sample-based counterpart.

²This assumption is not required by [RM11] but we included it for simple and interpretable result.

³Variants of the sample Fisher do not satisfy (A3), yet from the previous discussion we know that preconditioned update with $\mathbf{P} = (\mathbf{X}^\top \mathbf{X})^\dagger$ or $(\mathbf{X}^\top \mathbf{X} + \lambda \mathbf{I}_d)^{-1}$ also converges to the min-norm solution $\hat{\theta}_{\mathbf{I}}$.

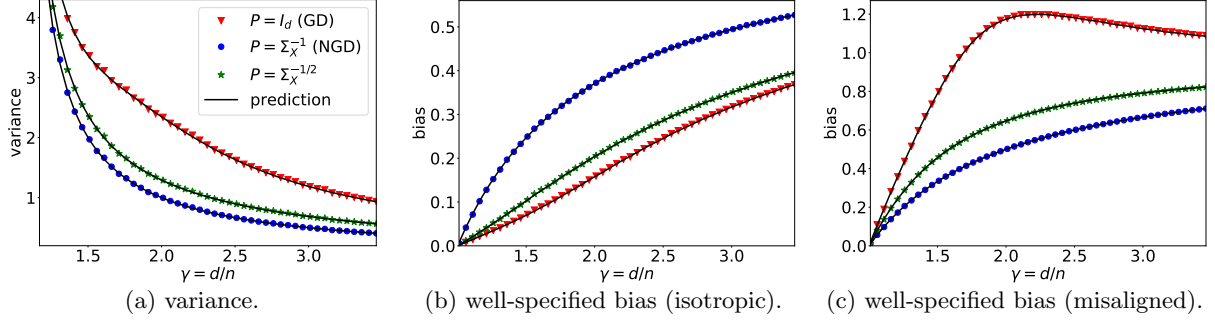


Figure 3: We set \mathbf{D}_X as two equally-weighted point masses with $\kappa_X = 20$ and $\|\mathbf{D}_X\|_F^2 = d$; empirical values (dots) are computed with $n = 300$. (a) NGD (blue) achieves minimum variance. (b) GD (red) achieves lower bias under isotropic signal: $\Sigma_\theta = \mathbf{I}_d$. (c) NGD achieves lower bias under “misalignment”: $\Sigma_X = \Sigma_\theta^{-1}$.

3.2 The Bias Term: Well-specified Case

We now consider the bias term when the teacher is also linear and well-specified, i.e. $y_i = \mathbf{x}_i^\top \boldsymbol{\theta}^*$. We assume a random effects model that is more general than that in [DW⁺18] and place the following prior on $\boldsymbol{\theta}^*$ ⁴:

- **(A4) Anisotropic Prior:** $\mathbb{E}[\boldsymbol{\theta}^*] = 0$, $\text{Cov}(\boldsymbol{\theta}^*) = d^{-1} \Sigma_\theta$. Σ_θ satisfies (A2-3). The empirical distributions of diagonal elements of \mathbf{D}_X , \mathbf{D}_θ , and $\mathbf{D}_{X\mathbf{P}}$ jointly converge to non-negative random variables (v_x, v_θ, v_{xp}) .

When $\mathbf{P} = \mathbf{I}_d$, previous works have considered the special case of the isotropic prior $\Sigma_\theta = d^{-1} \mathbf{I}_d$ [DW⁺18, XH19]. We note that our more general prior assumption gives rise to many interesting phenomena that are not captured by simplified settings, such as the non-monotonicity of the bias and variance for $\gamma > 1$ (see Figure 12), and the epoch-wise double descent (see Appendix A for discussion). Under our general setup, the asymptotic bias and the optimal \mathbf{P} can be characterize as follow:

Theorem 2. Under (A1-4), the expected bias $B(\hat{\boldsymbol{\theta}}_{\mathbf{P}}) := \mathbb{E}_{\boldsymbol{\theta}^*}[B(\hat{\boldsymbol{\theta}}_{\mathbf{P}})]$ is given as

$$B(\hat{\boldsymbol{\theta}}_{\mathbf{P}}) \rightarrow \lim_{\lambda \rightarrow 0^+} \frac{m'(-\lambda)}{m^2(-\lambda)} \mathbb{E} \left[\frac{v_x v_\theta}{(1 + v_{xp} m(-\lambda))^2} \right],$$

where expectation is taken over v and $m(z)$ is the Stieltjes transform defined in Theorem 1.

Furthermore, we have $B(\hat{\boldsymbol{\theta}}_{\mathbf{P}}) \geq \lim_{\lambda \rightarrow 0^+} [\gamma^{-1} m^{-1}(-\lambda)]$; the equality is obtained when $\mathbf{P} = \Sigma_\theta$.

Note that the optimal preconditioner does not depend on the data covariance Σ_X , but only on the orientation of the teacher Σ_θ , which is usually not known in practice. This result can thus be interpreted as a *no-free-lunch* characterization on choosing an optimal preconditioner (for the bias term) *a priori*. As a consequence of the theorem, when parameters of the teacher model have roughly equal magnitude (isotropic), GD achieves lower bias (see Figure 3(b) where $\Sigma_\theta = \mathbf{I}_d$). On the other hand, when Σ_X is “misaligned” with Σ_θ , i.e. when the most varying directions of the features \mathbf{X} contain little information about the signal $\boldsymbol{\theta}^*$ (see Figure 3(c) where $\Sigma_\theta = \Sigma_X^{-1}$), in which case the teacher is difficult to learn, then NGD results in lower bias. This is in contrast to the variance term, for which the NGD solution $\hat{\boldsymbol{\theta}}_{\mathbf{F}^{-1}}$ always dominates.

3.3 Misspecification \approx Label Noise

Under model misspecification, there does not exist a predictor $\boldsymbol{\theta} \in \mathbb{R}^d$ s.t. $B(\boldsymbol{\theta}) = 0$. In this case, we may decompose the teacher into a well-specified component and its residual: $f^*(\mathbf{x}) = \mathbf{x}^\top \boldsymbol{\theta}^* + f_c^*(\mathbf{x})$.

For simplicity, we first consider the residual to be a linear function of unobserved features (from [HMRT19, Section 5]). Formally, the label is generated as $y_i = \mathbf{x}_i^\top \boldsymbol{\theta}^* + \mathbf{x}_{c,i}^\top \boldsymbol{\theta}^c + \varepsilon_i$, where $\mathbf{x}_{c,i} \in \mathbb{R}^{d_c}$ are unobserved features independent on \mathbf{x}_i . Similar to the previous calculation, we assume \mathbf{x}_c has mean zero and covariance Σ_X^c and place the prior $\mathbb{E}[\boldsymbol{\theta}^c] = 0$, $\text{Cov}(\boldsymbol{\theta}^c) = d_c^{-1} \Sigma_\theta^c$, where Σ_X^c , Σ_θ^c satisfy (A2-3). The following proposition shows that in this setting the misspecification bias is the same as a scaled variance:

⁴We remark that the zero-mean assumption can be relaxed in the risk computation (see [WX20]).

Proposition 3. *Under model misspecification with unobserved features described above, the bias term can be decomposed as $B(\hat{\theta}) = B_{\theta}(\hat{\theta}_{\mathbf{P}}) + B_c(\hat{\theta}_{\mathbf{P}})$, where B_{θ} is the well-specified bias defined in Theorem 2, and $B_c = d_c^{-1} \text{tr}(\Sigma_{\mathbf{X}}^c \Sigma_{\theta}^c) (V(\hat{\theta}_{\mathbf{P}}) + 1)$, where $V(\hat{\theta}_{\mathbf{P}})$ is the variance given by Theorem 1.*

Model misspecification can thus be interpreted as additional label noise (also noted in [HMRT19, Thorem 4]). Therefore, Theorem 1 suggests that NGD is advantageous under misspecification. While Proposition 3 describes one specific example of misspecification, we expect such characterization to hold under broader settings. In particular, [MM19, Remark 5] indicates that for many nonlinear f_c^* , the misspecified bias is the same as variance caused by label noise. This result is only rigorously shown for isotropic data, but we empirically verify the same phenomenon under general covariances in Figure 1: we take $\Sigma_{\theta} = \mathbf{I}_d$ (favors GD) and f_c^* as a quadratic function: $f_c^*(\mathbf{x}) = \alpha((\mathbf{x}, \mathbf{x}) - \text{tr}(\Sigma_{\mathbf{X}}))$ (note that α controls the extent of nonlinearity). Predictions are generated by adding the same level of noise as the second moment of f_c^* . Observe that NGD leads to lower bias as we further misspecify the model by increasing α (nonlinearity of the teacher).

4 Bias-variance Tradeoff

Our characterization of the stationary risk suggests that preconditioners that achieve the optimal bias and variance are in general different (except when $\Sigma_{\mathbf{X}} = \Sigma_{\theta}^{-1}$). This section discusses how the bias-variance tradeoff can be realized by interpolating between preconditioners or by early stopping. Additionally, we analyze regression in the RKHS and show that by balancing the bias and variance, a preconditioned update that interpolates between GD and NGD also decreases the population risk faster than GD.

4.1 Interpolating between Preconditioners

Depending on the “shape” of the teacher model, we may expect a bias-variance tradeoff in choosing \mathbf{P} . Intuitively, given \mathbf{P}_1 that minimizes the bias and \mathbf{P}_2 that minimizes the variance, it is possible that a preconditioner interpolating between \mathbf{P}_1 and \mathbf{P}_2 could balance the bias and variance and thus generalize better. In the following proposition, we confirm this intuition in a setup of general data covariance and isotropic prior on the teacher⁵, for which GD ($\mathbf{P} = \mathbf{I}_d$) achieves optimal stationary bias and NGD ($\mathbf{P} = \mathbf{F}^{-1}$) achieves optimal stationary variance.

Proposition 4 (Informal). *Let $\Sigma_{\mathbf{X}} \neq \mathbf{I}_d$ and $\Sigma_{\theta} = \mathbf{I}_d$. Consider the following three interpolating preconditioners (under appropriate scaling of $\Sigma_{\mathbf{X}}$): (i) $\mathbf{P}_{\alpha} = \alpha \Sigma_{\mathbf{X}}^{-1} + (1 - \alpha) \mathbf{I}_d$, (ii) $\mathbf{P}_{\alpha} = (\alpha \Sigma_{\mathbf{X}} + (1 - \alpha) \mathbf{I}_d)^{-1}$, (iii) $\mathbf{P}_{\alpha} = \Sigma_{\mathbf{X}}^{-\alpha}$. The stationary variance monotonically decreases with $\alpha \in [0, 1]$ for all three choices. For (i), the stationary bias monotonically increases with $\alpha \in [0, 1]$, whereas for (ii) and (iii), the bias monotonically increases with α in a range that depends on $\Sigma_{\mathbf{X}}$.*

This proposition indicates that as the signal-to-noise ratio (SNR) decreases (i.e. more label noise or analogously, a more misspecified model), one can increase α , which makes the update closer to NGD, to improve generalization, and vice versa⁶ (small α entails GD-like update). This observation is supported by Figure 4 and 15(c), which illustrate that for a given SNR, a preconditioner that interpolates between $\Sigma_{\mathbf{X}}^{-1}$ and Σ_{θ} can achieve lower stationary risk than both GD and NGD.

Remark. *Two of the aforementioned interpolation schemes summarize choices often made in practice: The additive interpolation (ii) corresponds to damping added to the Fisher to stably compute the inverse, while the geometric interpolation (iii) includes the “conservative” square-root scaling in adaptive gradient methods such as Adagrad [DHS11] and Adam [KB14].*

⁵Note that this setup reduces to the random effects model studied in [DW+18, XH19].

⁶While Proposition 4 does not show the monotonicity of the bias of (ii)(iii) for all $\Sigma_{\mathbf{X}}$ and $\alpha \in [0, 1]$, in Appendix C.5 we empirically verify that the bias is monotone over $\alpha \in [0, 1]$ for a wide range of distributions beyond the proposition.

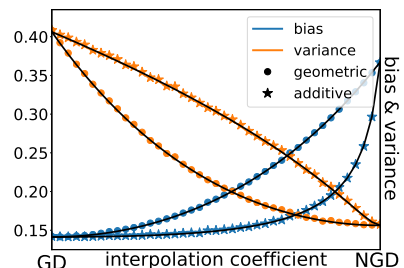


Figure 4: illustration of the bias-variance tradeoff with $\kappa_{\mathbf{X}} = 25$, $\Sigma_{\theta} = \mathbf{I}_d$ and $\text{SNR} = 32/5$. As we additively or geometrically interpolate from GD to NGD (left to right), the stationary bias (blue) increases and the stationary variance (orange) decreases.

4.2 The Role of Early Stopping

Previously, we considered the stationary solution of the unregularized objective. It is known that the bias-variance tradeoff can also be controlled by either explicit or algorithmic regularization. We briefly comment on the effect of early stopping, starting from the monotonicity of the variance term.

Proposition 5. *For all \mathbf{P} satisfying (A2-3), the variance $V(\boldsymbol{\theta}_{\mathbf{P}}(t))$ monotonically increases with time t .*

The proposition confirms the intuition that early stopping reduces overfitting to label noise. Variance reduction can be beneficial to GD in its comparison with NGD, which achieves the lowest stationary variance (this also holds for the misspecified bias, which is analogous to the variance). Indeed, Figure 2 and 14 show that GD may have better early stopping risk even when NGD has the advantage on the stationary risk.

On the other hand, early stopping may not always improve the bias in the well-specified case. While we do not give a full characterization due to the difficulty in handling the potentially non-monotonic bias term (see Appendix A), we speculate that previous observations on the stationary bias also translate to early stopping. To give a concrete example, we consider well-specified settings in which GD or NGD achieves the optimal stationary bias, and demonstrate that such optimality is also preserved under early stopping.

Proposition 6. *Denote the optimal early stopping bias as $B^{\text{opt}}(\boldsymbol{\theta}) = \inf_{t \geq 0} B(\boldsymbol{\theta}(t))$. Then for all \mathbf{P} satisfying (A2-3), when $\boldsymbol{\Sigma}_{\boldsymbol{\theta}} = \boldsymbol{\Sigma}_{\mathbf{X}}^{-1}$, $B^{\text{opt}}(\boldsymbol{\theta}_{\mathbf{P}}) \geq B^{\text{opt}}(\boldsymbol{\theta}_{\mathbf{F}-1})$. Whereas when $\boldsymbol{\Sigma}_{\boldsymbol{\theta}} = \mathbf{I}_d$, $B^{\text{opt}}(\boldsymbol{\theta}_{\mathbf{I}}) \leq B^{\text{opt}}(\boldsymbol{\theta}_{\mathbf{F}-1})$.*

Figure 14 illustrates that the observed trend in the stationary bias (well-specified) is indeed preserved in early stopping: GD or NGD achieves lower early stopping bias under isotropic or misaligned teacher model, respectively. We leave the precise characterization of this observation as future work.

4.3 Fast Decay of Population Risk

Our previous analysis suggests that certain preconditioners can achieve lower population risk (generalization error), but does not compare which method decreases the risk more efficiently. Knowing that preconditioned updates often accelerates optimization, one natural question to ask is, is this speedup also present for the population risk under fixed dataset? We answer this question in the affirmative in a slightly different model: we study least squares regression in the RKHS, and show that a preconditioned gradient update that interpolates between GD and NGD can achieve the minimax optimal rate in much fewer iterations than GD.

We defer the details to Appendix C and briefly outline the setup here. Let \mathcal{H} be an RKHS included in $L_2(P_X)$ equipped with a bounded kernel function k , and $K_{\mathbf{x}} \in \mathcal{H}$ be the Riesz representation of the kernel function. Define an operator S as the canonical embedding from \mathcal{H} to $L_2(P_X)$, and write $\Sigma = S^*S$ and $L = SS^*$. We consider a student-teacher setup with teacher model f^* and make the following assumptions:

- **(A5):** There exist $r \in (0, \infty)$ and $M > 0$ such that $f^* = L^r h^*$ for some $h^* \in L_2(P_X)$ and $\|f^*\|_{\infty} \leq M$.
- **(A6):** There exists $s > 1$ such that $\text{tr}(\Sigma^{1/s}) < \infty$ and $2r + s^{-1} > 1$.
- **(A7):** There exist $\mu \in [s^{-1}, 1]$ and $C_{\mu} > 0$ such that $\sup_{\mathbf{x} \in \text{supp}(P_X)} \|\Sigma^{1/2-1/\mu} K_{\mathbf{x}}\|_{\mathcal{H}} \leq C_{\mu}$.

The coefficient r in (A5) controls the complexity of the teacher model and relates to the notions of model misalignment and misspecification discussed in Section 3. In particular, large r indicates a smoother teacher model which is “easier” to learn, and vice versa. We remark that previous works mostly consider $r \geq 1/2$ which implies $f^* \in \mathcal{H}$. On the other hand, (A6)(A7) are common assumptions that control the capacity and the regularity of the RKHS [CDV07, PVRB18]. Given n training points $\{(\mathbf{x}_i, y_i)\}_{i=1}^n$, we consider the following preconditioned update on the student model $f_t \in \mathcal{H}$:

$$f_t = f_{t-1} - \eta(\Sigma + \alpha I)^{-1}(\hat{\Sigma} f_{t-1} - \hat{S}^* Y), \quad f_0 = 0, \quad (4.1)$$

where $\hat{\Sigma} = \frac{1}{n} \sum_{i=1}^n K_{\mathbf{x}_i} \otimes K_{\mathbf{x}_i}$ and $\hat{S}^* Y = \frac{1}{n} \sum_{i=1}^n y_i K_{\mathbf{x}_i}$. In this setup, the population Fisher corresponds to the covariance operator Σ , and thus (4.1) can be interpreted as additive interpolation between GD and NGD (discussed in Section 4.1): we expect update with large α to behave like GD, and small α like NGD. The following theorem shows that with appropriate damping α , preconditioning can lead to more efficient decrease in the population risk, due to the faster bias decay (similar to the role of momentum in [PR19]).

Theorem 7 (Informal). Under (A5-7) and sufficiently large n , the population risk of f_t can be written as $R(f_t) = \|Sf_t - f^*\|_{L_2(P_X)}^2 \leq B(t) + V(t)$, where $B(t)$ and $V(t)$ are defined in Appendix C. Given $r \geq 1/2$ or $\mu \leq 2r$, the preconditioned update (4.1) with $\alpha = n^{-\frac{2s}{2rs+1}}$ achieves the minimax optimal convergence rate $R(f_t) = \tilde{O}\left(n^{-\frac{2rs}{2rs+1}}\right)$ in $t = \Theta(\log n)$ steps, whereas ordinary gradient descent requires $t = \Theta\left(n^{\frac{2rs}{2rs+1}}\right)$ steps.

We remark that the optimal interpolation coefficient α and stopping time t are chosen to balance the bias $B(t)$ and variance $V(t)$. Note that α depends on the teacher model in the following way: for $n > 1$, α decreases as r becomes smaller, which corresponds to non-smooth and “difficult” teacher, and vice versa. This agrees with our previous observation that NGD is advantageous when the teacher is difficult to learn (either misaligned or misspecified). We defer empirical verification of this result to Appendix B.

5 Neural Network Experiments

5.1 Protocol

We compare the generalization performance of GD and NGD in neural network settings and illustrate the influence of the following factors: (i) label noise; (ii) model misspecification; (iii) signal misalignment. We also demonstrate that interpolating between GD and NGD can be advantageous due to bias-variance tradeoff.

We consider the MNIST and CIFAR10 [KH⁺09] datasets. To create a student-teacher setup, we split the original training set into two equal halves, one of which along with the original labels is used to pretrain the teacher, and the other along with the teacher’s labels is used to distill [HVD15, BCNM06] the student. We refer to the splits as the *pretrain* and *distill* split, respectively. In all scenarios, the teacher is either a two-layer fully-connected ReLU network [NH10] or a ResNet [HZRS16]; whereas the student model is a two-layer ReLU net. We normalize the teacher’s labels (logits) following [BC14] before potentially adding label noise and fit the student model by minimizing the L2 loss. Student models are trained on a subset of the distill split with full-batch updates. We implement NGD using Hessian-free optimization [Mar10]. To estimate the population Fisher, we use 100k training data obtained by possibly applying data augmentation. We report the test error when the training error is below 0.2% of the training error at initialization as a proxy for the stationary risk. We defer detailed setup to Appendix D and additional results to Appendix B.

5.2 Empirical Findings

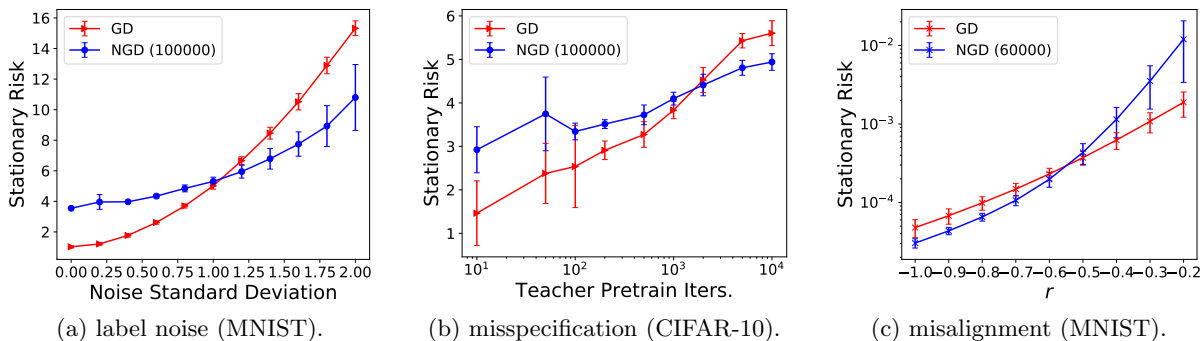


Figure 5: Comparison between NGD and GD. Error bar is one standard deviation away from mean over five independent runs. Numbers in parentheses denote amount of unlabeled examples for estimating the Fisher.

Label Noise. We pretrain the teacher with the full pretrain split and use 1024 examples from the distill split to fit the student. For both the student and teacher, we use a two-layer ReLU net with 80 hidden units. We corrupt the labels with isotropic Gaussian noise whose standard deviation we vary. Figure 5(a) shows that as the noise increases (variance begins to dominate), the stationary risk of both NGD and GD worsen, with GD worsening faster, which aligns with our observation in Figure 3.

Misspecification. We use ResNet-20 [HZRS16] for the teacher and the same two-layer student from the label noise experiment. To vary the misspecification, we take teacher models with the same initialization but varying amount of pretraining. Intuitively, large teacher models that are trained more should be more complex and thus more likely to be outside of functions that a small two-layer student can represent (therefore the problem is more misspecified). Indeed, Figure 5(b) shows that NGD eventually achieves better generalization as the number of training steps for the teacher increases. As a heuristic measure of misspecification, in Figure 6 we report $\sqrt{\mathbf{y}^\top \mathbf{K}^{-1} \mathbf{y} / n}$ studied in [ADH⁺19], in which \mathbf{y} is the label vector and \mathbf{K} is the student’s NTK matrix [JGH18]. We observe that the quantity is increasing as more label noise is added or as the teacher is trained longer. In Appendix A we provide a non-rigorous interpretation of how this quantity relates to label noise and misspecification.

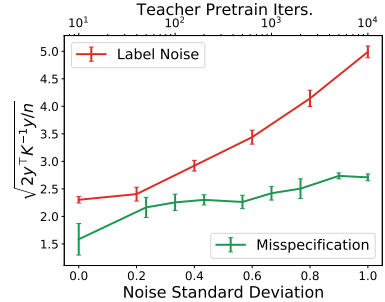
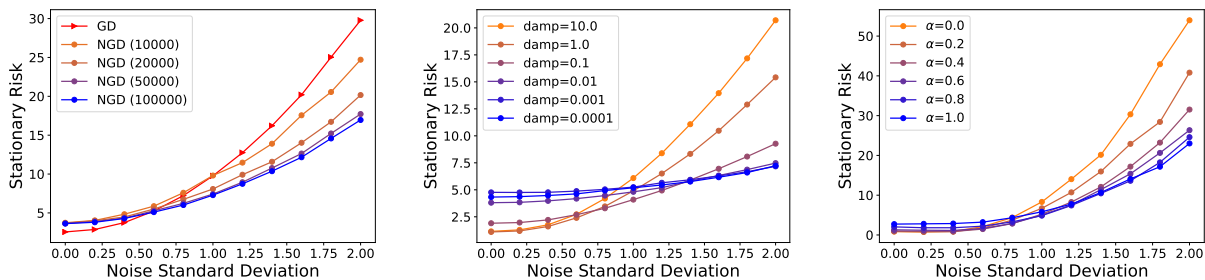


Figure 6: A heuristic measure of misspecification and label noise.

Misalignment. We use the same two-layer ReLU net (60 neurons) for the student and teacher (thus the setting is intuitively well-specified). We construct the teacher model by perturbing the student’s initialization, the direction of which is given by \mathbf{F}^r , where \mathbf{F} is the student’s Fisher (estimated using extra unlabeled data) and $r \in [-1, 0]$. Intuitively, as r approaches -1 , the “important” parameters of the teacher (i.e. larger update directions) lie in the small eigendirections of the student’s Hessian, and we therefore interpret the problem to be more misaligned, and vice versa. While this analogy is rather superficial due to the non-convex nature of neural network optimization, Figure 5(c) shows that as r becomes smaller (setup is more misaligned), NGD begins to generalize better than GD in terms of stationary risk.

Interpolating between Preconditioners. We also validate our observations in Section 3 and 4 on the difference between the sample Fisher and population Fisher, and the potential benefit of interpolating between GD and NGD, in neural network experiments. Figure 7(a) shows that as we decrease the number of unlabeled data in estimating the Fisher, which renders the preconditioner closer to the sample Fisher, the stationary risk becomes more akin to that of GD, especially in the large noise setting. This agrees with our remark on sample vs. population Fisher in Section 3 and Appendix A.

Figure 7(b)(c) confirms the finding in Section 4.1 that interpolating preconditioners provides bias-variance tradeoff also holds in neural network settings. In particular, we interpret the left end to correspond to a bias-dominant regime (due to the same architecture of two-layer MLP for the student and teacher), and the right end to correspond to the variance-dominant regime (due to the added label noise). Observe that at a certain SNR, a preconditioner that interpolates between GD and NGD achieves lower stationary risk.



(a) interpolation between sample and population Fisher (CIFAR-10). (b) additive interpolation between GD and NGD (MNIST). (c) geometric interpolation between GD and NGD (MNIST).

Figure 7: (a) numbers in parentheses indicate the amount of unlabeled data used in estimating the Fisher \mathbf{F} ; we expect the estimated Fisher to be closer to the sample Fisher when the number of unlabeled data is small. (a) additive interpolation $\mathbf{P} = (\mathbf{F} + \alpha \mathbf{I}_d)^{-1}$; larger damping parameter yields update closer to GD. (b) geometric interpolation $\mathbf{P} = \mathbf{F}^{-\alpha}$; larger α parameter yields update closer to that of NGD (blue). We use the singular value decomposition to compute the minus α power of the Fisher, as CG is not applicable in this scenario.

6 Discussion and Conclusion

We analyzed the generalization properties of a general class of preconditioned gradient descent under the squared loss, with particular emphasis on natural gradient descent. We identified three factors that affect the relative generalization performance of different optimizers, the influence of which we also empirically observed in neural network experiments⁷. We additionally determined the corresponding optimal preconditioner for each of the factors. While the optimal preconditioner is usually not known in practice, we provided justification for common algorithmic choices by discussing the bias-variance tradeoff. We remark that our least squares regression setup deals with a fixed preconditioner and thus does not cover many adaptive gradient methods; an interesting problem is to characterize the solution that these optimizers converge to in similar setting. In addition, beyond the analysis of this work, there are many other ingredients that influence the generalization performance of optimizers, such as different loss functions [TPT20, MNS+20], and explicit (e.g. weight decay⁸) or implicit regularization (e.g. learning rate and gradient noise); understanding their impact in the overparameterized regime would be a fruitful future direction.

It is worth noting that our optimal preconditioner requires knowledge on the population second-order statistics, which we empirically approximate using extra unlabeled data. Consequently, our characterization suggests that different “types” (sample vs. population) of second-order information may affect generalization differently. Broadly speaking, there are two types of practical approximate second-order optimizers for neural networks. Some algorithms, such as Hessian-free optimization [Mar10, MS12, DPCB13], approximate second-order matrices (typically the Hessian or Fisher) using the exact matrix on finite training examples. In high-dimensional problems, this sample-based approximation may be very different from the population quantity (e.g. it is necessarily degenerate in the overparameterized regime). Other algorithms fit a parametric approximation to the Fisher, such as diagonal [DHS11, KB14], quasi-diagonal [Oll15], or Kronecker-factored [MG15]. If the parametric assumption is accurate, these approximations are more statistically efficient and thus may lead to better approximation of the population Fisher. Our analysis reveals a separation between sample- and population-based preconditioned updates, which is observed in simple neural network problems as well (see Appendix A). As future work, we intend to investigate whether similar separation is also present for different approximate second-order optimizers in real-world problems.

Acknowledgement

The authors would like to thank Murat A. Erdogdu, Fartash Faghri, Ryo Karakida, Yiping Lu, Jiaxin Shi, Shengyang Sun, Yusuke Tsuzuku, Guodong Zhang, Michael Zhang and Tianzong Zhang for helpful comments and discussions. The authors are also grateful to Tomoya Murata for his contribution to preliminary studies on regression in the RKHS.

JB and RG were supported by the CIFAR AI Chairs program. JB and DW were partially supported by LG Electronics and NSERC. AN was partially supported by JSPS Kakenhi (19K20337) and JST-PRESTO. TS was partially supported by JSPS Kakenhi (26280009, 15H05707 and 18H03201), Japan Digital Design and JST-CREST. JX was supported by a Cheung-Kong Graduate School of Business Fellowship. Resources used in preparing this research were provided, in part, by the Province of Ontario, the Government of Canada through CIFAR, and companies sponsoring the Vector Institute.

⁷We note that observations in the analysis of linear or kernel models do not always translate to neural networks: many recent works have theoretically demonstrated such a gap (e.g. [Suz18, GMMM19, WLLM19, AZL19]).

⁸In a companion work [WX20] we characterize the impact of ℓ_2 regularization in overparameterized models.

References

- [ACHL19] Sanjeev Arora, Nadav Cohen, Wei Hu, and Yuping Luo, *Implicit regularization in deep matrix factorization*, Advances in Neural Information Processing Systems, 2019, pp. 7411–7422.
- [ADH⁺19] Sanjeev Arora, Simon S Du, Wei Hu, Zhiyuan Li, and Ruosong Wang, *Fine-grained analysis of optimization and generalization for overparameterized two-layer neural networks*, arXiv preprint arXiv:1901.08584 (2019).
- [AH18] Navid Azizan and Babak Hassibi, *Stochastic gradient/mirror descent: Minimax optimality and implicit regularization*, arXiv preprint arXiv:1806.00952 (2018).
- [AKT19] Alnur Ali, J Zico Kolter, and Ryan J Tibshirani, *A continuous-time view of early stopping for least squares*, International Conference on Artificial Intelligence and Statistics, vol. 22, 2019.
- [ALH19] Navid Azizan, Sahin Lale, and Babak Hassibi, *Stochastic mirror descent on overparameterized nonlinear models: Convergence, implicit regularization, and generalization*, arXiv preprint arXiv:1906.03830 (2019).
- [Ama97] Shun-ichi Amari, *Neural learning in structured parameter spaces-natural riemannian gradient*, Advances in neural information processing systems, 1997, pp. 127–133.
- [Ama98] Shun-Ichi Amari, *Natural gradient works efficiently in learning*, Neural computation **10** (1998), no. 2, 251–276.
- [APF00] Shun-Ichi Amari, Hyeyoung Park, and Kenji Fukumizu, *Adaptive method of realizing natural gradient learning for multilayer perceptrons*, Neural computation **12** (2000), no. 6, 1399–1409.
- [AZL19] Zeyuan Allen-Zhu and Yuanzhi Li, *What can resnet learn efficiently, going beyond kernels?*, arXiv preprint arXiv:1905.10337 (2019).
- [BBV04] Stephen Boyd, Stephen P Boyd, and Lieven Vandenberghe, *Convex optimization*, Cambridge university press, 2004.
- [BC14] Jimmy Ba and Rich Caruana, *Do deep nets really need to be deep?*, Advances in neural information processing systems, 2014, pp. 2654–2662.
- [BCNM06] Cristian Bucilu, Rich Caruana, and Alexandru Niculescu-Mizil, *Model compression*, Proceedings of ACM SIGKDD international conference on Knowledge discovery and data mining, 2006, pp. 535–541.
- [BES⁺20] Jimmy Ba, Murat A. Erdogdu, Taiji Suzuki, Denny Wu, and Tianzong Zhang, *Generalization of two-layer neural networks: An asymptotic viewpoint*, International Conference on Learning Representations (2020).
- [BHM18] Mikhail Belkin, Daniel J Hsu, and Partha Mitra, *Overfitting or perfect fitting? risk bounds for classification and regression rules that interpolate*, Advances in neural information processing systems, 2018, pp. 2300–2311.
- [BHMM18] Mikhail Belkin, Daniel Hsu, Siyuan Ma, and Soumik Mandal, *Reconciling modern machine learning and the bias-variance trade-off*, arXiv preprint arXiv:1812.11118 (2018).
- [BLLT19] Peter L Bartlett, Philip M Long, Gábor Lugosi, and Alexander Tsigler, *Benign overfitting in linear regression*, arXiv preprint arXiv:1906.11300 (2019).
- [BM19] Alberto Bietti and Julien Mairal, *On the inductive bias of neural tangent kernels*, Advances in Neural Information Processing Systems, 2019, pp. 12873–12884.
- [BRT18] Mikhail Belkin, Alexander Rakhlin, and Alexandre B Tsybakov, *Does data interpolation contradict statistical optimality?*, arXiv preprint arXiv:1806.09471 (2018).
- [CB20] Lenaic Chizat and Francis Bach, *Implicit bias of gradient descent for wide two-layer neural networks trained with the logistic loss*, arXiv preprint arXiv:2002.04486 (2020).
- [CDV07] Andrea Caponnetto and Ernesto De Vito, *Optimal rates for the regularized least-squares algorithm*, Foundations of Computational Mathematics **7** (2007), no. 3, 331–368.

- [CFW⁺19] Yuan Cao, Zhiying Fang, Yue Wu, Ding-Xuan Zhou, and Quanguan Gu, *Towards understanding the spectral bias of deep learning*, arXiv preprint arXiv:1912.01198 (2019).
- [CGH⁺19] Tianle Cai, Ruiqi Gao, Jikai Hou, Siyu Chen, Dong Wang, Di He, Zhihua Zhang, and Liwei Wang, *A gram-gauss-newton method learning overparameterized deep neural networks for regression problems*, arXiv preprint arXiv:1905.11675 (2019).
- [DHLZ19] Bin Dong, Jikai Hou, Yiping Lu, and Zhihua Zhang, *Distillation \approx early stopping? harvesting dark knowledge utilizing anisotropic information retrieval for overparameterized neural network*, arXiv preprint arXiv:1910.01255 (2019).
- [DHS11] John Duchi, Elad Hazan, and Yoram Singer, *Adaptive subgradient methods for online learning and stochastic optimization*, Journal of machine learning research **12** (2011), no. Jul, 2121–2159.
- [DKT19] Zeyu Deng, Abba Kammoun, and Christos Thrampoulidis, *A model of double descent for high-dimensional binary linear classification*, arXiv preprint arXiv:1911.05822 (2019).
- [DPBB17] Laurent Dinh, Razvan Pascanu, Samy Bengio, and Yoshua Bengio, *Sharp minima can generalize for deep nets*, arXiv preprint arXiv:1703.04933 (2017).
- [DPCB13] Guillaume Desjardins, Razvan Pascanu, Aaron Courville, and Yoshua Bengio, *Metric-free natural gradient for joint-training of boltzmann machines*, arXiv preprint arXiv:1301.3545 (2013).
- [dRBK20] Stéphane d’Ascoli, Maria Refinetti, Giulio Biroli, and Florent Krzakala, *Double trouble in double descent: Bias and variance (s) in the lazy regime*, arXiv preprint arXiv:2003.01054 (2020).
- [DW⁺18] Edgar Dobriban, Stefan Wager, et al., *High-dimensional asymptotics of prediction: Ridge regression and classification*, The Annals of Statistics **46** (2018), no. 1, 247–279.
- [GBLJ19] Gauthier Gidel, Francis Bach, and Simon Lacoste-Julien, *Implicit regularization of discrete gradient dynamics in deep linear neural networks*, arXiv preprint arXiv:1904.13262 (2019).
- [GLK⁺20] Federica Gerace, Bruno Loureiro, Florent Krzakala, Marc Mézard, and Lenka Zdeborová, *Generalisation error in learning with random features and the hidden manifold model*, arXiv preprint arXiv:2002.09339 (2020).
- [GLSS18a] Suriya Gunasekar, Jason Lee, Daniel Soudry, and Nathan Srebro, *Characterizing implicit bias in terms of optimization geometry*, arXiv preprint arXiv:1802.08246 (2018).
- [GLSS18b] Suriya Gunasekar, Jason D Lee, Daniel Soudry, and Nati Srebro, *Implicit bias of gradient descent on linear convolutional networks*, Advances in Neural Information Processing Systems, 2018, pp. 9461–9471.
- [GM16] Roger Grosse and James Martens, *A kronecker-factored approximate fisher matrix for convolution layers*, International Conference on Machine Learning, 2016, pp. 573–582.
- [GMMM19] Behrooz Ghorbani, Song Mei, Theodor Misiakiewicz, and Andrea Montanari, *Limitations of lazy training of two-layers neural networks*, arXiv preprint arXiv:1906.08899 (2019).
- [GWB⁺17] Suriya Gunasekar, Blake E Woodworth, Srinadh Bhojanapalli, Behnam Neyshabur, and Nati Srebro, *Implicit regularization in matrix factorization*, Advances in Neural Information Processing Systems, 2017, pp. 6151–6159.
- [HMRT19] Trevor Hastie, Andrea Montanari, Saharon Rosset, and Ryan J Tibshirani, *Surprises in high-dimensional ridgeless least squares interpolation*, arXiv preprint arXiv:1903.08560 (2019).
- [HVD15] Geoffrey Hinton, Oriol Vinyals, and Jeff Dean, *Distilling the knowledge in a neural network*, arXiv preprint arXiv:1503.02531 (2015).
- [HZRS16] Kaiming He, Xiangyu Zhang, Shaoqing Ren, and Jian Sun, *Deep residual learning for image recognition*, Proceedings of the IEEE conference on computer vision and pattern recognition, 2016, pp. 770–778.
- [IYS⁺20] Takashi Ishida, Ikko Yamane, Tomoya Sakai, Gang Niu, and Masashi Sugiyama, *Do we need zero training loss after achieving zero training error?*, arXiv preprint arXiv:2002.08709 (2020).
- [JGH18] Arthur Jacot, Franck Gabriel, and Clément Hongler, *Neural tangent kernel: Convergence and generalization in neural networks*, Advances in neural information processing systems, 2018, pp. 8571–8580.

- [JT18] Ziwei Ji and Matus Telgarsky, *Gradient descent aligns the layers of deep linear networks*, arXiv preprint arXiv:1810.02032 (2018).
- [JT19] ———, *The implicit bias of gradient descent on nonseparable data*, Conference on Learning Theory, 2019, pp. 1772–1798.
- [KAA18] Ryo Karakida, Shotaro Akaho, and Shun-ichi Amari, *Universal statistics of fisher information in deep neural networks: Mean field approach*, arXiv preprint arXiv:1806.01316 (2018).
- [KAA19] ———, *The normalization method for alleviating pathological sharpness in wide neural networks*, Advances in Neural Information Processing Systems, 2019, pp. 6403–6413.
- [Kar13] Nouredine El Karoui, *Asymptotic behavior of unregularized and ridge-regularized high-dimensional robust regression estimators: rigorous results*, arXiv preprint arXiv:1311.2445 (2013).
- [KB14] Diederik P Kingma and Jimmy Ba, *Adam: A method for stochastic optimization*, arXiv preprint arXiv:1412.6980 (2014).
- [KBH19] Frederik Kunstner, Lukas Balles, and Philipp Hennig, *Limitations of the empirical fisher approximation*, arXiv preprint arXiv:1905.12558 (2019).
- [KH⁺09] Alex Krizhevsky, Geoffrey Hinton, et al., *Learning multiple layers of features from tiny images*.
- [KMN⁺16] Nitish Shirish Keskar, Dheevatsa Mudigere, Jorge Nocedal, Mikhail Smelyanskiy, and Ping Tak Peter Tang, *On large-batch training for deep learning: Generalization gap and sharp minima*, arXiv preprint arXiv:1609.04836 (2016).
- [KS17] Nitish Shirish Keskar and Richard Socher, *Improving generalization performance by switching from adam to sgd*, arXiv preprint arXiv:1712.07628 (2017).
- [LBOM12] Yann A LeCun, Léon Bottou, Genevieve B Orr, and Klaus-Robert Müller, *Efficient backprop*, Neural networks: Tricks of the trade, Springer, 2012, pp. 9–48.
- [LC18] Zhenyu Liao and Romain Couillet, *The dynamics of learning: a random matrix approach*, arXiv preprint arXiv:1805.11917 (2018).
- [LD19] Daniel Levy and John C Duchi, *Necessary and sufficient geometries for gradient methods*, Advances in Neural Information Processing Systems, 2019, pp. 11491–11501.
- [LL19] Kaifeng Lyu and Jian Li, *Gradient descent maximizes the margin of homogeneous neural networks*, arXiv preprint arXiv:1906.05890 (2019).
- [LLC⁺18] Cosme Louart, Zhenyu Liao, Romain Couillet, et al., *A random matrix approach to neural networks*, The Annals of Applied Probability **28** (2018), no. 2, 1190–1248.
- [LMZ17] Yuanzhi Li, Tengyu Ma, and Hongyang Zhang, *Algorithmic regularization in over-parameterized matrix sensing and neural networks with quadratic activations*, arXiv preprint arXiv:1712.09203 (2017).
- [LP11] Olivier Ledoit and Sandrine Pécché, *Eigenvectors of some large sample covariance matrix ensembles*, Probability Theory and Related Fields **151** (2011), no. 1-2, 233–264.
- [LR17] Junhong Lin and Lorenzo Rosasco, *Optimal rates for multi-pass stochastic gradient methods*, The Journal of Machine Learning Research **18** (2017), no. 1, 3375–3421.
- [LR18] Tengyuan Liang and Alexander Rakhlin, *Just interpolate: Kernel” ridgeless” regression can generalize*, arXiv preprint arXiv:1808.00387 (2018).
- [LSO19] Mingchen Li, Mahdi Soltanolkotabi, and Samet Oymak, *Gradient descent with early stopping is provably robust to label noise for overparameterized neural networks*, arXiv preprint arXiv:1903.11680 (2019).
- [Mar10] James Martens, *Deep learning via hessian-free optimization.*, ICML, vol. 27, 2010, pp. 735–742.
- [Mar14] ———, *New insights and perspectives on the natural gradient method*, arXiv preprint arXiv:1412.1193 (2014).
- [MCO16] Gaétan Marceau-Caron and Yann Ollivier, *Practical riemannian neural networks*, arXiv preprint arXiv:1602.08007 (2016).

- [MG15] James Martens and Roger Grosse, *Optimizing neural networks with kronecker-factored approximate curvature*, International conference on machine learning, 2015, pp. 2408–2417.
- [Min17] Stanislav Minsker, *On some extensions of Bernstein’s inequality for self-adjoint operators*, Statistics & Probability Letters **127** (2017), 111–119.
- [MM19] Song Mei and Andrea Montanari, *The generalization error of random features regression: Precise asymptotics and double descent curve*, arXiv preprint arXiv:1908.05355 (2019).
- [MNS⁺20] Vidya Muthukumar, Adhyayan Narang, Vignesh Subramanian, Mikhail Belkin, Daniel Hsu, and Anant Sahai, *Classification vs regression in overparameterized regimes: Does the loss function matter?*, arXiv preprint arXiv:2005.08054 (2020).
- [MRSY19] Andrea Montanari, Feng Ruan, Youngtak Sohn, and Jun Yan, *The generalization error of max-margin linear classifiers: High-dimensional asymptotics in the overparametrized regime*, arXiv preprint arXiv:1911.01544 (2019).
- [MS12] James Martens and Ilya Sutskever, *Training deep and recurrent networks with hessian-free optimization*, Neural networks: Tricks of the trade, Springer, 2012, pp. 479–535.
- [NH10] Vinod Nair and Geoffrey E Hinton, *Rectified linear units improve restricted boltzmann machines*, Proceedings of the 27th international conference on machine learning (ICML-10), 2010, pp. 807–814.
- [NKB⁺19] Preetum Nakkiran, Gal Kaplun, Yamini Bansal, Tristan Yang, Boaz Barak, and Ilya Sutskever, *Deep double descent: Where bigger models and more data hurt*, arXiv preprint arXiv:1912.02292 (2019).
- [NW06] Jorge Nocedal and Stephen Wright, *Numerical optimization*, Springer Science & Business Media, 2006.
- [Oll15] Yann Ollivier, *Riemannian metrics for neural networks i: feedforward networks*, Information and Inference: A Journal of the IMA **4** (2015), no. 2, 108–153.
- [PB13] Razvan Pascanu and Yoshua Bengio, *Revisiting natural gradient for deep networks*, arXiv preprint arXiv:1301.3584 (2013).
- [PR19] Nicolò Pagliana and Lorenzo Rosasco, *Implicit regularization of accelerated methods in hilbert spaces*, Advances in Neural Information Processing Systems, 2019, pp. 14481–14491.
- [PVRB18] Loucas Pillaud-Vivien, Alessandro Rudi, and Francis Bach, *Statistical optimality of stochastic gradient descent on hard learning problems through multiple passes*, Advances in Neural Information Processing Systems, 2018, pp. 8114–8124.
- [QQ19] Qian Qian and Xiaoyuan Qian, *The implicit bias of adagrad on separable data*, Advances in Neural Information Processing Systems, 2019, pp. 7759–7767.
- [RC20] Noam Razin and Nadav Cohen, *Implicit regularization in deep learning may not be explainable by norms*, arXiv preprint arXiv:2005.06398 (2020).
- [RM11] Francisco Rubio and Xavier Mestre, *Spectral convergence for a general class of random matrices*, Statistics & probability letters **81** (2011), no. 5, 592–602.
- [RR17] Alessandro Rudi and Lorenzo Rosasco, *Generalization properties of learning with random features*, Advances in Neural Information Processing Systems, 2017, pp. 3215–3225.
- [RWC⁺] Alec Radford, Jeffrey Wu, Rewon Child, David Luan, Dario Amodei, and Ilya Sutskever, *Language models are unsupervised multitask learners*.
- [SHN⁺18] Daniel Soudry, Elad Hoffer, Mor Shpigel Nacson, Suriya Gunasekar, and Nathan Srebro, *The implicit bias of gradient descent on separable data*, The Journal of Machine Learning Research **19** (2018), no. 1, 2822–2878.
- [SMG13] Andrew M Saxe, James L McClelland, and Surya Ganguli, *Exact solutions to the nonlinear dynamics of learning in deep linear neural networks*, arXiv preprint arXiv:1312.6120 (2013).
- [SPR18] Arun Suggala, Adarsh Prasad, and Pradeep K Ravikumar, *Connecting optimization and regularization paths*, Advances in Neural Information Processing Systems, 2018, pp. 10608–10619.

- [Suz18] Taiji Suzuki, *Adaptivity of deep relu network for learning in besov and mixed smooth besov spaces: optimal rate and curse of dimensionality*, arXiv preprint arXiv:1810.08033 (2018).
- [SY19] Lili Su and Pengkun Yang, *On learning over-parameterized neural networks: A functional approximation perspective*, Advances in Neural Information Processing Systems, 2019, pp. 2637–2646.
- [TPT20] Hossein Taheri, Ramtin Pedarsani, and Christos Thrampoulidis, *Sharp asymptotics and optimal performance for inference in binary models*, arXiv preprint arXiv:2002.07284 (2020).
- [WGL⁺20] Blake Woodworth, Suriya Gunasekar, Jason D Lee, Edward Moroshko, Pedro Savarese, Itay Golan, Daniel Soudry, and Nathan Srebro, *Kernel and rich regimes in overparametrized models*, arXiv preprint arXiv:2002.09277 (2020).
- [WLLM19] Colin Wei, Jason D Lee, Qiang Liu, and Tengyu Ma, *Regularization matters: Generalization and optimization of neural nets vs their induced kernel*, Advances in Neural Information Processing Systems, 2019, pp. 9712–9724.
- [WMW18] Lei Wu, Chao Ma, and E Weinan, *How sgd selects the global minima in over-parameterized learning: A dynamical stability perspective*, Advances in Neural Information Processing Systems, 2018, pp. 8279–8288.
- [WRS⁺17] Ashia C Wilson, Rebecca Roelofs, Mitchell Stern, Nati Srebro, and Benjamin Recht, *The marginal value of adaptive gradient methods in machine learning*, Advances in Neural Information Processing Systems, 2017, pp. 4148–4158.
- [WTS⁺19] Francis Williams, Matthew Trager, Claudio Silva, Daniele Panozzo, Denis Zorin, and Joan Bruna, *Gradient dynamics of shallow univariate relu networks*, arXiv preprint arXiv:1906.07842 (2019).
- [WX20] Denny Wu and Ji Xu, *On the optimal weighted ℓ_2 regularization in overparameterized linear regression*, arXiv preprint arXiv:2006.05800 (2020).
- [XH19] Ji Xu and Daniel Hsu, *How many variables should be entered in a principal component regression equation?*, arXiv preprint arXiv:1906.01139 (2019).
- [XLS16] Bo Xie, Yingyu Liang, and Le Song, *Diverse neural network learns true target functions*, arXiv preprint arXiv:1611.03131 (2016).
- [XRM20] Peng Xu, Fred Roosta, and Michael W Mahoney, *Second-order optimization for non-convex machine learning: An empirical study*, Proceedings of the 2020 SIAM International Conference on Data Mining, SIAM, 2020, pp. 199–207.
- [ZBH⁺16] Chiyuan Zhang, Samy Bengio, Moritz Hardt, Benjamin Recht, and Oriol Vinyals, *Understanding deep learning requires rethinking generalization*, arXiv preprint arXiv:1611.03530 (2016).
- [ZLN⁺19] Guodong Zhang, Lala Li, Zachary Nado, James Martens, Sushant Sachdeva, George Dahl, Chris Shallue, and Roger B Grosse, *Which algorithmic choices matter at which batch sizes? insights from a noisy quadratic model*, Advances in Neural Information Processing Systems, 2019, pp. 8194–8205.
- [ZMG19] Guodong Zhang, James Martens, and Roger B Grosse, *Fast convergence of natural gradient descent for over-parameterized neural networks*, Advances in Neural Information Processing Systems, 2019, pp. 8080–8091.
- [ZWXG18] Guodong Zhang, Chaoqi Wang, Bowen Xu, and Roger Grosse, *Three mechanisms of weight decay regularization*, arXiv preprint arXiv:1810.12281 (2018).

A Discussion of Additional Results

A.1 Implicit Bias of GD vs. NGD

It is known that gradient descent is the steepest descent with respect to the ℓ_2 norm, i.e. the update direction is constructed to decrease the loss under small changes in the parameters measured by the ℓ_2 norm [GLSS18a]. Following this analogy, NGD is the steepest descent with respect to the KL divergence on the predictive distributions [Mar14]; this can be interpreted as a proximal update which penalizes how much the predictions change on the data distribution.

Intuitively, the above discussion suggests GD tend to find solution that is close to the initialization in the Euclidean distance between parameters, whereas NGD prefers solution close to the initialization in terms of the function outputs on P_X . This observation turns out to be exact in the case of ridgeless interpolant under the squared loss, as remarked in Section 3. Moreover, Figure 8 confirms the same trend in neural network optimization. In particular, we observe that

- GD results in small changes in the parameters, whereas NGD results in small changes in the function.
- preconditioning with the pseudo-inverse of the sample Fisher, i.e., $\mathbf{P} = (\mathbf{J}^\top \mathbf{J})^\dagger$, leads to implicit bias similar to that of GD (also pointed out in [ZMG19]), but not NGD with the population Fisher.
- interpolating between GD and NGD, e.g., $\mathbf{P} = \mathbf{F}^{-1/2}$ (green), results in solution with properties in between GD and NGD.

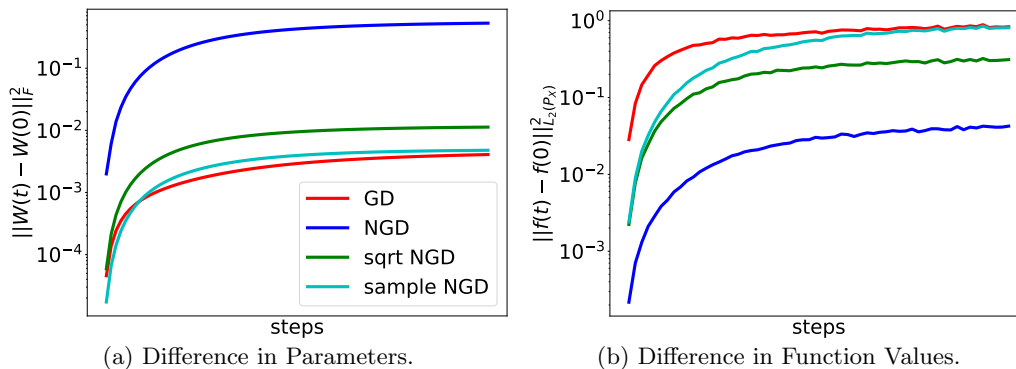


Figure 8: Illustration of the different implicit bias of GD and NGD. We set $n = 100$, $d = 50$, and regress a two-layer ReLU network with 50 hidden units towards a teacher model of the same architecture on Gaussian input. The x-axis is rescaled for each optimizer such that the final training error is below 10^{-3} . GD finds solution with small changes in the parameters, whereas NGD finds solution with small changes in the function. Note that the sample Fisher (cyan) has implicit bias similar to GD and does not resemble NGD (population Fisher).

In addition, we also speculate that as we interpolate from GD to NGD, the distance traveled by the parameter space would gradually increase, and distance traveled in the function space would decrease. Figure 9 and 20 demonstrate that this is indeed the case for linear model as well as neural network.

We remark that this observation also implies that wide neural networks trained with NGD (population Fisher) is less likely to stay in the kernel regime: the distance traveled from initialization can be large (see Figure 8(a)) and thus the Taylor expansion around the initialization is no longer an accurate description of the training dynamics. In other words, the analogy between wide neural net and its linearized kernel model (which we partially employed in Section 5) may not be valid in models trained with NGD⁹.

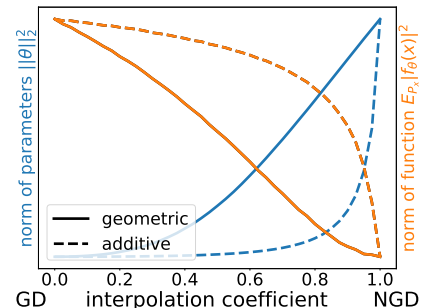


Figure 9: Euclidean and $\|\cdot\|_\Sigma$ norm (log scale) under additive and geometric interpolation in ridgeless regression.

⁹Note that this gap is only present when the population Fisher is used; previous works have shown the NTK-type global convergence for sample Fisher-related preconditioned update [ZMG19, CGH⁺19].

A.2 Non-monotonicity of the Bias Term

Many previous works on the high-dimensional characterization of linear regression assumed a random effects model with an isotropic prior on the true parameters [DW⁺18, HMRT19, XH19], which may not be realistic. As an example of the limitation of this assumption, we note that when $\Sigma_{\theta} = \mathbf{I}_d$, it can be shown that the expected bias $B(\hat{\theta}(t))$ monotonically decreases through time (see proof of Proposition 6 for details). In contrast, when the target parameters do not follow an isotropic prior, the bias of GD can exhibit non-monotonicity, which gives rise to the surprising “epoch-wise double descent” phenomenon also observed in deep learning [NKB⁺19, IYS⁺20].

We empirically demonstrate this non-monotonicity when the model is close to the interpolation threshold in Figure 10. We set $D_{\mathbf{X}}$ to be two equally-weighted point masses with $\kappa_{\mathbf{X}} = 32$, $\Sigma_{\theta} = \Sigma_{\mathbf{X}}^{-1}$ and $\gamma = 16/15$. Note that the GD trajectory (red) exhibits non-monotonicity in the bias term, whereas for NGD the bias is monotonically decreasing through time (which we confirm in the proof of Proposition 6). We remark that this mechanism of epoch-wise double descent may not be related to the empirical findings in deep neural networks (the robustness of which is also largely unknown), in which it is typically speculated that the variance term exhibits non-monotonicity.

A.3 Interpretation of $\sqrt{\mathbf{y}^{\top} \mathbf{K}^{-1} \mathbf{y} / n}$

The quantity which we empirically evaluated in Section 5 was first proposed as a measure of generalization for wide neural networks in the kernel regime. This quantity can be interpreted as a proxy for measuring how much signal and noise are distributed along the eigendirections of the NTK (see [LSO19, DHLZ19, SY19, CFW⁺19] for detailed discussion). Intuitively speaking, large $\sqrt{\mathbf{y}^{\top} \mathbf{K}^{-1} \mathbf{y} / n}$ implies that the problem is difficult to learn by GD, and vice versa.

Here we give a heuristic argument on how this quantity relates to label noise and misspecification in our setup. For the ridgeless regression model considered in Section 3, if we write the label as $y_i = f^*(\mathbf{x}_i) + f^c(\mathbf{x}_i) + \varepsilon_i$, where $f^*(\mathbf{x}) = \mathbf{x}^{\top} \theta^*$, f^c is the misspecified component that is independent to f^* , and ε_i is the label noise, we have the following heuristic calculation:

$$\begin{aligned} & \mathbb{E}[\mathbf{y}^{\top} \mathbf{K}^{-1} \mathbf{y}] \\ &= \mathbb{E}\left[\left(f^*(\mathbf{X}) + f^c(\mathbf{X}) + \varepsilon\right)^{\top} (\mathbf{X} \mathbf{X}^{\top})^{-1} \left(f^*(\mathbf{X}) + f^c(\mathbf{X}) + \varepsilon\right)\right] \\ &\stackrel{(i)}{\approx} \text{tr}\left(\theta^* \theta^{*\top} \mathbf{X}^{\top} (\mathbf{X} \mathbf{X}^{\top})^{-1} \mathbf{X}\right) + (\sigma^2 + \sigma_c^2) \text{tr}\left((\mathbf{X} \mathbf{X}^{\top})^{-1}\right), \quad (\text{A.1}) \end{aligned}$$

where we heuristically replaced the misspecified component with i.i.d. noise of the same variance σ_c^2 (as argued in Section 3). The first term of (A.1) resembles an RKHS norm of the true coefficients θ^* , whereas the second term is small when the data is well-conditioned (i.e. the inverse of $\mathbf{X} \mathbf{X}^{\top}$ is stable) or when the amount of label noise σ and misspecification σ_c^2 is small, as illustrated in Figure 11 (note that these are conditions under which GD achieves good generalization, as shown in Theorem 1 and Proposition 3). We also expect similar characterization to hold for neural networks close to the kernel regime. This provides a non-rigorous explanation of the trend we observed in Figure 6 as we increase the level of label noise and model misspecification.

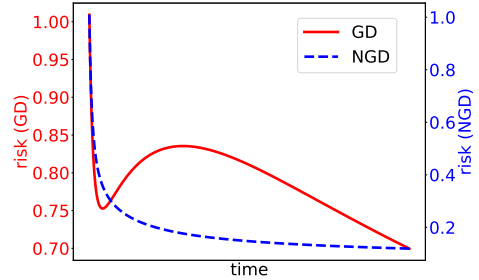


Figure 10: Epoch-wise double descent. Note that non-monotonicity of the bias term is present in GD but not NGD.

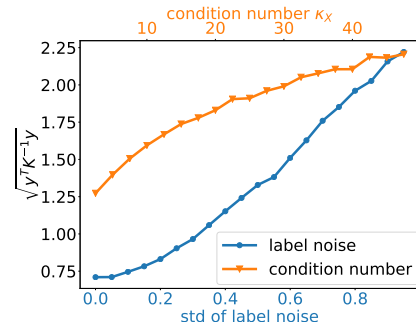


Figure 11: Demonstration of the growth of $\sqrt{\mathbf{y}^{\top} \mathbf{K}^{-1} \mathbf{y}}$ in linear regression as the amount of label noise (orange) or the condition number of $\Sigma_{\mathbf{X}}$ (blue) increases.

B Additional Figures

B.1 Ridgeless Regression

Non-monotonicity of the Risk. Under our generalized (anisotropic) assumption on the covariance of the features and the target (teacher model), both the bias and the variance term can exhibit non-monotonicity w.r.t. the overparameterization level $\gamma > 1$. For instance, in Figure 12 we observe two peaks in the bias term and three peaks in the variance term.

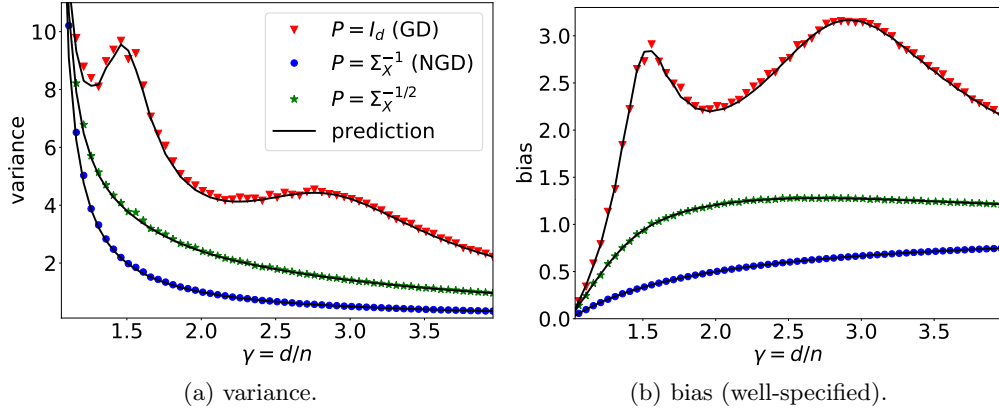


Figure 12: Illustration of the “multiple-descent” curve of the risk for $\gamma > 1$. We take $n = 300$, \mathbf{D}_X as three equally-spaced point masses with $\kappa_X = 5000$ and $\|\Sigma_X\|_F^2 = d$, and $\mathbf{D}_\theta = \mathbf{D}_X^{-1}$ (misaligned). Note that for GD, both the bias and the variance are highly non-monotonic for $\gamma > 1$.

Early Stopping Risk. Figure 13 compares the stationary risk with the optimal early stopping risk under varying misalignment level. To increase the extent of misalignment, we set $\Sigma_\theta = \Sigma_X^{-\alpha}$ and vary α from 0 to 1: larger α entails more “misaligned” teacher, and vice versa. Note that as the problem becomes more misaligned, NGD achieves lower stationary and early stopping risk.

Figure 14 reports the optimal early stopping risk under misspecification (exact same trend can be obtained when the x-axis is label noise). In contrast to the stationary risk (Figure 1), GD can be advantageous under early stopping even with large extent of misspecification (if parameters of the teacher are isotropic). This aligns with our finding in Section 4.2 that early stopping reduces the variance and the misspecified bias.

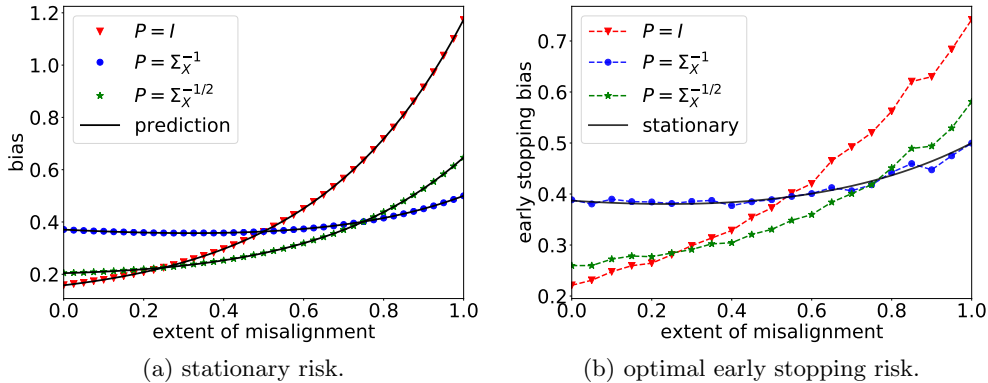


Figure 13: Well-specified bias against different extent of “alignment”. We set $n = 300$, \mathbf{D}_X as two point masses with $\kappa_X = 20$ and $\|\Sigma_X\|_F^2 = d$, and take $\Sigma_\theta = \Sigma_X^{-\alpha}$ and vary α from 0 to 1. (a) GD achieves lower bias when Σ_θ is isotropic, whereas NGD dominates when $\Sigma_X = \Sigma_\theta^{-1}$; $P = \Sigma_X^{-1/2}$ (interpolates between GD and NGD) is advantageous in between. (b) optimal early stopping bias follows similar trend as stationary risk (the optimal early stopping bias for NGD is the same as its stationary risk due to the monotonic bias term).

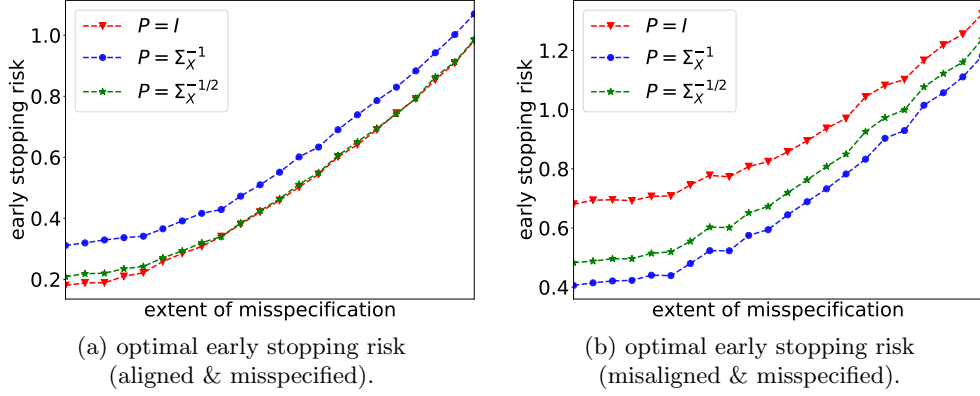


Figure 14: Optimal early stopping risk vs. increasing model misspecification. We follow the same setup as Figure 3(c). (a) $\Sigma_\theta = \mathbf{I}_d$ (favors GD); unlike Figure 3(c), GD has lower early stopping risk even under large extent of misspecification. (b) $\Sigma_\theta = \Sigma_X^{-1}$ (favors NGD); NGD is also advantageous under early stopping.

Complementary Figures for Section 3 and 4. We include additional figures on (a) well-specified bias when $\Sigma_\theta = \mathbf{I}_d$ (GD is optimal); (b) misspecified bias under unobserved features (predicted by Proposition 3); (c) bias-variance tradeoff by interpolating between preconditioners (SNR=5). Observe that in all cases the experimental values match the theoretical predictions.

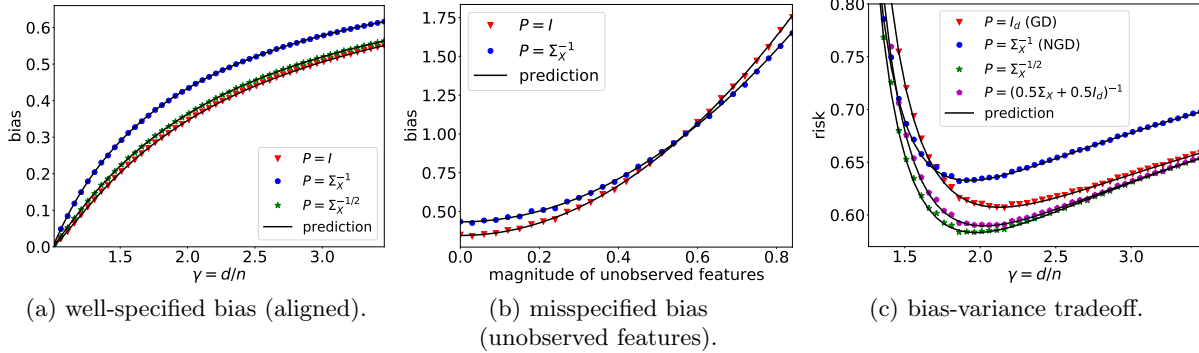


Figure 15: We set \mathbf{D}_X as a uniform distribution with $\kappa_X = 20$ and $\|\Sigma_X\|_F^2 = d$.

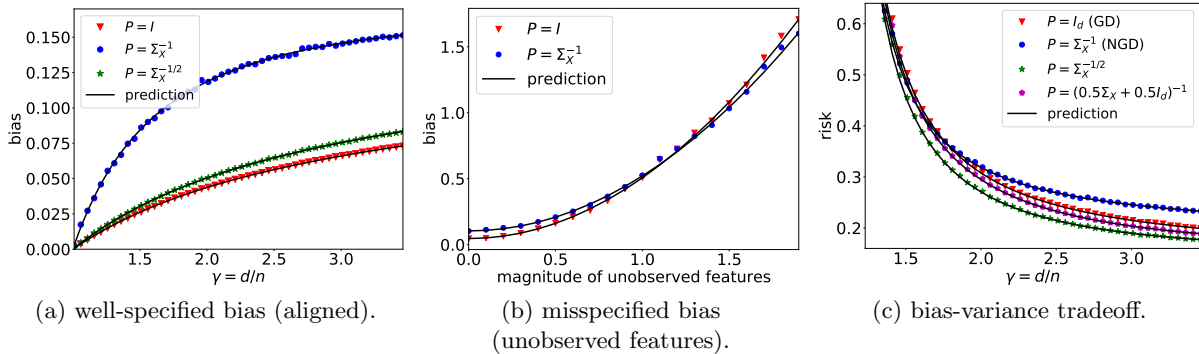


Figure 16: We construct \mathbf{D}_X with a polynomial decay: $\lambda_i(\mathbf{D}_X) = i^{-1}$ and then rescale the eigenvalues such that $\kappa_X = 500$ and $\|\Sigma_X\|_F^2 = d$.

B.2 RKHS Regression

We simulate the optimization in the coordinates of RKHS via a finite-dimensional approximation (using extra unlabeled data). In particular, we consider the teacher model in the form of $f^*(\mathbf{x}) = \sum_{i=1}^N h_i \mu_i^r \phi_i(\mathbf{x})$ for square summable $\{h_i\}_{i=1}^N$, in which r controls the “difficulty” of the learning problem. We find $\{\mu_i\}_{i=1}^N$ and $\{\phi_i\}_{i=1}^N$ by solving the eigenfunction problem for some kernel k . The student model takes the form of $f(\mathbf{x}) = \sum_{i=1}^N \frac{a_i}{\sqrt{\mu_i}} \phi_i(\mathbf{x})$ and we optimize the coefficients $\{a_i\}_{i=1}^N$ via the preconditioned update (4.1). We set $n = 1000$, $d = 5$, $N = 2500$ and consider the inverse multiquadratic (IMQ) kernel: $k(\mathbf{x}, \mathbf{y}) = \frac{1}{\sqrt{1 + \|\mathbf{x} - \mathbf{y}\|_2^2}}$.

Recall that Theorem 7 suggests that for small r , i.e. “difficult” problem, the damping coefficient λ would need to be small (which makes the update NGD-like), and vice versa. This result is (qualitatively) supported by Figure 17, from which we can see that small λ is beneficial when r is small, and vice versa. We remark that this observed trend is rather fragile and sensitive to various hyperparameters, and we leave a more comprehensive characterization of this observation as future work.

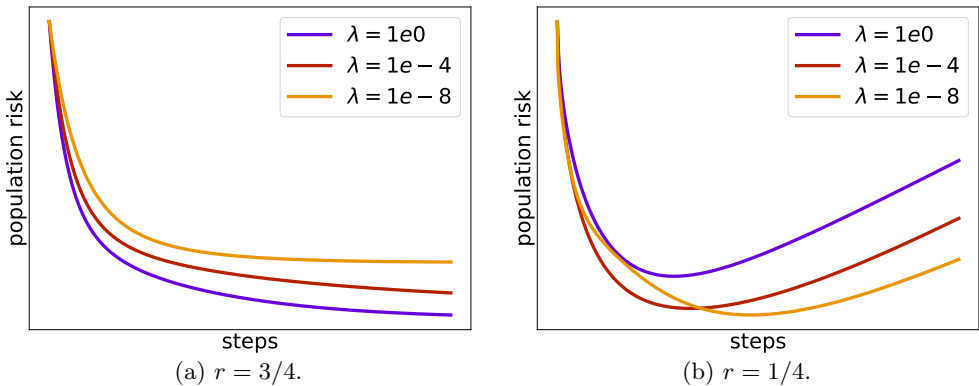


Figure 17: Population risk of the preconditioned update in RKHS that interpolates between GD and NGD. We use the IMQ kernel and set $n = 1000$, $d = 5$, $N = 2500$, $\sigma^2 = 5 \times 10^{-4}$. The x-axis has been rescaled for each curve and thus convergence speed is not directly comparable. Note that (a) large λ (i.e., GD-like update) is beneficial when r is large, and (b) small λ (i.e., NGD-like update) is beneficial when r is small.

B.3 Neural Networks

Label Noise. In Figure 18, (a) we observe the same phenomenon on CIFAR-10 that NGD generalizes better as more label noise is added to the training data, and vice versa. Figure 18 (b) shows that in all cases with varying amounts of label noise, the early stopping risk is however worse than that of GD, regardless of whether the preconditioner is the (pseudo-)inverse of the Fisher or its sample-based counterpart. This agrees with the observation in Section 4 and Figure 14(a) that early stopping can potentially favor GD due to the reduced variance.

Misalignment. We illustrate the finding in Proposition 6 and Figure 13(b) in neural networks under synthetic data: we consider 50-dimensional Gaussian input, and both the teacher model and the student model are two-layer ReLU networks with 50 hidden units. We construct the teacher by perturbing the initialization of the student, as described in Section 5. Figure 19 shows that as we decrease r , which we interpret as the problem becoming more “misaligned”¹⁰, NGD eventually achieves lower early stopping risk (b), whereas GD dominates the early stopping risk in less misaligned setting (a). We note that this phenomenon is difficult to observe in practical neural network training on real-world data, which may be partially due to the fragility of the analogy between neural nets and linear models, especially under NGD (discussed in Appendix A).

¹⁰We remark that this r is slightly different than that defined in the RKHS regression experiment.

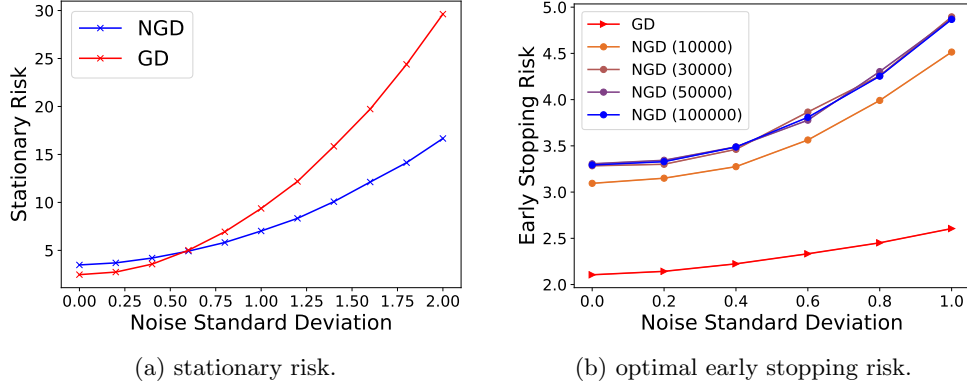


Figure 18: Additional label noise experiment on CIFAR-10.

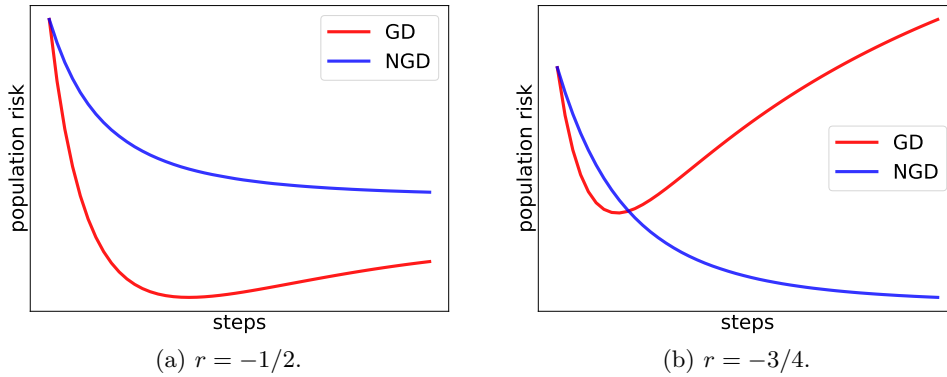


Figure 19: Population risk of two-layer neural networks in the misalignment setup (noiseless) with synthetic Gaussian data. We set $n = 200$, $d = 50$, the damping coefficient $\lambda = 10^{-6}$, and both the student and the teacher are two-layer ReLU networks with 50 hidden units. The x-axis and the learning rate have been rescaled for each curve. When r is sufficiently small, NGD achieves lower early stopping risk, and vice versa.

Implicit Bias of Interpolating Preconditioners. Figure 20 demonstrates that the implicit bias of preconditioned update that interpolates between GD and NGD. We use the same two-layer MLP setup on MNIST as in Figure 7. Note that updates that are closer to GD result in smaller change in the parameters, whereas ones close to NGD lead to smaller change in the function outputs.

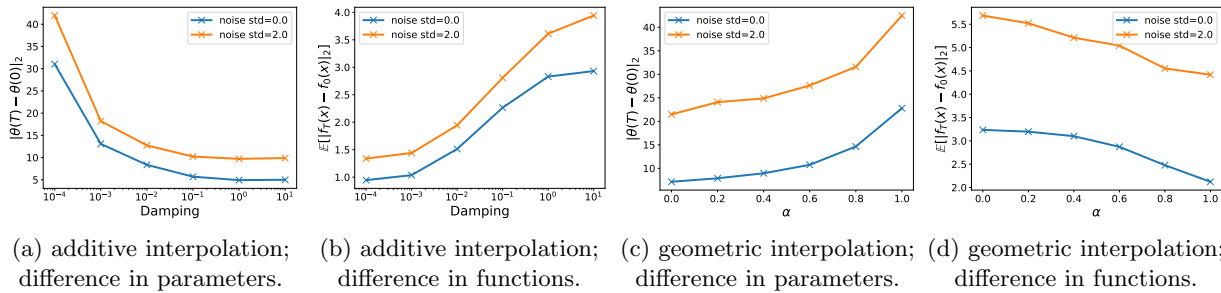


Figure 20: Illustration of the implicit bias of preconditioned gradient descent that interpolates between GD and NGD on MNIST. Note that as the update becomes more similar to NGD (smaller damping or larger α), the distance traveled in the parameter space increases, whereas the distance traveled on the output space decreases.

C Proofs and Derivations

C.1 Missing Derivations in Section 3

Gradient Flow of Preconditioned Updates. Given positive definite \mathbf{P} and $\gamma > 1$, it is clear that the gradient flow solution at time t can be written as

$$\boldsymbol{\theta}_{\mathbf{P}}(t) = \mathbf{P}\mathbf{X}^\top \left[\mathbf{I}_n - \exp\left(-\frac{t}{n}\mathbf{X}\mathbf{P}\mathbf{X}^\top\right) \right] (\mathbf{X}\mathbf{P}\mathbf{X}^\top)^{-1}\mathbf{y}.$$

Taking $t \rightarrow \infty$ yields the stationary solution $\hat{\boldsymbol{\theta}}_{\mathbf{P}} = \mathbf{P}\mathbf{X}^\top(\mathbf{X}\mathbf{P}\mathbf{X}^\top)^{-1}\mathbf{y}$. We remark that the damped inverse of the sample Fisher $\mathbf{P} = (\mathbf{X}\mathbf{X}^\top + \lambda\mathbf{I}_d)^{-1}$ leads to the same minimum-norm solution as GD $\hat{\boldsymbol{\theta}}_{\mathbf{I}} = \mathbf{X}^\top(\mathbf{X}\mathbf{X}^\top)^{-1}\mathbf{y}$ since $\mathbf{P}\mathbf{X}^\top$ and \mathbf{X} share the same eigenvectors. On the other hand, when \mathbf{P} is the pseudo-inverse of the sample Fisher $(\mathbf{X}\mathbf{X}^\top)^\dagger$ which is not full-rank, the trajectory can be obtained via the variation of constants formula:

$$\boldsymbol{\theta}(t) = \left[\frac{t}{n} \sum_{k=0}^{\infty} \frac{1}{(k+1)!} \left(-\frac{t}{n} \mathbf{X}^\top (\mathbf{X}\mathbf{X}^\top)^{-1} \mathbf{X} \right)^k \right] \mathbf{X}^\top (\mathbf{X}\mathbf{X}^\top)^{-1} \mathbf{y},$$

for which taking the large t limit also yields the minimum-norm solution $\mathbf{X}^\top(\mathbf{X}\mathbf{X}^\top)^{-1}\mathbf{y}$.

Minimum $\|\boldsymbol{\theta}\|_{\mathbf{P}^{-1}}$ Norm Interpolant. For positive definite \mathbf{P} and the corresponding stationary solution $\hat{\boldsymbol{\theta}}_{\mathbf{P}} = \mathbf{P}\mathbf{X}^\top(\mathbf{X}\mathbf{P}\mathbf{X}^\top)^{-1}\mathbf{y}$, note that given any other interpolant $\hat{\boldsymbol{\theta}}'$, we have $(\hat{\boldsymbol{\theta}}_{\mathbf{P}} - \hat{\boldsymbol{\theta}}')\mathbf{P}^{-1}\hat{\boldsymbol{\theta}}_{\mathbf{P}} = 0$ because both $\hat{\boldsymbol{\theta}}_{\mathbf{P}}$ and $\hat{\boldsymbol{\theta}}'$ achieves zero empirical risk. Therefore, $\|\hat{\boldsymbol{\theta}}'\|_{\mathbf{P}^{-1}}^2 - \|\hat{\boldsymbol{\theta}}_{\mathbf{P}}\|_{\mathbf{P}^{-1}}^2 = \|\hat{\boldsymbol{\theta}}' - \hat{\boldsymbol{\theta}}_{\mathbf{P}}\|_{\mathbf{P}^{-1}}^2 \geq 0$. This confirms that $\hat{\boldsymbol{\theta}}_{\mathbf{P}}$ is the minimum $\|\boldsymbol{\theta}\|_{\mathbf{P}^{-1}}$ norm solution.

C.2 Proof of Theorem 1

Proof. By the definition of the variance term and the stationary $\hat{\boldsymbol{\theta}}$,

$$V(\hat{\boldsymbol{\theta}}) = \text{tr}\left(\text{Cov}(\hat{\boldsymbol{\theta}})\boldsymbol{\Sigma}_{\mathbf{X}}\right) = \sigma^2 \text{tr}\left(\mathbf{P}\mathbf{X}^\top(\mathbf{X}\mathbf{P}\mathbf{X}^\top)^{-2}\mathbf{X}^\top\mathbf{P}\boldsymbol{\Sigma}_{\mathbf{X}}\right).$$

Write $\bar{\mathbf{X}} = \mathbf{X}\mathbf{P}^{1/2}$ with covariance $\mathbf{D}_{\mathbf{X}\mathbf{P}} = \mathbf{D}_{\mathbf{X}}\mathbf{D}_{\mathbf{P}}$. Similarly, we define $\boldsymbol{\Sigma}_{\mathbf{X}\mathbf{P}} = \boldsymbol{\Sigma}_{\mathbf{X}}\boldsymbol{\Sigma}_{\mathbf{P}}$. The equation above thus simplifies to

$$V(\hat{\boldsymbol{\theta}}_{\mathbf{P}}) = \sigma^2 \text{tr}\left(\bar{\mathbf{X}}^\top(\bar{\mathbf{X}}\bar{\mathbf{X}}^\top)^{-2}\bar{\mathbf{X}}^\top\boldsymbol{\Sigma}_{\mathbf{X}\mathbf{P}}\right).$$

The analytic expression of the variance term follows from a direct application of [HMRT19, Theorem 4], in which conditions on the population covariance are satisfied by (A2).

Taking the derivative of $m(-\lambda)$ yields

$$m'(-\lambda) = \left(\frac{1}{m^2(-\lambda)} - \gamma \int \frac{\tau^2}{(1 + \tau m(-\lambda))^2} dF_{\mathbf{X}\mathbf{P}}(\tau) \right)^{-1}.$$

Plugging the quantity into the expression of the variance (omitting the scaling σ^2 and constant shift),

$$\frac{m'(-\lambda)}{m^2(-\lambda)} = \left(1 - \gamma m^2(-\lambda) \int \frac{\tau^2}{(1 + \tau m(-\lambda))^2} dF_{\mathbf{X}\mathbf{P}}(\tau) \right)^{-1}.$$

From the monotonicity of $\frac{x}{1+x}$ on $x > 0$ or the Jensen's inequality we know that

$$1 - \gamma \int \left(\frac{\tau m(-\lambda)}{1 + \tau m(-\lambda)} \right)^2 dF_{\mathbf{X}\mathbf{P}}(\tau) \leq 1 - \gamma \left(\int \frac{\tau m(-\lambda)}{1 + \tau m(-\lambda)} dF_{\mathbf{X}\mathbf{P}}(\tau) \right)^2.$$

Taking $\lambda \rightarrow 0$ and omitting the scalar σ^2 , the RHS evaluates to $1 - 1/\gamma$. We thus arrive at the lower bound $V \geq (\gamma - 1)^{-1}$. Note that the equality is only achieved when $F_{\mathbf{X}\mathbf{P}}$ is a point mass, i.e. $\mathbf{P} = \Sigma_{\mathbf{X}}^{-1}$. In other words, the minimum variance is achieved by NGD. As a verification, the variance of the NGD solution $\hat{\boldsymbol{\theta}}_{\mathbf{F}^{-1}}$ agrees with the calculation in [HMRT19, A.3]. \square

C.3 Proof of Theorem 2

Proof. By the definition of the bias term,

$$\begin{aligned}
B(\hat{\boldsymbol{\theta}}_{\mathbf{P}}) &= \mathbb{E}_{\boldsymbol{\theta}^*} \left[\left\| \mathbf{P}\mathbf{X}^\top (\mathbf{X}\mathbf{P}\mathbf{X}^\top)^{-1} \mathbf{X}\boldsymbol{\theta}_* - \boldsymbol{\theta}^* \right\|_{\Sigma_{\mathbf{X}}}^2 \right] \\
&= \frac{1}{d} \text{tr} \left(\Sigma_{\boldsymbol{\theta}} \left(\mathbf{I}_d - \mathbf{P}\mathbf{X}^\top (\mathbf{X}\mathbf{P}\mathbf{X}^\top)^{-1} \mathbf{X} \right)^\top \Sigma_{\mathbf{X}} \left(\mathbf{I}_d - \mathbf{P}\mathbf{X}^\top (\mathbf{X}\mathbf{P}\mathbf{X}^\top)^{-1} \mathbf{X} \right) \right) \\
&\stackrel{(i)}{=} \frac{1}{d} \text{tr} \left(\Sigma_{\boldsymbol{\theta}/\mathbf{P}} \left(\mathbf{I}_d - \bar{\mathbf{X}}^\top (\bar{\mathbf{X}}\bar{\mathbf{X}}^\top)^{-1} \bar{\mathbf{X}} \right)^\top \Sigma_{\mathbf{X}\mathbf{P}} \left(\mathbf{I}_d - \bar{\mathbf{X}}^\top (\bar{\mathbf{X}}\bar{\mathbf{X}}^\top)^{-1} \bar{\mathbf{X}} \right) \right) \\
&\stackrel{(ii)}{=} \lim_{\lambda \rightarrow 0_+} \frac{\lambda^2}{d} \text{tr} \left(\Sigma_{\boldsymbol{\theta}/\mathbf{P}} \left(\frac{1}{n} \bar{\mathbf{X}}^\top \bar{\mathbf{X}} + \lambda \mathbf{I}_d \right)^{-1} \Sigma_{\mathbf{X}\mathbf{P}} \left(\frac{1}{n} \bar{\mathbf{X}}^\top \bar{\mathbf{X}} + \lambda \mathbf{I}_d \right)^{-1} \right) \\
&\stackrel{(iii)}{=} \lim_{\lambda \rightarrow 0_+} \frac{\lambda^2}{d} \text{tr} \left(\left(\frac{1}{n} \hat{\mathbf{X}}^\top \hat{\mathbf{X}} + \lambda \mathbf{D}_{\boldsymbol{\theta}/\mathbf{P}}^{-1} \right)^{-2} \Sigma_{\mathbf{X}\mathbf{P}} \Sigma_{\boldsymbol{\theta}/\mathbf{P}}^{-1} \right),
\end{aligned}$$

where we utilized (A3) and defined $\bar{\mathbf{X}} = \mathbf{X}\mathbf{P}^{1/2}$, $\Sigma_{\mathbf{X}\mathbf{P}} = \Sigma_{\mathbf{X}}\mathbf{P}$, $\Sigma_{\boldsymbol{\theta}/\mathbf{P}} = \Sigma_{\boldsymbol{\theta}}\mathbf{P}^{-1}$ in (i), applied the equality $(\mathbf{A}\mathbf{A}^\top)^\dagger \mathbf{A} = \lim_{\lambda \rightarrow 0} (\mathbf{A}^\top \mathbf{A} + \lambda \mathbf{I})^{-1} \mathbf{A}$ in (ii), and defined $\hat{\mathbf{X}} = \mathbf{X}\Sigma^{-1/2}\mathbf{P}$ with covariance $\mathbf{D}_{\mathbf{X}\mathbf{P}}\mathbf{D}_{\boldsymbol{\theta}/\mathbf{P}}^{-1}$ in (iii) (note that $\mathbf{D}_{\boldsymbol{\theta}/\mathbf{P}}$ is invertible by (A2-4)). To proceed, we first observe the following relation via a leave-one-out argument similar to that in [XH19],

$$\begin{aligned}
&\frac{1}{d} \text{tr} \left(\frac{1}{n} \hat{\mathbf{X}}^\top \hat{\mathbf{X}} \left(\frac{1}{n} \hat{\mathbf{X}}^\top \hat{\mathbf{X}} + \lambda \mathbf{D}_{\boldsymbol{\theta}/\mathbf{P}}^{-1} \right)^{-2} \right) \tag{C.1} \\
&\stackrel{(i)}{=} \frac{1}{d} \sum_{i=1}^n \frac{\frac{1}{n} \hat{\mathbf{x}}_i^\top \left(\frac{1}{n} \hat{\mathbf{X}}^\top \hat{\mathbf{X}} + \lambda \mathbf{D}_{\boldsymbol{\theta}/\mathbf{P}}^{-1} \right)^{-2}_{-i} \hat{\mathbf{x}}_i}{\left(1 + \frac{1}{n} \hat{\mathbf{x}}_i^\top \left(\frac{1}{n} \hat{\mathbf{X}}^\top \hat{\mathbf{X}} + \lambda \mathbf{D}_{\boldsymbol{\theta}/\mathbf{P}}^{-1} \right)^{-1}_{-i} \hat{\mathbf{x}}_i \right)^2} \\
&\stackrel{(ii)}{\xrightarrow{p}} \frac{\frac{1}{d} \text{tr} \left(\left(\frac{1}{n} \hat{\mathbf{X}}^\top \hat{\mathbf{X}} + \lambda \mathbf{D}_{\boldsymbol{\theta}/\mathbf{P}}^{-1} \right)^{-2} \Sigma_{\mathbf{X}\mathbf{P}} \Sigma_{\boldsymbol{\theta}/\mathbf{P}}^{-1} \right)}{\left(1 + \frac{1}{n} \text{tr} \left(\left(\frac{1}{n} \bar{\mathbf{X}}^\top \bar{\mathbf{X}} + \lambda \mathbf{I}_d \right)^{-1} \Sigma_{\mathbf{X}\mathbf{P}} \right) \right)^2}, \tag{C.2}
\end{aligned}$$

where (i) is due to the Woodbury identity and we defined $\left(\frac{1}{n} \hat{\mathbf{X}}^\top \hat{\mathbf{X}} + \lambda \mathbf{D}_{\boldsymbol{\theta}/\mathbf{P}}^{-1} \right)^{-2}_{-i} = \frac{1}{n} \hat{\mathbf{X}}^\top \hat{\mathbf{X}} - \frac{1}{n} \hat{\mathbf{x}}_i \hat{\mathbf{x}}_i^\top + \lambda \mathbf{D}_{\boldsymbol{\theta}/\mathbf{P}}^{-1}$ which is independent to $\hat{\mathbf{x}}_i$ (see [XH19, Eq. 58] for details), and in (ii) we used (A2), the convergence to trace [LP11, Lemma 2.1] and its stability under low-rank perturbation (e.g., see [LP11, Eq. 18]) which we elaborate below. In particular, denote $\hat{\Sigma} = \frac{1}{n} \hat{\mathbf{X}}^\top \hat{\mathbf{X}} + \lambda \mathbf{D}_{\boldsymbol{\theta}/\mathbf{P}}^{-1}$, for the denominator we have

$$\begin{aligned}
&\sup_i \left| \frac{\lambda}{n} \text{tr} \left(\hat{\Sigma}^{-1} \Sigma_{\mathbf{X}\mathbf{P}} \Sigma_{\boldsymbol{\theta}/\mathbf{P}}^{-1} \right) - \frac{\lambda}{n} \text{tr} \left(\hat{\Sigma}_{-i}^{-1} \Sigma_{\mathbf{X}\mathbf{P}} \Sigma_{\boldsymbol{\theta}/\mathbf{P}}^{-1} \right) \right| \\
&\leq \frac{\lambda}{n} \left\| \Sigma_{\mathbf{X}\mathbf{P}} \Sigma_{\boldsymbol{\theta}/\mathbf{P}}^{-1} \right\|_2 \sup_i \left| \text{tr} \left(\hat{\Sigma}^{-1} \left(\hat{\Sigma} - \hat{\Sigma}_{-i} \right) \hat{\Sigma}_{-i}^{-1} \right) \right| \\
&\leq \frac{\lambda}{n} \left\| \Sigma_{\mathbf{X}\mathbf{P}} \Sigma_{\boldsymbol{\theta}/\mathbf{P}}^{-1} \right\|_2 \left\| \hat{\Sigma}^{-1} \right\|_2 \sup_i \left\| \hat{\Sigma}_{-i}^{-1} \right\|_2 \text{tr} \left(\hat{\Sigma} - \hat{\Sigma}_{-i} \right) \stackrel{(i)}{\rightarrow} O_p \left(\frac{1}{n} \right),
\end{aligned}$$

where (i) is due to the definition of $\hat{\Sigma}_{-i}$ and (A1)(A2)(A4), which implies that the non-zero eigenvalues of $\Sigma_{\mathbf{X}\mathbf{P}}$, $\Sigma_{\theta/\mathbf{P}}$, $\hat{\Sigma}$ and $\hat{\Sigma}_{-i}$ are finite and lower-bounded away from zero as $n, d \rightarrow \infty$ (we take the pseudo-inverse of $\hat{\Sigma}$ when $\lambda \rightarrow 0$). The result on the numerator can be obtained via a similar calculation, the details of which we omit.

Note that the denominator can be evaluated by previous results (e.g. [DW⁺18, Theorem 2.1]) as follows,

$$\frac{1}{n} \text{tr} \left(\left(\frac{1}{n} \bar{\mathbf{X}}^\top \bar{\mathbf{X}} + \lambda \mathbf{I}_d \right)^{-1} \Sigma_{\mathbf{X}\mathbf{P}} \right) \xrightarrow{a.s.} \frac{1}{\lambda m(-\lambda)} - 1. \quad (\text{C.3})$$

On the other hand, following the same derivation as [DW⁺18, HMRT19], (C.1) can be decomposed as

$$\begin{aligned} & \frac{1}{d} \text{tr} \left(\frac{1}{n} \hat{\mathbf{X}}^\top \hat{\mathbf{X}} \left(\frac{1}{n} \hat{\mathbf{X}}^\top \hat{\mathbf{X}} + \lambda \mathbf{D}_{\theta/\mathbf{P}}^{-1} \right)^{-2} \right) \\ &= \frac{1}{d} \text{tr} \left(\left(\frac{1}{n} \bar{\mathbf{X}}^\top \bar{\mathbf{X}} + \lambda \mathbf{I}_d \right)^{-1} \Sigma_{\theta/\mathbf{P}} \right) - \frac{\lambda}{d} \text{tr} \left(\left(\frac{1}{n} \bar{\mathbf{X}}^\top \bar{\mathbf{X}} + \lambda \mathbf{I}_d \right)^{-2} \Sigma_{\theta/\mathbf{P}} \right) \\ &= \frac{1}{d} \text{tr} \left(\left(\frac{1}{n} \bar{\mathbf{X}}^\top \bar{\mathbf{X}} + \lambda \mathbf{I}_d \right)^{-1} \Sigma_{\theta/\mathbf{P}} \right) + \frac{\lambda}{d} \frac{d}{d\lambda} \text{tr} \left(\left(\frac{1}{n} \bar{\mathbf{X}}^\top \bar{\mathbf{X}} + \lambda \mathbf{I}_d \right)^{-1} \Sigma_{\theta/\mathbf{P}} \right). \end{aligned} \quad (\text{C.4})$$

We employ [RM11, Theorem 1] to characterize (C.4). In particular, For any deterministic sequence of matrices $\Theta_n \in \mathbb{R}^{d \times d}$ with finite trace norm, as $n, d \rightarrow \infty$ we have

$$\text{tr} \left(\Theta_n \left(\frac{1}{n} \bar{\mathbf{X}}^\top \bar{\mathbf{X}} - z \mathbf{I}_d \right)^{-1} - \Theta_n (c_n(z) \Sigma_{\mathbf{X}\mathbf{P}} - z \mathbf{I}_d)^{-1} \right) \xrightarrow{a.s.} 0,$$

in which $c_n(z) \rightarrow -zm(z)$ for $z \in \mathbb{C} \setminus \mathbb{R}^+$ and $m(z)$ is defined in Theorem 1 due to the dominated convergence theorem. By (A2)(A4) we are allowed to take $\Theta_n = \frac{1}{d} \Sigma_{\theta/\mathbf{P}}$. Thus we have

$$\begin{aligned} \frac{\lambda}{d} \text{tr} \left(\Sigma_{\theta/\mathbf{P}} \left(\frac{1}{n} \bar{\mathbf{X}}^\top \bar{\mathbf{X}} + \lambda \mathbf{I}_d \right)^{-1} \right) &\rightarrow \frac{\lambda}{d} \text{tr} \left(\Sigma_{\theta/\mathbf{P}} (\lambda m(-\lambda) \Sigma_{\mathbf{X}\mathbf{P}} + \lambda \mathbf{I}_d)^{-1} \right) \\ &\stackrel{(i)}{=} \mathbb{E} \left[\frac{v_x v_\theta v_{xp}^{-1}}{1 + m(-\lambda) v_{xp}} \right], \quad \forall \lambda > -c_l, \end{aligned} \quad (\text{C.5})$$

in which (i) is due to (A2)(A4), the fact that the LHS is almost surely bounded for $\lambda > -c_l$, where c_l is the lowest non-zero eigenvalue of $\frac{1}{n} \bar{\mathbf{X}}^\top \bar{\mathbf{X}}$, and the application of the dominated convergence theorem. Differentiating (C.5) (note that the derivative is also bounded on $\lambda > -c_l$) yields

$$\frac{\lambda}{d} \frac{d}{d\lambda} \text{tr} \left(\left(\frac{1}{n} \bar{\mathbf{X}}^\top \bar{\mathbf{X}} + \lambda \mathbf{I}_d \right)^{-1} \Sigma_{\theta/\mathbf{P}} \right) \rightarrow \mathbb{E} \left[\frac{v_x v_\theta v_{xp}^{-1}}{\lambda(1 + m(-\lambda) v_{xp})} - \frac{m'(-\lambda) v_x v_\theta}{(1 + m(-\lambda) v_{xp})^2} \right]. \quad (\text{C.6})$$

Finally, note that the numerator of (C.2) is the quantity of interest. Combining (C.1) (C.2) (C.3) (C.4) (C.5) (C.6) and taking $\lambda \rightarrow 0$ yields the formula of the bias term. We remark that similar (but less general) characterization can also be derived based on [LP11, Theorem 1.2] when the eigenvalues of $\mathbf{D}_{\mathbf{X}\mathbf{P}}$ and $\mathbf{D}_{\theta/\mathbf{P}}$ exhibit certain relations.

To show that $\mathbf{P} = \Sigma_\theta$ achieves the lowest bias, first note that under the definition of random variables in (A4), our claimed optimal preconditioner is equivalent to $v_{xp} \stackrel{a.s.}{=} v_x v_\theta$. We therefore define an interpolation $v_\alpha = \alpha v_x v_\theta + (1 - \alpha) \bar{v}$ for some \bar{v} and write the corresponding Stieltjes transform as $m_\alpha(-\lambda)$ and the bias term as B_α . We aim to show that $\text{argmin}_{\alpha \in [0,1]} B_\alpha = 1$.

For notational convenience define $g_\alpha \triangleq m_\alpha(0) v_x v_\theta$ and $h_\alpha \triangleq m_\alpha(0) v_\alpha$. One can check that

$$B_\alpha = \mathbb{E} \left[\frac{v_x v_\theta}{(1 + h_\alpha)^2} \right] \mathbb{E} \left[\frac{h_\alpha}{(1 + h_\alpha)^2} \right]^{-1}; \quad \left. \frac{dm_\alpha(-\lambda)}{d\alpha} \right|_{\lambda \rightarrow 0} = \frac{m_\alpha(0) \mathbb{E} \left[\frac{h_\alpha - g_\alpha}{(1 + h_\alpha)^2} \right]}{(1 - \alpha) \mathbb{E} \left[\frac{h_\alpha}{(1 + h_\alpha)^2} \right]}.$$

We now verify that the derivative of B_α w.r.t. α is non-positive for $\alpha \in [0, 1]$. A standard simplification of the derivative yields

$$\begin{aligned} \frac{dB_\alpha}{d\alpha} &\propto -2\mathbb{E}\left[\frac{(g_\alpha - h_\alpha)^2}{(1 + h_\alpha)^3}\right] \left(\mathbb{E}\left[\frac{h_\alpha}{(1 + h_\alpha)^2}\right]\right)^2 - 2\left(\mathbb{E}\left[\frac{g_\alpha - h_\alpha}{(1 + h_\alpha)^2}\right]\right)^2 \mathbb{E}\left[\frac{h_\alpha^2}{(1 + h_\alpha)^3}\right] \\ &\quad + 4\mathbb{E}\left[\frac{h_\alpha(g_\alpha - h_\alpha)}{(1 + h_\alpha)^3}\right] \mathbb{E}\left[\frac{g_\alpha - h_\alpha}{(1 + h_\alpha)^2}\right] \mathbb{E}\left[\frac{h_\alpha}{(1 + h_\alpha)^2}\right] \\ &\stackrel{(i)}{\leq} -4\sqrt{\mathbb{E}\left[\frac{(g_\alpha - h_\alpha)^2}{(1 + h_\alpha)^3}\right] \mathbb{E}\left[\frac{h_\alpha^2}{(1 + h_\alpha)^3}\right] \left(\mathbb{E}\left[\frac{g_\alpha - h_\alpha}{(1 + h_\alpha)^2}\right]\right)^2 \left(\mathbb{E}\left[\frac{h_\alpha}{(1 + h_\alpha)^2}\right]\right)^2} \\ &\quad + 4\mathbb{E}\left[\frac{h_\alpha(g_\alpha - h_\alpha)}{(1 + h_\alpha)^3}\right] \mathbb{E}\left[\frac{g_\alpha - h_\alpha}{(1 + h_\alpha)^2}\right] \mathbb{E}\left[\frac{h_\alpha}{(1 + h_\alpha)^2}\right] \stackrel{(ii)}{\leq} 0, \end{aligned}$$

where (i) is due to AM-GM and (ii) due to Cauchy-Schwarz on the first term. Note that the two equalities hold when $g_\alpha = h_\alpha$, from which one can easily deduce that the optimum is achieved when $v_{xp} \stackrel{a.s.}{=} v_x v_\theta$, and thus we know that $\mathbf{P} = \boldsymbol{\Sigma}_\theta$ is the optimal preconditioner for the bias term. \square

C.4 Proof of Proposition 3

Proof. Via a similar calculation as in [HMRT19, Section 5], the bias term can be decomposed as

$$\begin{aligned} \mathbb{E}[B(\hat{\boldsymbol{\theta}}_{\mathbf{P}})] &= \mathbb{E}_{\mathbf{x}, \hat{\mathbf{x}}, \boldsymbol{\theta}^*, \boldsymbol{\theta}^c} \left[\left(\mathbf{x}^\top \mathbf{P} \mathbf{X}^\top (\mathbf{X} \mathbf{P} \mathbf{X}^\top)^{-1} (\mathbf{X} \boldsymbol{\theta}^* + \mathbf{X}^c \boldsymbol{\theta}^c) - (\mathbf{x}^\top \boldsymbol{\theta}^* + \hat{\mathbf{x}}^\top \boldsymbol{\theta}^c) \right)^2 \right] \\ &\stackrel{(i)}{=} \mathbb{E}_{\mathbf{x}, \boldsymbol{\theta}^*} \left[\left(\mathbf{x}^\top \mathbf{P} \mathbf{X}^\top (\mathbf{X} \mathbf{P} \mathbf{X}^\top)^{-1} \mathbf{X} \boldsymbol{\theta}^* - \mathbf{x}^\top \boldsymbol{\theta}^* \right)^2 \right] + \mathbb{E}_{\mathbf{x}^c, \boldsymbol{\theta}^c} \left[(\hat{\mathbf{x}}^\top \boldsymbol{\theta}^c)^2 \right] \\ &\quad + \mathbb{E}_{\mathbf{x}, \boldsymbol{\theta}^c} \left[\left(\mathbf{x}^\top \mathbf{P} \mathbf{X}^\top (\mathbf{X} \mathbf{P} \mathbf{X}^\top)^{-1} \mathbf{X}^c \boldsymbol{\theta}^c \boldsymbol{\theta}^{c\top} \mathbf{X}^{c\top} (\mathbf{X} \mathbf{P} \mathbf{X}^\top)^{-1} \mathbf{X} \mathbf{P} \mathbf{x} \right)^2 \right] \\ &\stackrel{(ii)}{\rightarrow} B_\theta(\hat{\boldsymbol{\theta}}_{\mathbf{P}}) + \frac{1}{d^c} \text{tr}(\boldsymbol{\Sigma}_{\mathbf{X}^c} \boldsymbol{\Sigma}_{\boldsymbol{\theta}^c}) (1 + V(\hat{\boldsymbol{\theta}}_{\mathbf{P}})), \end{aligned}$$

where we used the independence of \mathbf{x} , $\hat{\mathbf{x}}$ and $\boldsymbol{\theta}^*$, $\boldsymbol{\theta}^c$ in (i), and (A2-4) as well as the definition of the well-specified bias $B_\theta(\hat{\boldsymbol{\theta}}_{\mathbf{P}})$ and variance $V(\hat{\boldsymbol{\theta}}_{\mathbf{P}})$ in (ii). \square

C.5 Proof of Proposition 4

Proof. We first outline a more general setup where $\mathbf{P}_\alpha = f(\boldsymbol{\Sigma}_{\mathbf{X}}; \alpha)$ for continuous and differentiable function of α and f applied to the eigenvalues of $\boldsymbol{\Sigma}_{\mathbf{x}}$. For any interval $\mathcal{I} \subseteq [0, 1]$, we claim that

- Suppose all four functions $\frac{1}{xf(x;\alpha)}$, $f(x;\alpha)$, $\frac{\partial f(x;\alpha)}{\partial \alpha}/f(x;\alpha)$ and $x \frac{\partial f(x;\alpha)}{\partial \alpha}$ are decreasing functions of x on the support of v_x for all $\alpha \in \mathcal{I}$. In addition, $\frac{\partial f(x;\alpha)}{\partial \alpha} \geq 0$ on the support of v_x for all $\alpha \in \mathcal{I}$. Then the stationary bias is an increasing function of α on \mathcal{I} .
- For all $\alpha \in \mathcal{I}$, suppose $xf(x;\alpha)$ is a monotonic function of x on the support of v_x and $\frac{\partial f(x;\alpha)}{\partial \alpha}/f(x;\alpha)$ is a decreasing function of x on the support of v_x . Then the stationary variance is a decreasing function of α on \mathcal{I} .

Let us verify the three choices of \mathbf{P}_α in Proposition 4 one by one.

- When $\mathbf{P}_\alpha = (1 - \alpha)\mathbf{I}_d + \alpha(\boldsymbol{\Sigma}_{\mathbf{X}})^{-1}$, the corresponding $f(x;\alpha)$ is $(1 - \alpha) + \alpha x$. It is clear that it satisfies all conditions in (a) and (b) for all $\alpha \in [0, 1]$. Hence, the stationary variance is a decreasing function and the stationary bias is an increasing function of $\alpha \in [0, 1]$.

- When $\mathbf{P}_\alpha = (\boldsymbol{\Sigma}_\mathbf{X})^{-\alpha}$, the corresponding $f(x; \alpha)$ is $x^{-\alpha}$. It is clear that it satisfies all conditions in (a) and (b) for all $\alpha \in [0, 1]$ except for the condition that $x \frac{\partial f(x; \alpha)}{\partial \alpha} = -x^{1-\alpha} \ln x$ is a decreasing function of x . Note that $x \frac{\partial f(x; \alpha)}{\partial \alpha} = -x^{1-\alpha} \ln x$ is a decreasing function of x on the support of v_x only for $\alpha \geq \frac{\ln(\kappa)-1}{\ln(\kappa)}$ where $\kappa = \sup v_x / \inf v_x$. Hence, the stationary variance is a decreasing function of $\alpha \in [0, 1]$ and the stationary bias is an increasing function of $\alpha \in [\max(0, \frac{\ln(\kappa)-1}{\ln(\kappa)}), 1]$.
- When $\mathbf{P}_\alpha = (\alpha \boldsymbol{\Sigma}_\mathbf{X} + (1-\alpha) \mathbf{I}_d)^{-1}$, the corresponding $f(x; \alpha)$ is $1/(\alpha x + (1-\alpha))$. It is clear that it satisfies all conditions in (a) and (b) for all $\alpha \in [0, 1]$ except for the condition that $x \frac{\partial f(x; \alpha)}{\partial \alpha} = \frac{x(1-x)}{(\alpha x + (1-\alpha))^2}$ is a decreasing function of x . Note that $x \frac{\partial f(x; \alpha)}{\partial \alpha} = \frac{x(1-x)}{(\alpha x + (1-\alpha))^2}$ is a decreasing function of x on the support of v_x only for $\alpha \geq \frac{\kappa-2}{\kappa-1}$. Hence, the stationary variance is a decreasing function of $\alpha \in [0, 1]$ and the stationary bias is an increasing function of $\alpha \in [\max(0, \frac{\kappa-2}{\kappa-1}), 1]$.

To show (a) and (b), note that under the conditions on $\boldsymbol{\Sigma}_\mathbf{x}$ and $\boldsymbol{\Sigma}_\boldsymbol{\theta}$ assumed in Proposition 4, the stationary bias $B(\hat{\boldsymbol{\theta}}_{\mathbf{P}_\alpha})$ and the stationary variance $V(\hat{\boldsymbol{\theta}}_{\mathbf{P}_\alpha})$ can be simplified to

$$B(\hat{\boldsymbol{\theta}}_{\mathbf{P}_\alpha}) = \frac{m'_\alpha(0)}{m_\alpha^2(0)} \mathbb{E} \frac{v_x}{(1 + v_x f(v_x; \alpha) m_\alpha(0))^2} \quad \text{and} \quad V(\hat{\boldsymbol{\theta}}_{\mathbf{P}_\alpha}) = \sigma^2 \cdot \left(\frac{m'_\alpha(0)}{m_\alpha^2(0)} - 1 \right),$$

where $m_\alpha(z)$ and $m'_\alpha(z)$ satisfy

$$1 = -z m_\alpha(z) + \gamma \mathbb{E} \frac{v_x f(v_x; \alpha) m_\alpha(z)}{1 + v_x f(v_x; \alpha) m_\alpha(z)} \quad (\text{C.7})$$

$$\frac{m'_\alpha(z)}{m_\alpha^2(z)} = \frac{1}{1 - \gamma \mathbb{E} \left(\frac{f(v_x; \alpha) m_\alpha(z)}{1 + f(v_x; \alpha) m_\alpha(z)} \right)^2}. \quad (\text{C.8})$$

For notation convenience, let $f_\alpha := v_x f(v_x; \alpha)$. From (C.8), we have the following equivalent expressions.

$$B(\hat{\boldsymbol{\theta}}_{\mathbf{P}_\alpha}) = \frac{\mathbb{E} \frac{v_x}{(1 + f_\alpha m_\alpha(0))^2}}{1 - \gamma \mathbb{E} \left(\frac{f_\alpha m_\alpha(0)}{1 + f_\alpha m_\alpha(0)} \right)^2}, \quad (\text{C.9})$$

$$V(\hat{\boldsymbol{\theta}}_{\mathbf{P}_\alpha}) = \sigma^2 \left(\frac{1}{1 - \gamma \mathbb{E} \left(\frac{f_\alpha m_\alpha(0)}{1 + f_\alpha m_\alpha(0)} \right)^2} - 1 \right). \quad (\text{C.10})$$

We first show that (b) holds. Note that from (C.10), we have

$$\frac{\partial V(\hat{\boldsymbol{\theta}}_{\mathbf{P}_\alpha})}{\partial \alpha} = \gamma \sigma^2 \left(\frac{1}{1 - \gamma \mathbb{E} \left(\frac{f_\alpha m_\alpha(0)}{1 + f_\alpha m_\alpha(0)} \right)^2} \right)^2 \mathbb{E} \left[\frac{2 f_\alpha m_\alpha(0)}{(1 + f_\alpha m_\alpha(0))^3} \left(f_\alpha \frac{\partial m_\alpha(z)}{\partial \alpha} \Big|_{z=0} + \frac{\partial f_\alpha}{\partial \alpha} m_\alpha(0) \right) \right]. \quad (\text{C.11})$$

To calculate $\frac{\partial m_\alpha(z)}{\partial \alpha} \Big|_{z=0}$, we take derivatives with respect to α on both sides of (C.7),

$$0 = \gamma \mathbb{E} \left[\frac{1}{(1 + f_\alpha m_\alpha(0))^2} \cdot \left(f_\alpha \frac{\partial m_\alpha(z)}{\partial \alpha} \Big|_{z=0} + \frac{\partial f_\alpha}{\partial \alpha} m_\alpha(0) \right) \right]. \quad (\text{C.12})$$

Therefore, plugging (C.12) into (C.11) yields

$$\begin{aligned} \frac{\partial V(\hat{\boldsymbol{\theta}}_{\mathbf{P}_\alpha})}{\partial \alpha} &= 2\gamma \sigma^2 \left(\frac{m_\alpha(0)}{1 - \gamma \mathbb{E} \left(\frac{f_\alpha m_\alpha(0)}{1 + f_\alpha m_\alpha(0)} \right)^2} \right)^2 \left(\mathbb{E} \frac{f_\alpha}{(1 + f_\alpha m_\alpha(0))^2} \right)^{-1} \\ &\quad \times \left(\mathbb{E} \frac{f_\alpha \frac{\partial f_\alpha}{\partial \alpha}}{(1 + f_\alpha m_\alpha(0))^3} \mathbb{E} \frac{f_\alpha}{(1 + f_\alpha m_\alpha(0))^2} - \mathbb{E} \frac{f_\alpha^2}{(1 + f_\alpha m_\alpha(0))^3} \mathbb{E} \frac{\frac{\partial f_\alpha}{\partial \alpha}}{(1 + f_\alpha m_\alpha(0))^2} \right) \end{aligned}$$

Thus showing $V(\hat{\theta}_{\mathbf{P}_\alpha})$ is a decreasing function of α is equivalent to showing that

$$\mathbb{E} \frac{f_\alpha^2}{(1 + f_\alpha m_\alpha(0))^3} \mathbb{E} \frac{\frac{\partial f_\alpha}{\partial \alpha}}{(1 + f_\alpha m_\alpha(0))^2} \geq \mathbb{E} \frac{f_\alpha \frac{\partial f_\alpha}{\partial \alpha}}{(1 + f_\alpha m_\alpha(0))^3} \mathbb{E} \frac{f_\alpha}{(1 + f_\alpha m_\alpha(0))^2}. \quad (\text{C.13})$$

Let μ_x be the probability measure of v_x . We define a new measure $\tilde{\mu}_x = \frac{f_\alpha \mu_x}{(1 + f_\alpha m_\alpha(0))^2}$, and let \tilde{v}_x follow the new measure. Since $\frac{\partial f(x; \alpha)}{\partial \alpha} / f(x; \alpha)$ is a decreasing function of x and $xf(x; \alpha)$ is a monotonic function of x ,

$$\mathbb{E} \frac{\tilde{v}_x f(\tilde{v}_x; \alpha)}{1 + \tilde{v}_x f(\tilde{v}_x; \alpha) m_\alpha(0)} \mathbb{E} \frac{\frac{\partial \tilde{v}_x f(\tilde{v}_x; \alpha)}{\partial \alpha}}{\tilde{v}_x f(\tilde{v}_x; \alpha)} \geq \mathbb{E} \frac{\frac{\partial \tilde{v}_x f(\tilde{v}_x; \alpha)}{\partial \alpha}}{1 + \tilde{v}_x f(\tilde{v}_x; \alpha) m_\alpha(0)}.$$

Changing \tilde{v}_x back to v_x , we arrive at (C.13) and thus (b).

For the bias term $B(\hat{\theta}_{\mathbf{P}_\alpha})$, note that from (C.7) and (C.9), we have

$$\begin{aligned} \frac{\partial B(\hat{\theta}_{\mathbf{P}_\alpha})}{\partial \alpha} &= \frac{1}{\gamma} \left(\frac{1}{\gamma} - \mathbb{E} \left(\frac{f_\alpha m_\alpha(0)}{1 + f_\alpha m_\alpha(0)} \right)^2 \right)^{-2} \\ &\quad \times \left(-\mathbb{E} \left[2 \frac{v_x}{(1 + f_\alpha m_\alpha(0))^3} \cdot \left(f_\alpha \frac{\partial m_\alpha(z)}{\partial \alpha} \Big|_{z=0} + \frac{\partial f_\alpha}{\partial \alpha} m_\alpha(0) \right) \right] \mathbb{E} \frac{f_\alpha m_\alpha(0)}{(1 + f_\alpha m_\alpha(0))^2} \right. \\ &\quad \left. + \mathbb{E} \frac{v_x}{(1 + f_\alpha m_\alpha(0))^2} \mathbb{E} \left[2 \frac{f_\alpha m_\alpha(0)}{(1 + f_\alpha m_\alpha(0))^3} \cdot \left(f_\alpha \frac{\partial m_\alpha(z)}{\partial \alpha} \Big|_{z=0} + \frac{\partial f_\alpha}{\partial \alpha} m_\alpha(0) \right) \right] \right). \quad (\text{C.14}) \end{aligned}$$

Similarly, we combine (C.12) and (C.14) and simplify the expression. To verify $B(\hat{\theta}_{\mathbf{P}_\alpha})$ is an increasing function of α , we need to show that

$$\begin{aligned} 0 \leq & \left(\mathbb{E} \frac{v_x f_\alpha m_\alpha(0)}{(1 + f_\alpha m_\alpha(0))^3} \mathbb{E} \frac{\frac{\partial f_\alpha}{\partial \alpha}}{(1 + f_\alpha m_\alpha(0))^2} - \mathbb{E} \frac{v_x \frac{\partial f_\alpha}{\partial \alpha}}{(1 + f_\alpha m_\alpha(0))^3} \mathbb{E} \frac{f_\alpha m_\alpha(0)}{(1 + f_\alpha m_\alpha(0))^2} \right) \mathbb{E} \frac{f_\alpha m_\alpha(0)}{(1 + f_\alpha m_\alpha(0))^2} \\ & - \mathbb{E} \frac{v_x}{(1 + f_\alpha m_\alpha(0))^2} \left(\mathbb{E} \frac{(f_\alpha m_\alpha(0))^2}{(1 + f_\alpha m_\alpha(0))^3} \mathbb{E} \frac{\frac{\partial f_\alpha}{\partial \alpha}}{(1 + f_\alpha m_\alpha(0))^2} - \mathbb{E} \frac{f_\alpha m_\alpha(0) \frac{\partial f_\alpha}{\partial \alpha}}{(1 + f_\alpha m_\alpha(0))^3} \mathbb{E} \frac{f_\alpha m_\alpha(0)}{(1 + f_\alpha m_\alpha(0))^2} \right), \quad (\text{C.15}) \end{aligned}$$

Let $h_\alpha \triangleq f_\alpha m_\alpha(0) = v_x f(v_x; \alpha) m_\alpha(0)$ and $g_\alpha \triangleq \frac{\partial f_\alpha}{\partial \alpha} = v_x \frac{\partial f(v_x; \alpha)}{\partial \alpha}$. Then (C.15) can be further simplified to the following equation

$$\begin{aligned} 0 \leq & \underbrace{\mathbb{E} \frac{v_x h_\alpha}{(1 + h_\alpha)^3} \mathbb{E} \frac{g_\alpha}{(1 + h_\alpha)^3} \mathbb{E} \frac{h_\alpha}{(1 + h_\alpha)^3} - \mathbb{E} \frac{v_x}{(1 + h_\alpha)^3} \mathbb{E} \frac{g_\alpha}{(1 + h_\alpha)^3} \mathbb{E} \frac{h_\alpha^2}{(1 + h_\alpha)^3}}_{\text{part 1}} \\ & + \underbrace{\mathbb{E} \frac{v_x}{(1 + h_\alpha)^3} \mathbb{E} \frac{g_\alpha h_\alpha}{(1 + h_\alpha)^3} \mathbb{E} \frac{h_\alpha}{(1 + h_\alpha)^3} - \mathbb{E} \frac{v_x g_\alpha}{(1 + h_\alpha)^3} \mathbb{E} \frac{h_\alpha}{(1 + h_\alpha)^3} \mathbb{E} \frac{h_\alpha}{(1 + h_\alpha)^3}}_{\text{part 2}} \\ & + \underbrace{2 \mathbb{E} \frac{v_x h_\alpha}{(1 + h_\alpha)^3} \mathbb{E} \frac{g_\alpha h_\alpha}{(1 + h_\alpha)^3} \mathbb{E} \frac{h_\alpha}{(1 + h_\alpha)^3} - 2 \mathbb{E} \frac{v_x g_\alpha}{(1 + h_\alpha)^3} \mathbb{E} \frac{h_\alpha^2}{(1 + h_\alpha)^3} \mathbb{E} \frac{h_\alpha}{(1 + h_\alpha)^3}}_{\text{part 3}} \\ & + \underbrace{\mathbb{E} \frac{v_x h_\alpha}{(1 + h_\alpha)^3} \mathbb{E} \frac{g_\alpha h_\alpha}{(1 + h_\alpha)^3} \mathbb{E} \frac{h_\alpha^2}{(1 + h_\alpha)^3} - \mathbb{E} \frac{v_x g_\alpha}{(1 + h_\alpha)^3} \mathbb{E} \frac{h_\alpha^2}{(1 + h_\alpha)^3} \mathbb{E} \frac{h_\alpha^2}{(1 + h_\alpha)^3}}_{\text{part 4}}. \quad (\text{C.16}) \end{aligned}$$

Note that under condition of (a), we know that both h_α and v_x/h_α are increasing functions of v_x ; and both g_α/h_α and g_α are decreasing functions of v_x . Hence, with calculation similar to (C.13), we know part 1,2,3,4 in (C.16) are all non-negative, and therefore (C.16) holds. \square

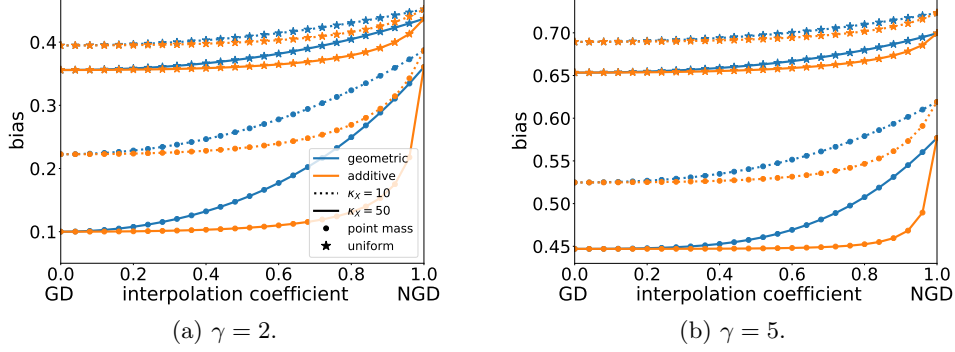


Figure 21: Illustration of the monotonicity of the bias term under $\Sigma_{\theta} = \mathbf{I}_d$. We consider two distributions of eigenvalues for $\Sigma_{\mathbf{X}}$: two equally weighted point masses (circle) and a uniform distribution (star), and vary the condition number $\kappa_{\mathbf{X}}$ and overparameterization level γ . In all cases the bias is monotone in $\alpha \in [0, 1]$.

Remark. *The above characterization provides sufficient but not necessary conditions for the monotonicity of the bias term. In general, the expression of the bias is rather opaque, and determining the sign of its derivative can be tedious, except for certain special cases (e.g. $\gamma = 2$ and the eigenvalues of $\Sigma_{\mathbf{X}}$ are two equally weighted point masses, for which m_{α} has a simple form and one may analytically check the monotonicity). We conjecture that the bias is monotone for $\alpha \in [0, 1]$ for a much wider class of $\Sigma_{\mathbf{X}}$, as shown in Figure 21.*

C.6 Proof of Proposition 5

Proof. Taking the derivative of $V(\theta_{\mathbf{P}}(t))$ w.r.t. time yields (omitting the scalar σ^2),

$$\begin{aligned} \frac{dV(\theta_{\mathbf{P}}(t))}{dt} &= \frac{d}{dt} \left\| \Sigma_{\mathbf{X}}^{1/2} \mathbf{P} \mathbf{X}^{\top} \left(\mathbf{I}_n - \exp\left(-\frac{t}{n} \mathbf{X} \mathbf{P} \mathbf{X}^{\top}\right) \right) \left(\mathbf{X} \mathbf{P} \mathbf{X}^{\top} \right)^{-1} \right\|_F^2 \\ &\stackrel{(i)}{=} \frac{1}{n} \text{tr} \left(\underbrace{\Sigma_{\mathbf{X} \mathbf{P}} \bar{\mathbf{X}}^{\top} \mathbf{S}_{\mathbf{P}} \exp\left(-\frac{t}{n} \mathbf{S}_{\mathbf{P}}\right) \mathbf{S}_{\mathbf{P}}^{-2} \left(\mathbf{I}_n - \exp\left(-\frac{t}{n} \mathbf{S}_{\mathbf{P}}\right) \right) \bar{\mathbf{X}}}_{p.s.d.} \right) \stackrel{(ii)}{>} 0, \end{aligned}$$

where we defined $\bar{\mathbf{X}} = \mathbf{X} \mathbf{P}^{1/2}$ and $\mathbf{S}_{\mathbf{P}} = \mathbf{X} \mathbf{P} \mathbf{X}^{\top}$ in (i), and (ii) is due to (A2-3) the inequality $\text{tr}(\mathbf{A} \mathbf{B}) \geq \lambda_{\min}(\mathbf{A}) \text{tr}(\mathbf{B})$ for positive semi-definite \mathbf{A} and \mathbf{B} . \square

C.7 Proof of Proposition 6

Proof. Recall the definition of the bias (well-specified) of $\hat{\theta}_{\mathbf{P}}(t)$,

$$\begin{aligned} B(\theta_{\mathbf{P}}(t)) &\stackrel{(i)}{=} \frac{1}{d} \text{tr} \left(\Sigma_{\theta} \left(\mathbf{I}_d - \mathbf{P} \mathbf{X}^{\top} \mathbf{W}_{\mathbf{P}}(t) \mathbf{S}_{\mathbf{P}}^{-1} \mathbf{X} \right)^{\top} \Sigma_{\mathbf{X}} \left(\mathbf{I}_d - \mathbf{P} \mathbf{X}^{\top} \mathbf{W}_{\mathbf{P}}(t) \mathbf{S}_{\mathbf{P}}^{-1} \mathbf{X} \right) \right) \\ &\stackrel{(ii)}{=} \frac{1}{d} \text{tr} \left(\Sigma_{\theta/\mathbf{P}} \left(\mathbf{I}_d - \bar{\mathbf{X}}^{\top} \mathbf{W}_{\mathbf{P}}(t) \mathbf{S}_{\mathbf{P}}^{-1} \bar{\mathbf{X}} \right)^{\top} \Sigma_{\mathbf{X} \mathbf{P}} \left(\mathbf{I}_d - \bar{\mathbf{X}}^{\top} \mathbf{W}_{\mathbf{P}}(t) \mathbf{S}_{\mathbf{P}}^{-1} \bar{\mathbf{X}} \right) \right) \\ &\stackrel{(iii)}{\geq} \frac{1}{d} \text{tr} \left(\left(\Sigma_{\mathbf{X} \mathbf{P}}^{1/2} \left(\mathbf{I}_d - \bar{\mathbf{X}}^{\top} \mathbf{W}_{\mathbf{P}}(t) \mathbf{S}_{\mathbf{P}}^{-1} \bar{\mathbf{X}} \right) \Sigma_{\theta/\mathbf{P}}^{1/2} \right)^2 \right), \end{aligned} \tag{C.17}$$

where we defined $\mathbf{S}_{\mathbf{P}} = \mathbf{X} \mathbf{P} \mathbf{X}^{\top}$, $\mathbf{W}_{\mathbf{P}}(t) = \mathbf{I}_n - \exp\left(-\frac{t}{n} \mathbf{S}_{\mathbf{P}}\right)$ in (i), $\bar{\mathbf{X}} = \mathbf{X} \mathbf{P}^{1/2}$ in (ii), and (iii) is due to the inequality $\text{tr}(\mathbf{A}^{\top} \mathbf{A}) \geq \text{tr}(\mathbf{A}^2)$.

When $\Sigma_{\mathbf{X}} = \Sigma_{\boldsymbol{\theta}}^{-1}$, i.e. NGD achieves lowest stationary bias, (C.17) simplifies to

$$B(\boldsymbol{\theta}_{\mathbf{P}}(t)) \geq \frac{1}{d} \text{tr} \left(\left(\mathbf{I}_d - \bar{\mathbf{X}}^\top \mathbf{W}_{\mathbf{P}}(t) \mathbf{S}_{\mathbf{P}}^{-1} \bar{\mathbf{X}} \right)^2 \right) = \left(1 - \frac{1}{\gamma} \right) + \frac{1}{d} \sum_{i=1}^n \exp \left(-\frac{t}{n} \bar{\lambda}_i \right)^2, \quad (\text{C.18})$$

where $\bar{\lambda}$ is the eigenvalue of $\mathbf{S}_{\mathbf{P}}$. On the other hand, since $\mathbf{F} = \Sigma_{\mathbf{X}}$, for the NGD iterate $\hat{\boldsymbol{\theta}}_{\mathbf{F}^{-1}}(t)$ we have

$$B(\boldsymbol{\theta}_{\mathbf{F}^{-1}}(t)) = \frac{1}{d} \text{tr} \left(\left(\mathbf{I}_d - \hat{\mathbf{X}}^\top \mathbf{W}_{\mathbf{F}^{-1}}(t) \mathbf{S}_{\mathbf{F}^{-1}}^{-1} \hat{\mathbf{X}} \right)^2 \right) = \left(1 - \frac{1}{\gamma} \right) + \frac{1}{d} \sum_{i=1}^n \exp \left(-\frac{t}{n} \hat{\lambda}_i \right)^2, \quad (\text{C.19})$$

where $\hat{\mathbf{X}} = \mathbf{X} \Sigma_{\mathbf{X}}^{-1/2}$ and $\bar{\lambda}$ is the eigenvalue of $\mathbf{S}_{\mathbf{F}^{-1}} = \hat{\mathbf{X}} \hat{\mathbf{X}}^\top$. Comparing (C.18)(C.19), we see that given $\hat{\boldsymbol{\theta}}_{\mathbf{P}}(t)$ at a fixed t , if we run NGD for time $T > \frac{\bar{\lambda}_{\max}}{\bar{\lambda}_{\min}} t$ (note that $T/t = O(1)$ by (A2-3)), then we have $B(\boldsymbol{\theta}_{\mathbf{P}}(t)) \geq B(\boldsymbol{\theta}_{\mathbf{F}^{-1}}(T))$ for any \mathbf{P} satisfying (A3). This thus implies that $B^{\text{opt}}(\boldsymbol{\theta}_{\mathbf{P}}) \geq B^{\text{opt}}(\boldsymbol{\theta}_{\mathbf{F}^{-1}})$.

On the other hand, when $\Sigma_{\boldsymbol{\theta}} = \mathbf{I}_d$, we can show that the bias term of GD is monotonically decreasing through time by taking its derivative,

$$\begin{aligned} \frac{d}{dt} B(\boldsymbol{\theta}_{\mathbf{I}}(t)) &= \frac{1}{d} \frac{d}{dt} \text{tr} \left(\left(\mathbf{I}_d - \mathbf{X}^\top \mathbf{W}_{\mathbf{I}}(t) \mathbf{S}_{\mathbf{I}}^{-1} \mathbf{X} \right)^\top \Sigma_{\mathbf{X}} \left(\mathbf{I}_d - \mathbf{X}^\top \mathbf{W}_{\mathbf{I}}(t) \mathbf{S}_{\mathbf{I}}^{-1} \mathbf{X} \right) \right) \\ &= -\frac{1}{nd} \text{tr} \left(\underbrace{\Sigma_{\mathbf{X}} \mathbf{X}^\top \mathbf{S} \exp \left(-\frac{t}{n} \mathbf{S} \right) \mathbf{S}^{-1} \mathbf{X} \left(\mathbf{I}_d - \mathbf{X}^\top \mathbf{W}_{\mathbf{I}}(t) \mathbf{S}_{\mathbf{I}}^{-1} \mathbf{X} \right)}_{p.s.d.} \right) < 0. \end{aligned} \quad (\text{C.20})$$

Similarly, one can verify that the expected bias of NGD is monotonically decreasing for all choices of $\Sigma_{\mathbf{X}}$ and $\Sigma_{\boldsymbol{\theta}}$ satisfying (A2-4),

$$\begin{aligned} &\frac{d}{dt} \text{tr} \left(\Sigma_{\boldsymbol{\theta}} \left(\mathbf{I}_d - \mathbf{F}^{-1} \mathbf{X}^\top \mathbf{W}_{\mathbf{F}^{-1}}(t) \mathbf{S}_{\mathbf{F}^{-1}}^{-1} \mathbf{X} \right)^\top \Sigma_{\mathbf{X}} \left(\mathbf{I}_d - \mathbf{F}^{-1} \mathbf{X}^\top \mathbf{W}_{\mathbf{F}^{-1}}(t) \mathbf{S}_{\mathbf{F}^{-1}}^{-1} \mathbf{X} \right) \right) \\ &= \frac{d}{dt} \text{tr} \left(\Sigma_{\mathbf{X} \boldsymbol{\theta}} \left(\mathbf{I}_d - \hat{\mathbf{X}}^\top \mathbf{W}_{\mathbf{F}^{-1}}(t) \mathbf{S}_{\mathbf{F}^{-1}}^{-1} \hat{\mathbf{X}} \right)^\top \left(\mathbf{I}_d - \hat{\mathbf{X}}^\top \mathbf{W}_{\mathbf{F}^{-1}}(t) \mathbf{S}_{\mathbf{F}^{-1}}^{-1} \hat{\mathbf{X}} \right) \right) \stackrel{(i)}{<} 0, \end{aligned}$$

where (i) follows from calculation similar to (C.20). Since the expected bias is decreasing through time for both GD and NGD when $\Sigma_{\boldsymbol{\theta}} = \mathbf{I}_d$, and from Theorem 2 we know that $B(\boldsymbol{\theta}_{\mathbf{I}}) \leq B(\hat{\boldsymbol{\theta}}_{\mathbf{F}^{-1}})$, we conclude that $B^{\text{opt}}(\boldsymbol{\theta}_{\mathbf{I}}) \leq B^{\text{opt}}(\boldsymbol{\theta}_{\mathbf{F}^{-1}})$. \square

C.8 Proof of Theorem 7

C.8.1 Setup and Result

We first state the setting and assumptions (which has been slightly updated compare to that of the main text). \mathcal{H} is an RKHS included in $L_2(P_X)$ equipped with a bounded kernel function k . $K_{\mathbf{x}} \in \mathcal{H}$ is the Riesz representation of the kernel function $k(x, \cdot)$, that is, $k(\mathbf{x}, \mathbf{y}) = \langle K_{\mathbf{x}}, K_{\mathbf{y}} \rangle_{\mathcal{H}}$. S is the canonical embedding operator from \mathcal{H} to $L_2(P_X)$. We write $\Sigma = S^* S : \mathcal{H} \rightarrow \mathcal{H}$ and $L = S S^*$. Note that the boundedness of the kernel gives $\|Sf\|_{L_2(P_X)} \leq \sup_{\mathbf{x}} |f(\mathbf{x})| = \sup_{\mathbf{x}} |\langle K_{\mathbf{x}}, f \rangle| \leq \|K_{\mathbf{x}}\|_{\mathcal{H}} \|f\|_{\mathcal{H}} \leq \|f\|_{\mathcal{H}}$. Hence we know $\|\Sigma\| \leq 1$ and $\|L\| \leq 1$. Our analysis will be made under the following assumptions.

- there exist $r \in (0, \infty)$ and $M > 0$ such that $f^* = L^r h^*$ for some $h^* \in L_2(P_X)$ and $\|f^*\|_{\infty} \leq M$.
- there exists $s > 1$ s.t. $\text{tr}(\Sigma^{1/s}) < \infty$ and $2r + s^{-1} > 1$.
- There exist $\mu \in [s^{-1}, 1]$ and $C_{\mu} > 0$ such that $\sup_{\mathbf{x} \in \text{supp}(P_X)} \|\Sigma^{1/2-1/\mu} K_{\mathbf{x}}\|_{\mathcal{H}} \leq C_{\mu}$.
- $\sup_{\mathbf{x} \in \text{supp}(P_X)} k(\mathbf{x}, \mathbf{x}) \leq 1$.

The training data is generated as $y_i = f^*(\mathbf{x}_i) + \varepsilon_i$, where ε_i is an i.i.d. noise satisfying $|\varepsilon_i| \leq \sigma$ almost surely. Let $\mathbf{y} \in \mathbb{R}^n$ be the label vector. We identify \mathbb{R}^n with $L_2(P_n)$ and define

$$\hat{\Sigma} = \frac{1}{n} \sum_{i=1}^n K_{\mathbf{x}_i} \otimes K_{\mathbf{x}_i} : \mathcal{H} \rightarrow \mathcal{H}, \quad \hat{S}^* Y = \frac{1}{n} \sum_{i=1}^n Y_i K_{\mathbf{x}_i}, \quad (Y \in L_2(P_n)).$$

We consider the following preconditioned update on $f_t \in \mathcal{H}$:

$$f_t = f_{t-1} - \eta(\Sigma + \lambda I)^{-1}(\hat{\Sigma} f_{t-1} - \hat{S}^* Y), \quad f_0 = 0.$$

We aim to show the following theorem:

Theorem 8. *Given the assumptions above, if the sample size n is sufficiently large so that $1/(n\lambda) \ll 1$, then for $\eta < \|\Sigma\|$ with $\eta t \geq 1$ and $0 < \delta < 1$ and $0 < \lambda < 1$, it holds that*

$$\|Sf_t - f^*\|_{L_2(P_X)}^2 \leq C(B(t) + V(t)),$$

with probability $1 - 3\delta$, where C is a constant and

$$B(t) := \exp(-\eta t) \vee \left(\frac{\lambda}{\eta t}\right)^{2r},$$

$$V(t) := V_1(t) + (1 + \eta t) \left(\frac{\lambda^{-1} B(t) + \sigma^2 \text{tr}(\Sigma^{1/s}) \lambda^{-1/s}}{n} + \frac{\lambda^{-1}(\sigma + M + (1 + t\eta)\lambda^{-(\frac{1}{2}-r)_+})^2}{n^2} \right) \log(1/\delta)^2,$$

in which

$$V_1(t) := \left[\exp(-\eta t) \vee \left(\frac{\lambda}{\eta t}\right)^{2r} + (t\eta)^2 \left(\frac{\beta'(1 \vee \lambda^{2r-\mu}) \text{tr}(\Sigma^{1/s}) \lambda^{-1/s}}{n} + \frac{\beta'^2(1 + \lambda^{-\mu}(1 \vee \lambda^{2r-\mu}))}{n^2} \right) \right] (1 + t\eta)^2,$$

for $\beta' = \log\left(\frac{28C_\mu^2(2^{2r-\mu} \vee \lambda^{-\mu+2r}) \text{tr}(\Sigma^{1/s}) \lambda^{-1/s}}{\delta}\right)$. When $r \geq 1/2$, if we set $\lambda = n^{-\frac{s}{2rs+1}} =: \lambda^*$ and $t = \Theta(\log(n))$, then the overall convergence rate becomes

$$\|Sg_t - f^*\|_{L_2(P_X)}^2 = \tilde{O}_p\left(n^{-\frac{2rs}{2rs+1}}\right),$$

which is the minimax optimal rate ($\tilde{O}_p(\cdot)$ hides a poly-log(n) factor). On the other hand, when $r < 1/2$, the bound is also $\tilde{O}_p\left(n^{-\frac{2rs}{2rs+1}}\right)$ except the term $V_1(t)$. In this case, if $2r \geq \mu$ holds additionally, we have $V_t(t) = \tilde{O}_p\left(n^{-\frac{2rs}{2rs+1}}\right)$, which again recovers the optimal rate.

Note that if the naive GD (with iterates \tilde{f}_t) is employed, from previous works [LR17], we know that the bias term $\left(\frac{\lambda}{\eta t}\right)^{2r}$ is replaced by $\left(\frac{1}{\eta t}\right)^{2r}$, and therefore the upper bound translates to

$$\|S\tilde{f}_t - f^*\|_{L_2(P_X)}^2 \leq C \left\{ (\eta t)^{-2r} + \frac{1}{n} \left(\text{tr}(\Sigma^{1/s}) (\eta t)^{1/s} + \frac{\eta t}{n} \right) \left(\sigma^2 + \left(\frac{1}{\eta t}\right)^{2r} + \frac{M^2 + (\eta t)^{-(2r-1)}}{n} \right) \right\},$$

with high probability. In other words, by the condition $\eta = O(1)$, we need $t = \Theta(n^{\frac{2rs}{2rs+1}})$ steps to sufficiently diminish the bias term. In contrast, the preconditioned update that interpolates between GD and NGD (4.1) only require $t = O(\log(n))$ steps to make the bias term negligible. This is because the NGD amplifies the high frequency component and rapidly captures the detailed ‘‘shape’’ of the target function f^* .

C.8.2 Proof of Main Result

Proof. We follow the proof strategy of [LR17]. First we define a reference optimization problem with iterates \bar{f}_t that directly minimize the population risk:

$$\bar{f}_t = \bar{f}_{t-1} - \eta(\Sigma + \lambda I)^{-1}(\Sigma \bar{f}_{t-1} - S^* f^*), \quad \bar{f}_0 = 0.$$

Note that $\mathbb{E}[f_t] = \bar{f}_t$. In addition, we define the degrees of freedom and its related quantity as

$$\mathcal{N}_\infty(\lambda) := \mathbb{E}_{\mathbf{x}}[\langle K_{\mathbf{x}}, \Sigma_\lambda^{-1} K_{\mathbf{x}} \rangle_{\mathcal{H}}] = \text{tr}(\Sigma \Sigma_\lambda^{-1}), \quad \mathcal{F}_\infty(\lambda) := \sup_{\mathbf{x} \in \text{supp}(P_X)} \|\Sigma_\lambda^{-1/2} K_{\mathbf{x}}\|_{\mathcal{H}}^2.$$

We can see that the risk admits the following bias-variance decomposition

$$\|Sf_t - f^*\|_{L_2(P_X)}^2 \leq 2 \underbrace{\|Sf_t - S\bar{f}_t\|_{L_2(P_X)}^2}_{V(t), \text{ variance}} + \underbrace{\|\bar{f}_t - f^*\|_{L_2(P_X)}^2}_{B(t), \text{ bias}}.$$

We upper bound the bias and variance separately.

Bounding the bias term $B(t)$: Note that by the update rule (4.1), it holds that

$$\begin{aligned} S\bar{f}_t - f^* &= S\bar{f}_{t-1} - f^* - \eta S(\Sigma + \lambda I)^{-1}(\Sigma \bar{f}_{t-1} - S^* f^*) \\ \Leftrightarrow S\bar{f}_t - f^* &= (I - \eta S(\Sigma + \lambda I)^{-1} S^*)(S\bar{f}_{t-1} - f^*). \end{aligned}$$

Therefore, unrolling the recursion gives $S\bar{f}_t - f^* = (I - \eta S(\Sigma + \lambda I)^{-1} S^*)^t (S\bar{f}_0 - f^*) = (I - \eta S(\Sigma + \lambda I)^{-1} S^*)^t (-f^*) = -(I - \eta S(\Sigma + \lambda I)^{-1} S^*)^t L^r h^*$. Write the spectral decomposition of L as $L = \sum_{j=1}^{\infty} \sigma_j \phi_j \phi_j^*$ for $\phi_j \in L_2(P_X)$ for $\sigma_j \geq 0$. We have $\|(I - \eta S(\Sigma + \lambda I)^{-1} S^*)^t L^r h^*\|_{L_2(P_X)} = \sum_{j=1}^{\infty} (1 - \eta \frac{\sigma_j}{\sigma_j + \lambda})^{2t} \sigma_j^{2r} h_j^2$, where $h = \sum_{j=1}^{\infty} h_j \phi_j$. We then apply Lemma 9 to obtain

$$B(t) \leq \exp(-\eta t) \sum_{j: \sigma_j \geq \lambda} h_j^2 + \left(\frac{2r}{e} \frac{\lambda}{\eta t}\right)^{2r} \sum_{j: \sigma_j < \lambda} h_j^2 \leq C \left[\exp(-\eta t) \vee \left(\frac{\lambda}{\eta t}\right)^{2r} \right] \|h^*\|_{L_2(P_X)}^2,$$

where C is a constant depending only on r .

Bounding the variance term $V(t)$: We now handle the variance term $V(t)$. For notational convenience, we write $A_\lambda := A + \lambda I$ for a linear operator A from a Hilbert space H to H . By the definition of f_t , we know

$$\begin{aligned} f_t &= (I - \eta(\Sigma + \lambda I)^{-1} \hat{\Sigma}) f_{t-1} + \eta(\Sigma + \lambda I)^{-1} \hat{S}^* Y \\ &= \sum_{j=0}^{t-1} (I - \eta(\Sigma + \lambda I)^{-1} \hat{\Sigma})^j \eta(\Sigma + \lambda I)^{-1} \hat{S}^* Y \\ &= \Sigma_\lambda^{-1/2} \eta \left[\sum_{j=0}^{t-1} (I - \eta \Sigma_\lambda^{-1/2} \hat{\Sigma} \Sigma_\lambda^{-1/2})^j \right] \Sigma_\lambda^{-1/2} \hat{S}^* Y =: \Sigma_\lambda^{-1/2} G_t \Sigma_\lambda^{-1/2} \hat{S}^* Y, \end{aligned}$$

where we defined $G_t := \eta \left[\sum_{j=0}^{t-1} (I - \eta \Sigma_\lambda^{-1/2} \hat{\Sigma} \Sigma_\lambda^{-1/2})^j \right]$. Accordingly, we decompose $V(t)$ as

$$\begin{aligned} \|Sf_t - S\bar{f}_t\|_{L_2(P_X)}^2 &\leq 2 \underbrace{\|S(f_t - \Sigma_\lambda^{-1/2} G_t \Sigma_\lambda^{-1/2} \hat{\Sigma} \bar{f}_t)\|_{L_2(P_X)}^2}_{(a)} \\ &\quad + \underbrace{\|S(\Sigma_\lambda^{-1/2} G_t \Sigma_\lambda^{-1/2} \hat{\Sigma} \bar{f}_t - \bar{f}_t)\|_{L_2(P_X)}^2}_{(b)}. \end{aligned}$$

We bound (a) and (b) separately.

Step 1. Bounding (a). Decompose (a) as

$$\begin{aligned} & \|S(f_t - \Sigma_\lambda^{-1/2} G_t \Sigma_\lambda^{-1/2} \hat{\Sigma}_\lambda \bar{f}_t)\|_{L_2(P_X)}^2 = \|S \Sigma_\lambda^{-1/2} G_t \Sigma_\lambda^{-1/2} (\hat{S}^* Y - \hat{\Sigma}_\lambda \bar{f}_t)\|_{L_2(P_X)}^2 \\ & \leq \|S \Sigma_\lambda^{-1/2}\|^2 \|G_t \Sigma_\lambda^{-1/2} \hat{\Sigma}_\lambda \Sigma_\lambda^{-1/2}\|^2 \|\Sigma_\lambda^{1/2} \hat{\Sigma}_\lambda^{-1} \Sigma_\lambda^{1/2}\|^2 \|\Sigma_\lambda^{-1/2} (\hat{S}^* Y - \hat{\Sigma}_\lambda \bar{f}_t)\|_{\mathcal{H}}^2. \end{aligned}$$

We bound the terms in the RHS individually.

(i) $\|S \Sigma_\lambda^{-1/2}\|^2 = \|\Sigma_\lambda^{-1/2} \Sigma \Sigma_\lambda^{-1/2}\| \leq 1.$

(ii) Note that $\Sigma_\lambda^{-1/2} \hat{\Sigma}_\lambda \Sigma_\lambda^{-1/2} = I - \Sigma_\lambda^{-1/2} (\Sigma - \hat{\Sigma}) \Sigma_\lambda^{-1/2} \succeq (1 - \|\Sigma_\lambda^{-1/2} (\Sigma - \hat{\Sigma}) \Sigma_\lambda^{-1/2}\|) I.$

Proposition 6 of [RR17] and its proof implies that for $\lambda \leq \|\Sigma\|$ and $0 < \delta < 1$, it holds that

$$\|\Sigma_\lambda^{-1/2} (\Sigma - \hat{\Sigma}) \Sigma_\lambda^{-1/2}\| \leq \sqrt{\frac{2\beta \mathcal{F}_\infty(\lambda)}{n}} + \frac{2\beta(1 + \mathcal{F}_\infty(\lambda))}{3n} =: \Xi_n, \quad (\text{C.21})$$

with probability $1 - \delta$, where $\beta = \log\left(\frac{4\text{tr}(\Sigma \Sigma_\lambda^{-1})}{\delta}\right) = \log\left(\frac{4\mathcal{N}_\infty(\lambda)}{\delta}\right)$. By Lemma 12, $\beta \leq \log\left(\frac{4\text{tr}(\Sigma^{1/s}) \lambda^{-1/s}}{\delta}\right)$ and $\mathcal{F}_\infty(\lambda) \leq \lambda^{-1}$. Therefore, if $\lambda = o(n^{-1} \log(n))$ and $\lambda = \Omega(n^{-1/s})$, the RHS can be smaller than $1/2$ for sufficiently large n , i.e. $\Xi_n = O(\sqrt{\log(n)/(n\lambda)}) \leq 1/2$. In this case we have,

$$\Sigma_\lambda^{-1/2} \hat{\Sigma}_\lambda \Sigma_\lambda^{-1/2} \succeq \frac{1}{2} I.$$

We denote this event as \mathcal{E}_1 .

(iii) Note that

$$\begin{aligned} G_t \Sigma_\lambda^{-1/2} \hat{\Sigma}_\lambda \Sigma_\lambda^{-1/2} &= \eta \left[\sum_{j=0}^{t-1} (I - \eta \Sigma_\lambda^{-1/2} \hat{\Sigma}_\lambda \Sigma_\lambda^{-1/2})^j \right] \Sigma_\lambda^{-1/2} \hat{\Sigma}_\lambda \Sigma_\lambda^{-1/2} \\ &= \eta \left[\sum_{j=0}^{t-1} (I - \eta \Sigma_\lambda^{-1/2} \hat{\Sigma}_\lambda \Sigma_\lambda^{-1/2})^j \right] (\Sigma_\lambda^{-1/2} \hat{\Sigma}_\lambda \Sigma_\lambda^{-1/2} + \lambda \Sigma_\lambda^{-1}). \end{aligned}$$

Thus, by Lemma 10 we have

$$\begin{aligned} & \|G_t \Sigma_\lambda^{-1/2} \hat{\Sigma}_\lambda \Sigma_\lambda^{-1/2}\| \\ & \leq \underbrace{\left\| \eta \left[\sum_{j=0}^{t-1} (I - \eta \Sigma_\lambda^{-1/2} \hat{\Sigma}_\lambda \Sigma_\lambda^{-1/2})^j \right] \Sigma_\lambda^{-1/2} \hat{\Sigma}_\lambda \Sigma_\lambda^{-1/2} \right\|}_{\leq 1 \text{ (due to Lemma 10)}} + \left\| \eta \left[\sum_{j=0}^{t-1} (I - \eta \Sigma_\lambda^{-1/2} \hat{\Sigma}_\lambda \Sigma_\lambda^{-1/2})^j \right] \lambda \Sigma_\lambda^{-1} \right\| \\ & \leq 1 + \eta \sum_{j=0}^{t-1} \|(I - \eta \Sigma_\lambda^{-1/2} \hat{\Sigma}_\lambda \Sigma_\lambda^{-1/2})^j\| \|\lambda \Sigma_\lambda^{-1}\| \leq 1 + \eta t. \end{aligned}$$

(iv) Note that

$$\|\Sigma_\lambda^{-1/2} (\hat{S}^* Y - \hat{\Sigma}_\lambda \bar{f}_t)\|_{\mathcal{H}}^2 \leq 2(\|\Sigma_\lambda^{-1/2} [(\hat{S}^* Y - \hat{\Sigma}_\lambda \bar{f}_t) - (S^* f^* - \Sigma \bar{f}_t)]\|_{\mathcal{H}}^2 + \|\Sigma_\lambda^{-1/2} (S^* f^* - \Sigma \bar{f}_t)\|_{\mathcal{H}}^2).$$

First we bound the first term of the RHS. Let $\xi_i = \Sigma_\lambda^{-1/2} [K_{\mathbf{x}_i} y_i - K_{\mathbf{x}_i} \bar{f}_t(\mathbf{x}_i) - (S^* f^* - \Sigma \bar{f}_t)]$. Then, $\{\xi_i\}_{i=1}^n$ is an i.i.d. sequence of zero-centered random variables taking value in \mathcal{H} and thus we have

$$\|\Sigma_\lambda^{-1/2} [(\hat{S}^* Y - \hat{\Sigma}_\lambda \bar{f}_t) - (S^* f^* - \Sigma \bar{f}_t)]\|_{\mathcal{H}}^2 = \left\| \frac{1}{n} \sum_{i=1}^n \xi_i \right\|_{\mathcal{H}}^2.$$

The RHS can be bounded by using Bernstein's inequality in Hilbert space [CDV07]. To apply the inequality, we need to bound the variance and sup-norm of the random variable. The variance can be bounded as

$$\begin{aligned}
\mathbb{E}[\|\xi_i\|_{\mathcal{H}}^2] &\leq \mathbb{E}_{(\mathbf{x},y)} \left[\|\Sigma_\lambda^{-1/2}(K_{\mathbf{x}}(f^*(\mathbf{x}) - \bar{f}_t(\mathbf{x})) + K_\xi \epsilon)\|_{\mathcal{H}}^2 \right] \\
&\leq 2 \left\{ \mathbb{E}_{(\mathbf{x},y)} \left[\|\Sigma_\lambda^{-1/2}(K_{\mathbf{x}}(f^*(\mathbf{x}) - \bar{f}_t(\mathbf{x}))\|_{\mathcal{H}}^2 + \|\Sigma_\lambda^{-1/2}(K_{\mathbf{x}}\epsilon)\|_{\mathcal{H}}^2 \right] \right\} \\
&\leq 2 \left\{ \sup_{\mathbf{x} \in \text{supp}(P_X)} \|\Sigma_\lambda^{-1/2} K_{\mathbf{x}}\|^2 \|f^* - S\bar{f}_t\|_{L_2(P_X)}^2 + \sigma^2 \text{tr}(\Sigma_\lambda^{-1}\Sigma) \right\} \\
&\leq 2 \{ \mathcal{F}_\infty(\lambda) B(t) + \sigma^2 \text{tr}(\Sigma_\lambda^{-1}\Sigma) \} \\
&\leq 2 \{ \lambda^{-1} B(t) + \sigma^2 \text{tr}(\Sigma_\lambda^{-1}\Sigma) \},
\end{aligned}$$

The sup-norm can be bounded as follows. Observe that $\|\bar{f}_t\|_\infty \leq \|\bar{f}_t\|_{\mathcal{H}}$, and thus by Lemma 11,

$$\begin{aligned}
\|\xi_i\|_{\mathcal{H}} &\leq 2 \sup_{\mathbf{x} \in \text{supp}(P_X)} \|\Sigma_\lambda^{-1/2} K_{\mathbf{x}}\|_{\mathcal{H}} (\sigma + \|f^*\|_\infty + \|\bar{f}_t\|_\infty) \\
&\lesssim \mathcal{F}_\infty^{1/2}(\lambda) (\sigma + M + (1+t\eta)\lambda^{-(1/2-r)_+}) \\
&\lesssim \lambda^{-1/2} (\sigma + M + (1+t\eta)\lambda^{-(1/2-r)_+}).
\end{aligned}$$

Therefore, for $0 < \delta < 1$, Bernstein's inequality (see Proposition 2 of [CDV07]) yields that

$$\left\| \frac{1}{n} \sum_{i=1}^n \xi_i \right\|_{\mathcal{H}}^2 \leq C \left(\sqrt{\frac{\lambda^{-1} B(t) + \sigma^2 \text{tr}(\Sigma_\lambda^{-1}\Sigma)}{n}} + \frac{\lambda^{-1/2} (\sigma + M + (1+t\eta)\lambda^{-(1/2-r)_+})}{n} \right)^2 \log(1/\delta)^2$$

with probability $1 - \delta$ where C is a universal constant. We define this event as \mathcal{E}_2 .

For the second term $\|\Sigma_\lambda^{-1/2}(S^* f^* - \Sigma \bar{f}_t)\|_{\mathcal{H}}^2$ we have

$$\|\Sigma_\lambda^{-1/2}(S^* f^* - \Sigma \bar{f}_t)\|_{\mathcal{H}}^2 \leq \|\Sigma_\lambda^{-1/2}(f^* - S\bar{f}_t)\|_{\mathcal{H}}^2 = \|f^* - S\bar{f}_t\|_{L_2(P_X)}^2 \leq B(t).$$

Combining these evaluations, on the event \mathcal{E}_2 where $P(\mathcal{E}_2) \geq 1 - \delta$ for $0 < \delta < 1$ we have

$$\begin{aligned}
&\|\Sigma_\lambda^{-1/2}(\hat{S}^* Y - \hat{\Sigma} \bar{f}_t)\|_{\mathcal{H}}^2 \\
&\stackrel{(i)}{\leq} C \left(\sqrt{\frac{\lambda^{-1} B(t) + \sigma^2 \text{tr}(\Sigma_\lambda^{-1}\Sigma)}{n}} + \frac{\lambda^{-1/2} (\sigma + M + (1+t\eta)\lambda^{-(1/2-r)_+})}{n} \right)^2 \log(1/\delta)^2 + B(t).
\end{aligned}$$

where we used Lemma 12 in (i).

Step 2. Bounding (b). On the event \mathcal{E}_1 , the term (b) can be evaluated as

$$\begin{aligned}
&\|S(\Sigma_\lambda^{-1/2} G_t \Sigma_\lambda^{-1/2} \hat{\Sigma} \bar{f}_t - \bar{f}_t)\|_{L_2(P_X)}^2 \\
&\leq \|\Sigma^{1/2}(\Sigma_\lambda^{-1/2} G_t \Sigma_\lambda^{-1/2} \hat{\Sigma} \bar{f}_t - \bar{f}_t)\|_{\mathcal{H}}^2 \\
&\leq \|\Sigma^{1/2} \Sigma_\lambda^{-1/2} (G_t \Sigma_\lambda^{-1/2} \hat{\Sigma} \Sigma_\lambda^{-1/2} - I) \Sigma_\lambda^{1/2} \bar{f}_t\|_{\mathcal{H}}^2 \\
&\leq \|\Sigma^{1/2} \Sigma_\lambda^{-1/2} \| (G_t \Sigma_\lambda^{-1/2} \hat{\Sigma} \Sigma_\lambda^{-1/2} - I) \Sigma_\lambda^{1/2} \bar{f}_t\|_{\mathcal{H}}^2 \\
&\leq \|(G_t \Sigma_\lambda^{-1/2} \hat{\Sigma} \Sigma_\lambda^{-1/2} - I) \Sigma_\lambda^{1/2} \bar{f}_t\|_{\mathcal{H}}^2.
\end{aligned} \tag{C.22}$$

where we used Lemma 11 in the last inequality. The term $\|(G_t \Sigma_\lambda^{-1/2} \hat{\Sigma} \Sigma_\lambda^{-1/2} - I) \Sigma_\lambda^{1/2} \bar{f}_t\|_{\mathcal{H}}$ can be bounded as follows. First, note that

$$(G_t \Sigma_\lambda^{-1/2} \hat{\Sigma} \Sigma_\lambda^{-1/2} - I) \Sigma_\lambda^{1/2} = \left\{ \eta \left[\sum_{j=0}^{t-1} (I - \eta \Sigma_\lambda^{-1/2} \hat{\Sigma} \Sigma_\lambda^{-1/2})^j \right] \Sigma_\lambda^{-1/2} \hat{\Sigma} \Sigma_\lambda^{-1/2} - I \right\} \Sigma_\lambda^{1/2}$$

$$= (I - \eta \Sigma_\lambda^{-1/2} \hat{\Sigma} \Sigma_\lambda^{-1/2})^t \Sigma_\lambda^{1/2}.$$

Therefore, the RHS of (C.22) can be further bounded by

$$\begin{aligned}
& \|(I - \eta \Sigma_\lambda^{-1/2} \hat{\Sigma} \Sigma_\lambda^{-1/2})^t \Sigma_\lambda^{1/2} \bar{f}_t\|_{\mathcal{H}} \\
&= \|(I - \eta \Sigma_\lambda^{-1/2} \Sigma \Sigma_\lambda^{-1/2} + \eta \Sigma_\lambda^{-1/2} (\Sigma - \hat{\Sigma}) \Sigma_\lambda^{-1/2})^t \Sigma_\lambda^{1/2} \bar{f}_t\|_{\mathcal{H}} \\
&= \left\| \sum_{k=0}^{t-1} (I - \eta \Sigma_\lambda^{-1/2} \hat{\Sigma} \Sigma_\lambda^{-1/2})^k (\eta \Sigma_\lambda^{-1/2} (\Sigma - \hat{\Sigma}) \Sigma_\lambda^{-1/2}) (I - \eta \Sigma_\lambda^{-1} \Sigma)^{t-k-1} \Sigma_\lambda^{1/2} \bar{f}_t - (I - \eta \Sigma_\lambda^{-1} \Sigma)^t \Sigma_\lambda^{1/2} \bar{f}_t \right\|_{\mathcal{H}} \\
&\stackrel{(i)}{\leq} \|(I - \eta \Sigma_\lambda^{-1} \Sigma)^t \Sigma_\lambda^{1/2} \bar{f}_t\|_{\mathcal{H}} \\
&\quad + \eta \sum_{k=0}^{t-1} \|(I - \eta \Sigma_\lambda^{-1/2} \hat{\Sigma} \Sigma_\lambda^{-1/2})^k \Sigma_\lambda^{-1/2} (\Sigma - \hat{\Sigma}) \Sigma_\lambda^{-1/2+r} (I - \eta \Sigma_\lambda^{-1} \Sigma)^{t-k-1} \Sigma_\lambda^{1/2-r} \bar{f}_t\|_{\mathcal{H}} \\
&\leq \|(I - \eta \Sigma_\lambda^{-1} \Sigma)^t \Sigma_\lambda^{1/2} \bar{f}_t\|_{\mathcal{H}} + t\eta \|\Sigma_\lambda^{-1/2} (\Sigma - \hat{\Sigma}) \Sigma_\lambda^{-1/2+r}\| \|\Sigma_\lambda^{1/2-r} \bar{f}_t\|_{\mathcal{H}} \\
&= \|(I - \eta \Sigma_\lambda^{-1} \Sigma)^t \Sigma_\lambda^r\| \|\Sigma_\lambda^{1/2-r} \bar{f}_t\|_{\mathcal{H}} + t\eta \|\Sigma_\lambda^{-1/2} (\Sigma - \hat{\Sigma}) \Sigma_\lambda^{-1/2+r}\| \|\Sigma_\lambda^{1/2-r} \bar{f}_t\|_{\mathcal{H}} \\
&\lesssim \|(I - \eta \Sigma_\lambda^{-1} \Sigma)^t \Sigma_\lambda^r\| + t\eta \|\Sigma_\lambda^{-1/2} (\Sigma - \hat{\Sigma}) \Sigma_\lambda^{-1/2+r}\| (1 + t\eta) \|h^*\|_{L_2(P_X)}, \tag{C.23}
\end{aligned}$$

where (i) is due to exchangeability of Σ_λ and Σ . By Lemma 9, for the RHS we have

$$\|(I - \eta \Sigma_\lambda^{-1} \Sigma)^t \Sigma_\lambda^r\| \leq \exp(-\eta t/2) \vee \left(\frac{1}{e} \frac{\lambda}{\eta t}\right)^r.$$

Next, as in the (C.21), by applying the Bernstein inequality for asymmetric operators (Corollary 3.1 of [Min17] with the argument in its Section 3.2), it holds that

$$\begin{aligned}
& \|\Sigma_\lambda^{-1/2} (\Sigma - \hat{\Sigma}) \Sigma_\lambda^{-1/2+r}\| \\
&\leq C' \left(\sqrt{\frac{\beta' C_\mu^2 (2^{2r-\mu} \vee \lambda^{2r-\mu}) \mathcal{N}_\infty(\lambda)}{n}} + \frac{\beta' ((1+\lambda)^r + C_\mu^2 \lambda^{-\mu/2} (2^{2r-\mu} \vee \lambda^{r-\mu/2}))}{n} \right) =: \Xi'_n,
\end{aligned}$$

with probability $1 - \delta$, where C' is a universal constant and $\beta' \leq \log\left(\frac{28C_\mu^2 (2^{2r-\mu} \vee \lambda^{-\mu+2r}) \text{tr}(\Sigma^{1/s}) \lambda^{-1/s}}{\delta}\right)$. We also used the following bounds on the sup-norm and the second order moments:

$$\begin{aligned}
(\text{sup-norm}) \quad & \|\Sigma_\lambda^{-1/2} (K_{\mathbf{x}} K_{\mathbf{x}}^* - \Sigma) \Sigma_\lambda^{-1/2+r}\| \\
& \leq \|\Sigma_\lambda^{-1/2} K_{\mathbf{x}} K_{\mathbf{x}}^* \Sigma_\lambda^{-1/2+r}\| + \|\Sigma_\lambda^r\| \\
& \leq \|\Sigma_\lambda^{-\mu/2} \Sigma_\lambda^{\mu/2-1/2} K_{\mathbf{x}} K_{\mathbf{x}}^* \Sigma_\lambda^{-1/2+\mu/2} \Sigma_\lambda^{r-\mu/2}\| + \|\Sigma_\lambda^r\| \\
& \leq C_\mu^2 \lambda^{-\mu/2} (2^{r-\mu/2} \vee \lambda^{r-\mu/2}) + (1+\lambda)^r \quad (\text{a.s.}), \\
(2\text{nd order moment 1}) \quad & \|\mathbb{E}_{\mathbf{x}} [\Sigma_\lambda^{-1/2} (K_{\mathbf{x}} K_{\mathbf{x}}^* - \Sigma) \Sigma_\lambda^{-1+2r} (K_{\mathbf{x}} K_{\mathbf{x}}^* - \Sigma) \Sigma_\lambda^{-1/2}]\| \\
& \leq \|\Sigma_\lambda^{-1/2} \Sigma \Sigma_\lambda^{-1/2}\| \sup_{\mathbf{x} \in \text{supp}(P_X)} [K_{\mathbf{x}}^* \Sigma_\lambda^{-1/2+\mu/2} \Sigma_\lambda^{-\mu+2r} \Sigma_\lambda^{-1/2+\mu/2} K_{\mathbf{x}}] \\
& \leq C_\mu^2 (2^{2r-\mu} \vee \lambda^{2r-\mu}), \\
(2\text{nd order moment 2}) \quad & \|\mathbb{E}_{\mathbf{x}} [\Sigma_\lambda^{-1/2+r} (K_{\mathbf{x}} K_{\mathbf{x}}^* - \Sigma) \Sigma_\lambda^{-1/2} \Sigma_\lambda^{-1/2} (K_{\mathbf{x}} K_{\mathbf{x}}^* - \Sigma) \Sigma_\lambda^{-1/2+r}]\| \\
& \leq \|\mathbb{E}_{\mathbf{x}} [\Sigma_\lambda^{-1/2+r} K_{\mathbf{x}} K_{\mathbf{x}}^* \Sigma_\lambda^{-1} K_{\mathbf{x}} K_{\mathbf{x}}^* \Sigma_\lambda^{-1/2+r}]\| \\
& \leq C_\mu^2 (2^{2r-\mu} \vee \lambda^{2r-\mu}) \mathbb{E}_{\mathbf{x}} [K_{\mathbf{x}}^* \Sigma_\lambda^{-1} K_{\mathbf{x}}] \\
& = C_\mu^2 (2^{2r-\mu} \vee \lambda^{2r-\mu}) \text{tr}(\Sigma \Sigma_\lambda^{-1}) \\
& = C_\mu^2 (2^{2r-\mu} \vee \lambda^{2r-\mu}) \mathcal{N}_\infty(\lambda).
\end{aligned}$$

We define this event as \mathcal{E}_3 . Therefore, the RHS of (C.23) can be further bounded by

$$\begin{aligned} & \|[(I - \eta \Sigma_\lambda^{-1} \Sigma)^t \Sigma_\lambda^r + Ct\eta \|\Sigma_\lambda^{-1/2} (\Sigma - \hat{\Sigma}) \Sigma_\lambda^{-1/2+r}\|](1 + t\eta) \|h^*\|_{L_2(P_X)} \\ & \leq \left[\exp(-\eta t/2) \vee \left(\frac{1}{e} \frac{\lambda}{\eta t} \right)^r + t\eta \Xi'_n \right] (1 + t\eta) \|h^*\|_{L_2(P_X)}. \end{aligned}$$

Finally, note that when $\lambda = \lambda^*$ and $2r \geq \mu$,

$$\Xi_n^{r/2} = \tilde{O} \left(\frac{\lambda^{*2r-\mu-1/s}}{n} + \frac{\lambda^{*2(r-\mu)}}{n^2} \right) \leq \tilde{O} \left(n^{-\frac{s(4r-\mu)}{2rs+1}} + n^{-\frac{s(4r-2\mu)+2}{2rs+1}} \right) \leq \tilde{O} \left(n^{-\frac{2rs}{2rs+1}} \right).$$

Step 3. Combining the calculations in Step 1 and 2 leads to the desired result. \square

C.8.3 Auxiliary lemmas

Lemma 9. For $t \in \mathbb{N}$, $0 < \eta < 1$, $0 < \sigma \leq 1$ and $0 \leq \lambda$, it holds that

$$\left(1 - \eta \frac{\sigma}{\sigma + \lambda} \right)^t \sigma^r \leq \begin{cases} \exp(-\eta t/2) & (\sigma \geq \lambda) \\ \left(\frac{2r}{e} \frac{\lambda}{\eta t} \right)^r & (\sigma < \lambda) \end{cases}.$$

Proof. When $\sigma \geq \lambda$, we have

$$\left(1 - \eta \frac{\sigma}{\sigma + \lambda} \right)^t \sigma^r \leq \left(1 - \eta \frac{\sigma}{2\sigma} \right)^t \sigma^r = (1 - \eta/2)^t \sigma^r \leq \exp(-\eta t/2) \sigma^r \leq \exp(-\eta t/2)$$

due to $\sigma \leq 1$. On the other hand, note that

$$\begin{aligned} \left(1 - \eta \frac{\sigma}{\sigma + \lambda} \right)^t \sigma^r & \leq \exp\left(-\eta t \frac{\sigma}{\sigma + \lambda}\right) \times \left(\frac{\sigma \eta t}{\sigma + \lambda} \right)^r \left(\frac{\sigma + \lambda}{\eta t} \right)^r \\ & \leq \sup_{x>0} \exp(-x) x^r \left(\frac{\sigma + \lambda}{\eta t} \right)^r \leq \left(\frac{\sigma + \lambda}{\eta t e} \right)^r, \end{aligned}$$

where we used $\sup_{x>0} \exp(-x) x^r = (r/e)^r$. \square

Lemma 10. For $t \in \mathbb{N}$, $0 < \eta$ and $0 \leq \sigma$ such that $\eta\sigma < 1$, it holds that $\eta \sum_{j=0}^{t-1} (1 - \eta\sigma)^j \sigma \leq 1$.

Proof. If $\sigma = 0$, then the statement is obvious. Assume that $\sigma > 0$, then

$$\sum_{j=0}^{t-1} (1 - \eta\sigma)^j \sigma = \frac{1 - (1 - \eta\sigma)^t}{1 - (1 - \eta\sigma)} \sigma = \frac{1}{\eta} [1 - (1 - \eta\sigma)^t] \leq \eta^{-1}.$$

This yields the desired claim. \square

Lemma 11. Under (A5-7), for any $0 < \lambda < 1$ and $q \leq r$, it holds that

$$\|\Sigma_\lambda^{-s} \bar{f}_t\|_{\mathcal{H}} \lesssim (1 + \lambda^{-(1/2+(q-r))_+} + \lambda t \eta \lambda^{-(3/2+(q-r))_+}) \|h^*\|_{L_2(P_X)}.$$

Proof. Recall that

$$\bar{f}_t = (I - \eta(\Sigma + \lambda I)^{-1} \Sigma) \bar{f}_{t-1} + \eta(\Sigma + \lambda I)^{-1} S^* f^* = \sum_{j=0}^{t-1} (I - \eta(\Sigma + \lambda I)^{-1} \Sigma)^j \eta(\Sigma + \lambda I)^{-1} S^* f^*.$$

Therefore, we obtain the following

$$\begin{aligned}
\|\Sigma_\lambda^{-q} \bar{f}_t\|_{\mathcal{H}} &= \eta \left\| \sum_{j=0}^{t-1} (I - \eta \Sigma_\lambda^{-1} \Sigma)^j \Sigma_\lambda^{-1-q} S^* L^r h^* \right\|_{\mathcal{H}} \\
&= \eta \left\| \sum_{j=0}^{t-1} (I - \eta \Sigma_\lambda^{-1} \Sigma)^j \Sigma_\lambda^{-1} (\Sigma + \lambda I) \Sigma_\lambda^{-q-1} S^* L^r h^* \right\|_{\mathcal{H}} \\
&\leq \eta \left\| \sum_{j=0}^{t-1} (I - \eta \Sigma_\lambda^{-1} \Sigma)^j \Sigma_\lambda^{-1} \Sigma \Sigma_\lambda^{-q-1} S^* L^r h^* \right\|_{\mathcal{H}} + \lambda \eta \left\| \sum_{j=0}^{t-1} (I - \eta \Sigma_\lambda^{-1} \Sigma)^j \Sigma_\lambda^{-1} \Sigma_\lambda^{-q-1} S^* L^r h^* \right\|_{\mathcal{H}} \\
&\leq \eta \left\| \sum_{j=0}^{t-1} (I - \eta \Sigma_\lambda^{-1} \Sigma)^j \Sigma_\lambda^{-1} \Sigma \right\| \left\| \Sigma_\lambda^{-q-1} S^* L^r h^* \right\|_{\mathcal{H}} + \lambda \eta \left\| \sum_{j=0}^{t-1} (I - \eta \Sigma_\lambda^{-1} \Sigma)^j \Sigma_\lambda^{-1} \Sigma_\lambda^{-q-1} S^* L^r h^* \right\|_{\mathcal{H}} \\
&\leq \left\| \Sigma_\lambda^{-q-1} S^* L^r h^* \right\|_{\mathcal{H}} + \lambda t \eta \left\| \Sigma_\lambda^{-1} \Sigma_\lambda^{-q-1} S^* L^r h^* \right\|_{\mathcal{H}} \\
&\leq \left\| S^* L_\lambda^{-q-1+r} h^* \right\|_{\mathcal{H}} + \lambda t \eta \left\| S^* L_\lambda^{-q-2+r} h^* \right\|_{\mathcal{H}} \\
&\leq \sqrt{\langle h^*, L_\lambda^{-q-1+r} S S^* L_\lambda^{-q-1+r} h^* \rangle_{L_2(P_X)}} + \lambda t \eta \sqrt{\langle h^*, L_\lambda^{-q-2+r} S S^* L_\lambda^{-q-2+r} h^* \rangle_{L_2(P_X)}} \\
&= \sqrt{\langle h^*, L_\lambda^{-q-1+r} L L_\lambda^{-q-1+r} h^* \rangle_{L_2(P_X)}} + \lambda t \eta \sqrt{\langle h^*, L_\lambda^{-q-2+r} L L_\lambda^{-q-2+r} h^* \rangle_{L_2(P_X)}} \\
&\leq (\lambda^{-1/2-(q-r)} + \lambda t \eta \lambda^{-3/2-(q-r)}) \|h^*\|_{L_2(P_X)} \leq (1 + t \eta) \lambda^{-1/2-(q-r)} \|h^*\|_{L_2(P_X)}.
\end{aligned}$$

□

Lemma 12. Under (A5-7) and for $\lambda \in (0, 1)$, it holds that $\mathcal{N}_\infty(\lambda) \leq \text{tr}(\Sigma^{1/s}) \lambda^{-1/s}$, and $\mathcal{F}_\infty(\lambda) \leq 1/\lambda$.

Proof. For the first inequality, we have

$$\begin{aligned}
\mathcal{N}_\infty(\lambda) &= \text{tr}(\Sigma \Sigma_\lambda^{-1}) = \text{tr}(\Sigma^{1/s} \Sigma^{1-1/s} \Sigma_\lambda^{-(1-1/s)} \Sigma_\lambda^{-1/s}) \\
&\leq \text{tr}(\Sigma^{1/s} \Sigma^{1-1/s} \Sigma_\lambda^{-(1-1/s)}) \lambda^{-1/s} \leq \text{tr}(\Sigma^{1/s}) \lambda^{-1/s}.
\end{aligned}$$

As for the second inequality, note that

$$\mathcal{F}_\infty(\lambda) = \sup_{\mathbf{x}} \langle K_{\mathbf{x}}, \Sigma_\lambda^{-1} K_{\mathbf{x}} \rangle_{\mathcal{H}} \leq \sup_{\mathbf{x}} \lambda^{-1} \langle K_{\mathbf{x}}, K_{\mathbf{x}} \rangle_{\mathcal{H}} \leq \lambda^{-1} \sup_{\mathbf{x}} k(\mathbf{x}, \mathbf{x}) \leq \lambda^{-1}.$$

□

D Experiment Setup

D.1 Processing the Datasets

To obtain extra unlabeled data to estimate the Fisher, we zero pad pixels on the borders of each image before randomly cropping; a random horizontal flip is also applied for CIFAR10 images. We preprocess all images by dividing pixel values by 255 before centering them to be located within $[-0.5, 0.5]$ with the subtraction by $1/2$. For experiments on CIFAR10, we downsample the original images using a max pooling layer with kernel size 2 and stride 2.

D.2 Setup and Implementation for Optimizers

In all settings, GD uses a learning rate of 0.01 that is exponentially decayed every 1k updates with the parameter value 0.999. For NGD, we use a fixed learning rate of 0.03. Since inverting a parameter-by-parameter-sized Fisher estimate per iteration would be costly, we adopt the Hessian free approach [Mar10] which computes approximate matrix-inverse-vector products using the conjugate gradient (CG) method [NW06, BBV04]. For each approximate inversion, we run CG for 200 iterations starting from the solution returned by the previous CG run. The precise number of CG iterations and the initialization heuristic roughly follow [MS12]. For the first run of CG, we initialize the vector from a standard Gaussian, and run CG for 5k iterations. To ensure invertibility, we apply a very small amount of damping (0.00001) in most scenarios.

D.3 Other Details

For experiments in the label noise and misspecification sections, we pretrain the teacher using the Adam optimizer [KB14] with its default hyperparameters and a learning rate of 0.001.

For experiments in the misalignment section, we downsample all images twice using max pooling with kernel size 2 and stride 2. Moreover, only for experiments in this section, we implement natural gradient descent by exactly computing the Fisher on a large batch of unlabeled data and inverting the matrix by calling PyTorch’s `torch.inverse` before right multiplying the gradient.